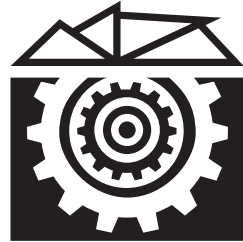


A F T
ACTA
FACULTATIS
TECHNICAЕ



TECHNICKÁ UNIVERZITA VO ZVOLENE

1

**ROČNÍK: XXIV
ZVOLEN 2019**

Medzinárodný zbor recenzentov / International Reviewers Board

Alexander A. Bartashevich (BY)

Belarusian State Technological University

Witold Biały (PL)

Silesian University of Technology, Faculty of Organization and Management

Jiří Dvořák (CZ)

Czech University of Life Sciences Prague, Faculty of Forestry and Wood Sciences

Ladislav Dzurenda (SK)

Technical University in Zvolen, Faculty of Wood Sciences and Technology

Zhivko Gochev (BG)

University of Forestry, Faculty of Forest Industry

Karel Janák (CZ)

Mendel University in Brno, Faculty of Forestry and Wood Technology

Radek Knoflíček (CZ)

Brno University of Technology, Faculty of Mechanical Engineering

Ján Kosiba (SK)

Slovak University of Agriculture in Nitra, Faculty of Engineering

Dražan Kožák (HR)

Josip Juraj Strossmayer University of Osijek, Mechanical Engineering Faculty

Antonín Kříž (CZ)

University of West Bohemia, Faculty of Mechanical Engineering

Stanisław Legutko (PL)

Poznan University of Technology

Oleg Machuga (UA)

National Forestry University of Ukraine, Lviv

Aleksandar Makedonski (BG)

Technical University of Sofia

Milan Malcho (SK)

University of Zilina, The Faculty of Mechanical Engineering

Stanislav Marchevský (SK)

Technical University of Košice, Faculty of Electrical Engineering and Informatics

Ján Mihalík (SK)

Technical University of Košice, Faculty of Electrical Engineering and Informatics

Miroslav Müller (CZ)

Czech University of Life Sciences Prague, Faculty of Engineering

Nataša Náprstková (CZ)

UJEP in Ustí nad Labem, Faculty of Production Technology and Management

Jindřich Neruda (CZ)

Mendel University in Brno, Faculty of Forestry and Wood Technology

Alena Očkajová (SK)

Matej Bel University, Faculty of Natural Sciences

Marián Peciar (SK)

Slovak University of Technology in Bratislava, Faculty of Mechanical Engineering

Krzysztof Zbigniew Rokosz (PL)

University of Technology

Miroslav Rousek (CZ)

Mendel University in Brno, Faculty of Forestry and Wood Technology

Pavel V. Rudak (BY)

Belarusian State Technological University

Juraj Ružbarský (SK)

University of Zilina, Faculty of Mechanical Engineering

Ruslan Safin (RU)

Kazan National Research Technological University

Sergey Spiridonov (RU)

State Institution of Higher Professional Education, Saint Petersburg State

Forest Technical University

Vladimír Štollmann (SK)

Technical University in Zvolen, Faculty of Forestry

Marian Šušniar (HR)

University of Zagreb, Faculty of Forestry

Pawel Tylek (PL)

University of Agriculture in Krakow, Faculty of Forestry

OBSAH

VEDECKÉ ČLÁNKY

HARD IRON AND SOFT IRON COMPENSATION OF THREE AXIS MAGNETOMETER MEASUREMENTS KOMPENZÁCIA HARD IRON A SOFT IRON VPLYVOV NA MERANIE TROJOSÉHO MAGNETOMETRA Marián Kišev, Patrik Kósa, Lukáš Vacho, Juraj Baláži, Vladimír Cviklovič	9
COMMUNICATION BETWEEN A PLC AND A RASPBERRY PI VIA OPENPOWERLINK KOMUNIKÁCIA MEDZI PLC A RASPBERRY PI PROSTREDNÍCTVOM OPENPOWERLINK Patrik Kósa, Marián Kišev, Juraj Baláži, Lukáš Vacho, Martin Olejár	17
ASSESSMENT OF ADHESIVE PROPERTIES OF SUMMER AND WINTER TYRES UNDER SPECIFIED CONDITIONS POSÚDENIE ADHÉZNYCH VLASTNOSTÍ LETNÝCH A ZIMNÝCH PNEUMATÍK ZA STANOVENÝCH PODMIENOK Peter Kuchar, Marek Halenár, Jozef Nosian, Juraj Tulík, Michal Holubek, Adam Fürstenzeller	27
IMPORTANT CHANGES IN ISO 9001:2015 FROM ISO 9001:2008 AND THEIR IMPACT ON SUPPLIER COMPLAINTS MANAGEMENT VÝZNAMNÉ ZMENY NORMY ISO 9001:2015 OPROTI ISO 9001:2008 A ICH DOPAD NA RIADENIE DODÁVATEĽSKÝCH REKLAMÁCIÍ Adéla Melicharová	37
MONITORING OF THE HOUSEHOLDS' ENERGY CONSUMPTION AS INDICATOR OF LIFE QUALITY IN RURAL MICRO- REGIONS MONITOROVANIE KVALITY ŽIVOTA MIKROREGIÓNOV VIDIEKA SO ZRETEL'OM NA SPOTREBU ENERGIE Petra Procházková	45
CHIPLESS CUTTING OF WOOD – DELIMBING KNIVES BEZTRIESKOVÉ DELENIE DREVA – ODVETVOVACIE NOŽE Ján Melicherčík, Jozef Krilek	53
LOCATION OF VEHICLE REGISTRATION PLATES IN REAL SCENE IMAGES LOKALIZÁCIA Evidenčných Čísel Vozidiel V REÁLNYCH OBRAZOCH Ladislav Karrach, Elena Pivarčiová	63

ENERGY AND TRANSPORT INFRASTRUCTURE IN LOW POPULATION AREAS, TECHNICAL POSSIBILITIES OF CHARGING STATION FOR ELECTRIC VEHICLES IN THESE AREAS ENERGETICKÁ A DOPRAVNÁ INFRAŠTRUKTÚRA V OBLASTIACH S NÍZKOU HUSTOTOU OBÝVATEĽSTVA, TECHNICKÉ MOŽNOSTI DOBÍJACÍCH STANÍC ELEKTROMOBILOV V TÝCHTO OBLASTIACH Miroslav Krumbholc	71
ANALYSIS OF ROLLING RESISTANCE OF TYRES FOR AGRICULTURAL AND FORESTRY MACHINES ON PAVED SURFACES ANALÝZA VALIVÉHO ODPORU PNEUMATÍK AGROLESNÍCKYCH STROJOV NA SPEVNENEJ PODLOŽKE Michal Berák, Ján Kováč, Milan Helexa	79
DESIGN OF A DEVICE FOR VERIFICATION OF A HYDRAULIC PUMP OPERATION KONŠTRUKCIA ZARIADENIA NA OVEROVANIE PREVÁDZKY HYDRAULICKÉHO ČERPADLA Jozef Nosian, Marek Halenár Peter Kuchar, Juraj Tulík, Adam Fürstenzeller, Marian Kučera	89
REFERÁTY	
USE OF HARVESTER HEADS IN FORESTRY VYUŽITIE HARVESTOROVÝCH HLAVÍC V LESNÍCTVE Veronika Ľuptáčiková, Richard Hnilica	101

VEDECKÉ ČLÁNKY

HARD IRON AND SOFT IRON COMPENSATION OF THREE AXIS MAGNETOMETER MEASUREMENTS

KOMPENZÁCIA HARD IRON A SOFT IRON VPLYVOV NA MERANIE TROJOSÉHO MAGNETOMETRA

Marián Kišev, Patrik Kósa, Lukáš Vacho, Juraj Baláži, Vladimír Cviklovič

*Department of Electrical Engineering, Automation and Informatics, Faculty of Engineering,
Slovak University of Agriculture in Nitra, Tr. A. Hlinku 2, 949 76, Nitra, Slovakia, dtf@uniag.sk*

ABSTRACT: Nowadays, the navigation systems are more and more used. They are mainly used in the transport, but they come into the field of autonomous systems. The navigation systems use a combination of GPS and inertial sensors. One of the inertial sensors is a magnetometer that measures the resulting magnetic field vector of the Earth. When it is measuring acceleration and distance, it is necessary to know the heading. The absolute heading value can be determined by the magnetometer. The magnetic field is deformed by magnetic materials which change the final magnetic induction vector and the magnetic field needs to be compensated. The device itself, on which the sensor is located, affects the measured magnetic field and therefore the magnetometer has to be directly compensated on the device on which it is located. The calibration constants are determined from the measured data that are subsequently applied to the individual measured samples. The calibration algorithm is implemented directly into the microcontroller that acquires the measured data.

Key words: magnetometer, microcontroller, calibration, ellipsoid

ABSTRAKT: V súčasnosti sa čoraz častejšie používajú navigačné systémy. Používajú sa najmä v doprave, ale dostávajú sa aj do oblasti autonómnych systémov. Pri navigačných systémoch sa používa kombinácia GPS spolu s inerciálnymi snímačmi. Jedným z inerciálnych snímačov je magnetometer, ktorý meria výsledný vektor magnetického poľa Zeme. Pri meraní zrýchlenia a prejdenej dráhy je treba poznať natočenie, ktorého absolútну hodnotu je možné určiť magnetometrom. Magnetické pole sa pôsobením magnetických materiálov deformuje, čím sa mení výsledný vektor magnetickej indukcie, ktorý treba ďalej kompenzovať. Samotné zariadenie, na ktorom je umiestnený snímač ovplyvňuje merané magnetické pole a preto je treba magnetometer kompenzovať priamo na zariadení, na ktorom bude umiestnený. Z nameraných údajov je možné určiť kalibračné konštanty, ktoré sú následne aplikované na jednotlivé namerané vzorky. Kalibračný algoritmus je implementovaný priamo do mikrokontroléra, ktorý zbiera namerané údaje.

Krúčové slová: magnetometer, mikrokontrolér, kalibrácia, snímač, elipsoid

INTRODUCTION

At present, the potential of using inertial sensors in mobile robotics is increasing. Inertial sensors used to be extremely costly in the past, but the introduction of sensors produced by the micro-electro-mechanical technology (MEMS) into consumer technology greatly contributes to the availability and to affordability of these sensors.

In this study, we are conducting the tri-axis magnetometer calibration using the least square method and subsequent absolute measurement of the heading angle in order to increase its accuracy and reliability for use in practice. Its precision is influenced by a variety of factors from the environment and from the device on which it is located. Among the factors, which are influencing the magnetometer we mainly classify noise measurement, manufacturing inaccuracies and at least, errors caused by foreign magnetic fields or materials, which are deforming the measured magnetic field of the Earth. Errors caused by deformation of the magnetic field or by the effect of a foreign magnetic field, which do not change over time, can be partially compensated by calibration of the sensors.

Hemanth et al. (2012) estimated bias and scale factors for all axes, using a simpler 2 step procedure. The proposed technique exploits the relation between the body axis rates and the Euler angles to define a limited rotation and an associated optimization problem to determine the calibration parameters. In results of Pylvänäinen (2008) report there is proposed an automatic calibration algorithm based on recursive fitting of an ellipsoid to collected samples from the sensor which can adaptively update the calibration parameters. Three different calibration strategies were analyzed and compared by Shitu et al. (2013). Calibration and magnetic disturbance compensation can be solved by computing nonlinear equations (Hongfeng et al. 2016). There are also researches which are especially analyzed calibration of errors caused by sensors deviations and the error separation based on non-magnetic three axis rotation platform (Včelák et al. 2005, Zhiwei et al. 2016, Gorkem & Billur 2016). More information about sensors and its calibration can be found in the literature (Farrell 2008, Groves 2008).

MATERIAL AND METHODS

Magnetometers are used in systems where it is necessary to determine absolute direction of orientation, which is an advantage, because while using relative sensors, the error increases rapidly. The used sensor is a MEMS LSM303DLHC sensor. These sensors have become very popular because of their price. Their disadvantage is their dependence on the environment that disturbs the magnetic field and then the error rises.

Magnetic induction of the geomagnetic field ranges from 20 to 130 μT . The vector of the magnetic induction of the Earth contains elements in all three axes of the coordinate system and they help us to determine the North Magnetic Pole. The North Magnetic Pole is located near the Northern Geographic Pole and it is unstable. The horizontal plane is given by the B_{eh} vector, which consists of two components B_{ex} and B_{ey} . The resulting vector of the geomagnetic field is then given by the sum of the horizontal component B_{ex} vector and the vertical component B_{ey} vector. The angle between the vector of the geomagnetic field and the horizontal plane is called as the inclination angle. The angle between the magnetic pole and the geographic pole is called as the declination angle. Its value is within $\pm 20^\circ$.

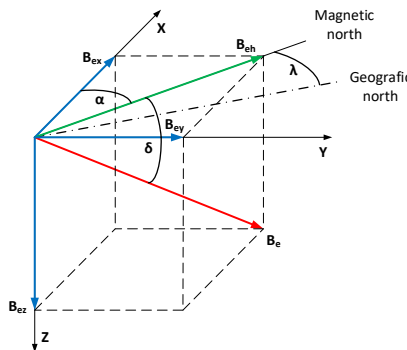


Fig. 1. Components of the magnetic induction vector
Obr. 1. Rozloženie vektora magnetickéj indukcie Zeme

The electromagnetic field is known to be different from other physical quantities by the fact that its sources are in the vicinity of every magnetic induction sensor and they cannot be removed. The only solution is to calibrate the sensor on a complete device with all its structural elements. The first disturbing phenomenon in magnetometers is the so-called “hard-iron” interference of magnetic field generated by ferromagnetic materials. Their electromagnetic field is constant over time and it is added to the Earth’s electromagnetic field. It reflects as an offset on the output of the magnetic induction sensor. The so-called “soft-iron” electromagnetic field interference is generated by the inner segments of the sensor device. It can be caused by electric currents flowing through a printed circuit board or by the soft magnetization of materials. These sources generate an electromagnetic field that is changing over time.

The effect of the so-called “soft-iron” distortion causes an error in the entire rotation of the sensor, which is evident in the tilt of the ellipsoid described by the rotation of the sensor in a space with a constant magnetic induction. Another interfering phenomenon is gain factor, which is defined as a sensitivity error of the sensor. In the best case, the electromagnetic field sensor has the same sensitivity in all three axes of the coordinate system.

In real conditions, each of the sensors in all three axes (x, y and z) has a different sensitivity. The effect is that after rotating the device around one of the axes, the vector of the measured magnetic induction describes an ellipse. If the device does not contain the so-called “hard-iron” and “soft-iron” interferential magnetic fields, the sensitivity of the sensors in the individual axes are the same and if the frame of the device and of the sensor are identical, then the measured vector of magnetic induction upon rotation describes the same surface of the sphere with its centre at centre of coordinate system.

The LSM303DLHC is an integrated circuit, featuring an integrated three-axis accelerometer and a three-axis magnetometer. The magnetic induction can be measured in ranges of $\pm 130 \mu\text{T}$, $\pm 190 \mu\text{T}$, $\pm 250 \mu\text{T}$, $\pm 400 \mu\text{T}$, $\pm 470 \mu\text{T}$, $\pm 560 \mu\text{T}$ and $\pm 810 \mu\text{T}$. The common circuit for both sensors that was produced by MEMS technology minimizes energy demands with the simultaneous absence of additional geometric adjustment of the axes of the both sensors. The measured data is read by a microcontroller via the I²C communication standard. The magnetometer and accelerometer have in applications that require

an electronic compass an advantage in their ability to compensate the inclination, which extends the compass usability for a variety of applications in research and practice.

RESULTS

The aim of the calibration of the geomagnetic induction sensor is to determine the correction parameters, so that the measured data is later compensated with minimal measurement uncertainty. Verification of the so-called “soft-iron” effect is done through a graphical rendering of the magnetic induction vector in space for various device rotations. The vector must describe the surface of the sphere.

The first connection of the LSM303DLHC with the EFM32WG990F256 microcontroller on the STK3800 development board was done only through the wires, but this had a negative impact on the measurement. The currents flowing through the wires created an interfering magnetic field. For this reason, we created a module that is directly connected to the development board. The module contains a SD card slot that is used to store the measured data used for calculating the calibration constants on the computer. To determine the tilt compensation, it includes a gyroscope together with an accelerometer. Fig. 2 shows the development board with the designed measurement module.

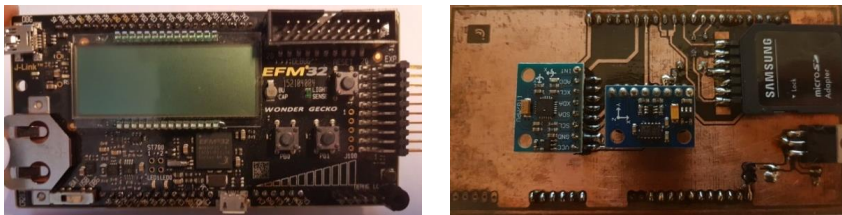


Fig. 2. Measurement device

(a – development board STK3800, b – designed measurement module LSM303DLHC)

Obr. 2. Meracie zariadenie

(a – vývojové zariadenie STK3800, b – vyhotovený prídavný merací modul s LSM303DLHC)

The communication is controlled by a microcontroller, which output provides data for tilt and heading angle after it gets calibration constants. Tilt is calculated from the accelerometer and gyroscope data. Measured sensor data has to be compensated according to the calibration protocol to assess the heading angle accurately. The microcontroller must compensate all the measured data in real time and, at the same time, perform all the necessary calculations.

The microcontroller has the ability to directly measure the data using the software low-pass filter of the specified frequency, thus sensor output is stabilized slightly.

The components of the vector of magnetic induction B are for simpler calculations normalized to its absolute value. Their value after normalization ranges from -1 to $+1$. If the calculated absolute value is not equal to 1 , it informs us of the presence of another interfering electromagnetic field and the measured directional angle is not accurate.

The measured values needed for calibrations are then processed in the Matlab to get calibration constants using least square ellipsoid fitting method. By a surface we mean a set of points in a space whose right-angled coordinates correspond to the equation $F(x, y, z) = 0$, where F is a function having at each point a continuous partial derivation of at least the first order. The general equation of quadratic surface has four so-called invariants, whose values do not change in the transformation of the coordinates by displacement and rotation. The general equation of quadratic surface:

$$a_{11}x^2 + a_{22}y^2 + a_{33}z^2 + 2a_{12}xy + 2a_{13}xz + 2a_{23}yz + 2a_{14}x + 2a_{24}y + 2a_{34}z + a_{44} = 0 \quad (1)$$

where $a_{11}.. a_{44}$ are constants that describes quadratic surface [-],
 x, y, z are parameters of quadratic surface [-].

The measured values are given in the general equation of the quadratic surface. The number of samples corresponds to the total number of rows stored in matrix D . The ellipsoid can be mathematically described by the least square method, which gives us the best equation for ellipsoid to get the individual calibration constants for the both cases of distortion. Accuracy increases with the number of measured vectors at different turns. However, the prerequisite here is a pre-calibrated accelerometer to measure the tilt and climb angles. It is unacceptable to calibrate the sensor itself, because it needs to be calibrated on a complete device on which no further adjustments will be made. Least square method is realized by equation 2.

$$V = (D^T D)^{-1} D^T Y \quad (2)$$

where V is result matrix of the quadratic surface [-],
 D is data matrix [-].

From the matrix of the quadratic surface we can obtain the values of the length of the half-axes and of the center, which are used as calibration constants for the magnetometer. Matrix of quadratic the surface is described in equation 3.

$$V = \begin{bmatrix} a_{11} & a_{12} & a_{13} & a_{14} \\ a_{12} & a_{22} & a_{23} & a_{24} \\ a_{13} & a_{23} & a_{33} & a_{34} \\ a_{14} & a_{24} & a_{34} & a_{44} \end{bmatrix} \quad (3)$$

Measurement was performed by free movement of the sensor around all the axes. The calibration consists of 10,000 measured samples. The first measurement proved only hard-iron offset (fig. 3a). To properly demonstrate the functionality of the algorithm, we placed a ferromagnetic material near the sensor, which influenced the resulting vector of magnetic induction and then we repeated the measurement. In the second measurement, a considerable magnetic field deformation occurred (fig. 3b), on which the vector describes the surface of an ellipsoid that has its center out of the center of the coordinate system and its being rotated. The red points indicate the measured values and the blue dots indicate the calibrated magnetic induction values.

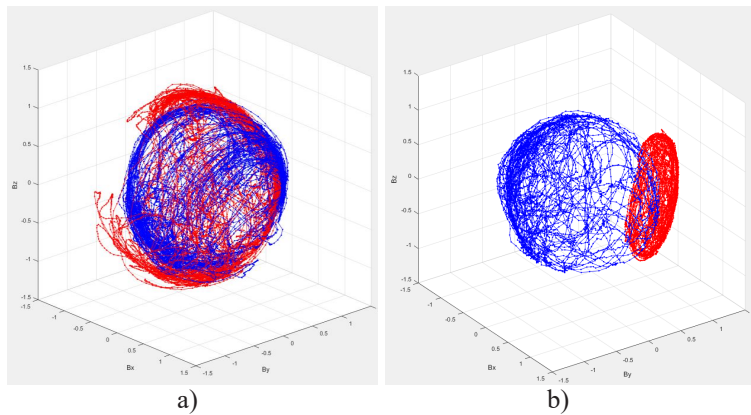


Fig. 3. Normalized measured values of magnetic induction
(a – without affecting of magnetic material, b – affected by magnetic material)

Obr. 3. Normalizované namerané údaje magnetickej indukcie

(a – bez ovplyvnenia magnetickým materiálom, b – ovplyvnenie magnetickým materiálom)

If the sensor is in a horizontal position, the tilt angle is equal to zero. The z-axis component is not required to specify the heading angle. In that case, we calculate the heading angle ψ from the relation:

$$\psi = \operatorname{arctg} \frac{B_{ym}}{B_{xm}} \quad (4)$$

where ψ is the heading angle [rad],

B_{ym} , B_{xm} are the measured components of the magnetic induction vector [μT].

The gravitational acceleration vector data from the accelerometer serves to correct the magnetic induction vector from which the heading angle of the device relative to the North Magnetic Pole is calculated. The tilt and the rise of the device were set from the distribution of the gravitational vector, from which the vector of the Earth's magnetic induction was also transformed. The relations from whom the components of the magnetic induction vector required to determine the heading angle were calculated are as follows:

$$\begin{aligned} B_x &= B_{xm} \cos(\theta) + B_{zm} \sin(\theta) \\ B_y &= B_{xm} \sin(\phi) \sin(\theta) + B_{ym} \cos(\phi) - B_{zm} \sin(\phi) \cos(\theta) \end{aligned} \quad (5)$$

where B_x , B_y are the compensated components of the magnetic induction vector [μT], B_{xm} , B_{ym} , B_{zm} are the measured components of the magnetic induction vector [μT], ϕ , θ are the tilt angles [rad].

After the compensation, it is possible to calculate the heading angle according to the equation 4, but it is necessary to use the compensated components of the magnetic induc-

tion. The calculated calibration constants are then load to the microcontroller which then compensates the measured values of the magnetic field in real time as follows:

$$\begin{bmatrix} B_{xc} \\ B_{yc} \\ B_{zc} \end{bmatrix} = \begin{bmatrix} M_{11} & M_{12} & M_{13} \\ M_{21} & M_{22} & M_{23} \\ M_{31} & M_{32} & M_{33} \end{bmatrix} \cdot \left(\begin{bmatrix} B_{xm} \\ B_{ym} \\ B_{zm} \end{bmatrix} - \begin{bmatrix} B_{xo} \\ B_{yo} \\ B_{zo} \end{bmatrix} \right) \quad (6)$$

where B_{xc} , B_{yc} , B_{zc} are calibrated components of magnetic induction vector [μT],
 B_{xo} , B_{yo} , B_{zo} are offsets of magnetic induction [μT],
 M is transformation matrix that contains rotation and gain factor of ellipsoid [-].

CONCLUSION

In this paper we present the application of the least square method for calibration of the magnetic induction sensor. When the measured magnetic induction vector is properly calibrated; it describes the surface area of a sphere. In case of incorrect calibration, the magnetic field vector will describe an ellipsoid, which can have its centre deflected from the centre of the coordinate system, and it can be also rotated. In the initial measurement the sensor has shown only a hard-iron interference, which has resulted in the shift of the sphere's centre. In order to demonstrate the accuracy and the functionality of the calibration, we have placed materials near the sensor that have induced not only hard-iron interference, but also soft-iron interference. Calculation of calibration constants was performed in mathematical simulation software Matlab.

To apply the least square method to find the approximate equation for the ellipsoid we have used 10,000 samples. Calculation with all collected samples could not be performed directly in the microcontroller due to lack of operating memory and computing power. After applying the calculated calibration constants to the measured data to the sensor, it shows correct values and the resulting vector describes the surface of a sphere. With correctly selected samples that do not contain a large measurement error, caused for example by interference, it is possible to approximate the equation for the ellipsoid with at least nine samples.

LITERATURE

- BROWN, P. ET. AL. 2008. Calibration techniques for magnetometers implementing on-board de-spinning algorithms. *Advances in Space Research*, Volume 41, Issue 10, pp 1571-1578, ISSN 0273-1177.
- FARRELL, Jay A. 2008. Aided Navigation. *McGraw-Hill Companies*, 2008, New York, s. 530, ISBN 978-0-07-149329-1.
- GORKEM, S., BILLUR B. 2016. Improvements in deterministic error modeling and calibration of inertial sensors and magnetometers. *Sensors and Actuators A: Physical*, Volume 247, pp 522-538, ISSN 0924-4247.
- GROVES, Paul D. 2008. Principles of GNSS, Inertial, and Multisensor Integrated Navigation Systems. *Artech House*, 2008, Boston, s. 505, ISBN 978-1-58053-255-6.

- HEMANTH, K.S., VISWANATH T., SHRIKANT R. 2012. Calibration of 3-axis Magnetometers. *IFAC Proceedings Volumes*, Volume 45, Issue 1, 2012, pp 175-178, ISSN 1474-6670, ISBN 9783902823298.
- HONGFENG, P., ET. AL. 2016. Integrated calibration and magnetic disturbance compensation of three-axis magnetometers. *Measurement*, Volume 93, pp 409-413, ISSN 0263-2241.
- PYLVÄNÄINEN T. 2008. Automatic and adaptive calibration of 3D field sensors. *Applied Mathematical Modelling*, Volume 32, Issue 4, pp 575-587, ISSN 0307-904X.
- SHITU L., ET. AL. 2013. Calibration strategy and generality test of three-axis magnetometers. *Measurement*, Volume 46, Issue 10, pp 3918-3923, ISSN 0263-2241.
- VČELÁK, J., ET. AL. 2005. AMR navigation systems and methods of their calibration. *Sensors and Actuators A: Physical*, Volumes 123–124, 2005, pp 122-128, ISSN 0924-4247.
- ZHIWEI, CH., ET. AL. 2016. Error-separation method for the calibration of magnetic compass. *Sensors and Actuators A: Physical*, Volume 250, pp 195-201, ISSN 0924-4247.

Corresponding author:

Marián Kišev, tel.: +421 37 641 4723, e-mail: xkisevm@is.uniag.sk

COMMUNICATION BETWEEN A PLC AND A RASPBERRY PI VIA OPENPOWERLINK

KOMUNIKÁCIA MEDZI PLC A RASPBERRY PI PROSTREDNÍCTVOM OPENPOWERLINK

Patrik Kósa, Marián Kišev, Juraj Baláži, Lukáš Vacho, Martin Olejár

*Department of Electrical Engineering, Automation and Informatics, Faculty of Engineering,
Slovak University of Agriculture Nitra, Tr. A. Hlinku 2, 949 76, Nitra, Slovak Republic, dtf@uniag.sk*

ABSTRACT: Nowadays, communication between industrial PLCs and programmable platforms is increasingly required in practise. Usage of a programmable platform like Raspberry PI offers in addition to simple programming features also low price while the processing power is preserved. One of the areas, where the advantages of the communication between a PLC and a Raspberry PI can be used is data processing of industrial cameras and other sensors in the industry. The most common methods of measuring and sensing of quantities are focused on usage of a communication protocol which is compatible with the used control system. Since these methods are in the most cases expensive, we have decided to modify an existing technology based on a Raspberry PI single-board PC. The objects of this research are Hall-effect current sensors and an industrial camera from Keyence, which are incompatible with the control system B&R X20CP1584 without usage of additional modules. The solution for incompatibility is adaptation of the openPOWERLINK communication protocol, which is supported by the Raspberry Pi and its connection to the PLC, which supports POWERLINK protocol. This solution provides an easily programmable and a cheap method how to reduce designing costs of any industrial solution effectively.

Key words: OPENPOWERLINK, PLC, Raspberry PI, industrial camera

ABSTRAKT: V súčasnosti je v praxi čoraz častejšie požadovaná komunikácia medzi komerčnými programovateľnými platformami a priemyselnými PLC. Použitie programovateľnej platformy akou je aj Raspberry PI ponúka okrem jednoduchého programovania aj možnosť zníženia nákladov pri zachovaní výpočtového výkonu daného systému. Jednou z oblastí, kde je možné aplikovať výhody komunikácie medzi PLC a Raspberry PI je spracovanie údajov z priemyselných kamier a rôznych iných snímačov v priemysle. Najpoužívanejšie spôsoby merania a snímania veličín sú zamerané na použitie komunikačného rozhrania kompatibilného s použitým riadiacim systémom. Keďže tie-to spôsoby merania a snímania veličín sú často nákladné, preto sme sa na základe tohto rozhodli upraviť existujúcu technológiu založenú na platforme Raspberry PI. Objektmi skúmania sú Hallove snímače prúdu a priemyselná kamera od firmy Keyence, ktoré sú bez použitia rozširujúcich modulov nekompatibilné s riadiacim systémom B&R X20CP1584. Riešením na nekompatibilitu bola adaptácia komunikačného protokolu openPOWERLINK podporovaného platformou Raspberry Pi na komunikáciu s PLC, ktorý podporuje komunikačný protokol POWERLINK. Vďaka tomuto riešeniu sme vytvorili jednoducho programovateľný a cenovo nenáročný spôsob ako efektívne znížiť náklady pri návrhu určitého technologického riešenia.

Kľúčové slová: OPENPOWERLINK, PLC, Raspberry PI, priemyselná kamera

INTRODUCTION

Minimalization and rising of effectiveness of control systems and their peripheries is nowadays a commonly resolved problem, which creates space for usage of unconventional methods. One of the areas where unconventional methods can be applied is usage of affordable hardware components, which are incompatible with the used control system. Innovative solutions allow designing affordable devices with similar parameters to the professional devices. These devices can replace expensive extending modules, which are used for data processing of used hardware components. Usually, the limiting factor in usage of affordable components is the fact that they do not support communication via standardised industrial communication protocols. In this research we have concentrated to develop a system based on a Raspberry Pi 2 platform, which will process and send data via POWERLINK communication protocol. The backbone of the system is an existing openPOWERLINK communication protocol package that was developed for communication between two or more Raspberry Pi's without the possibility to communicate with a PLC. Modification of this package allows creating a device that is able to communicate via POWERLINK communication protocol, which can be adapted to any specific requirements.

MATERIAL AND METHODS

The goal of this work is adaptation of openPOWERLINK communication protocol for communication and data transfer of an industrial camera and of Hall-effect current sensors to a B&R X20CP1584 PLC, which supports POWERLINK communication protocol. While designing, we had to know the characteristics of the POWERLINK communication protocol from which the openPOWERLINK software package was modified. We had to modify it to make it able to establish communication between Raspberry Pi and PLC. After its adaptation, a measuring device was developed, which will process data from the used sensors and from the industrial camera. To process data from the Raspberry pi 2, we had to set up the parameters of the communication protocol and create a control program on the PLC.

Ethernet POWERLINK

Ethernet POWERLINK is a deterministic and a real-time variant of the Ethernet communication protocol, which is based on the IEE802.3 standard with its full compatibility (Zurawski, 2014). The principle of the communication is based on sending requests for deterministic data transfer (Kubacki, 2016; Mozdik *et al.*, 2015). This way of communication guarantees a transfer of critically time dependent data in very short cycles with configurable timing. The structure of the data processing is divided into two parts:

- 1. Isochronous part** – in this part, the transfer of time dependent data, which requires time synchronisation, is located. The data transfer is addicted to the sent communication requests.
- 2. Asynchronous part** – in this part, the less time dependent data and packets (parametric data or link overload) are transferred.

The data layer of the network consists of one master device “Managing node” (MN) and of maximally 240 slave devices “Controlled nodes” (CN). The MN device is defining the synchronisation pulses for all devices in the network and it processes data from the communication cycle (Lindner, 2018). The communication of the CN with the MN is possible only after the CN has received a communication request from the MN (Thomesse, 2005). The principle of the data transmission is shown in Figure 1.

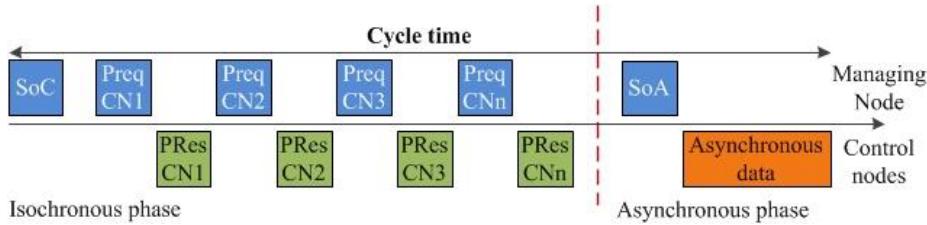


Fig. 1. POWERLINK data transmission
Obr. 1. Prenosový cyklus protokolu POWERLINK

The data transmission of the POWERLINK communication protocol consists of three periods:

1. The data transmission cycle begins with “Start period”, when the MN sends a SoC (Start of Cycle Frame) message to all CN devices for synchronisation of the communication.
2. Communication between the MN and the CN begins in the second period called “Isochronous phase”, when the MN sends a PollRequest (PReq) message to establish the data transfer between the CN and the MN. The CN sends their data via PollResponse (PRes) message.
3. The third period indicates the start of the asynchronous phase by sending a SoA (Start of Asynchronous) message from the MN. In this phase, the less critical packets or data are transferred (Kubacki, 2016).

The application layer of the POWERLINK protocol is based on the application layer and on the services of the CANopen communication protocol (Luvisotto, 2017). Its main feature is that every device has its own interface, which is expressed to the other devices through files called object dictionaries (OD). The participants of the communication can communicate with each other via access to the OD of every device in these ways:

1. **Synchronously:** via Process Data Objects (PDOs).
2. **Asynchronously:** via Service Data Objects (SDOs).

The Object dictionary is a structured list of objects in CANopen style. This list defines the main interface between devices and it also allows exposing data, parameters and services to other devices in the network. The objects of the OD can be accessible through SDO or PDO services. The description of the OD plays a very important role in XML Device Description (XDD) file, which contains the description of the used objects and subobjects in the POWERLINK communication protocol. All of them are defined with specific pro-

perties like index, name, predefined and actual value. These properties are declared in the definition of the object dictionary for all POWERLINK devices (nodes) and they have to be signed in the XDD file of the specific node identically (Knezic et al., 2017).

Raspberry Pi 2, model B

Raspberry Pi 2 is a single-board platform, which is with its architecture a device between embedded systems (e. g. Arduino) and desktop PC's. This platform is based on a 4-core 900 MHz Broadcom BCM2836 processor with 32-bit ARMv7 Cortex-A7 cores. Its RAM memory size is 1 GB and it also contains 4 USB ports, 10/100 BaseT Ethernet port, HDMI port, microSD card slot and many other peripheries (Girling, 2016).

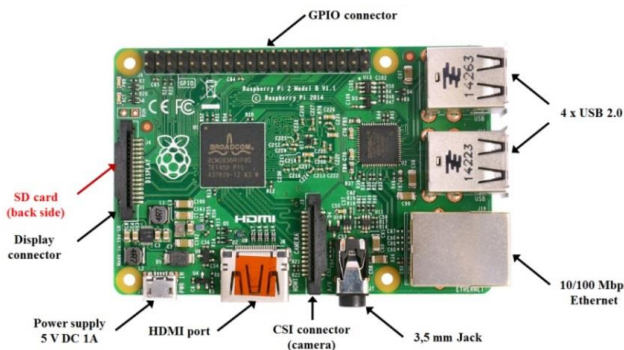


Fig. 2. Raspberry Pi 2 model B

Obr. 2. Raspberry Pi 2 model B

GPIO (General Purpose Input Output) connector is a periphery where the pins for digital inputs and UART, I2C and SPI communication buses are located. These pins can be used to process data from sensors (Girling, 2016). The GPIO connector pinout is shown in Figure 3.



Fig. 3. GPIO connector pinout

Obr. 3. Rozloženie vývodov na konektore GPIO

Hall-effect current sensor

The Hall-effect current sensor is a sensor, which functionality is based on the Hall-effect. Hall-effect is an effect when a potential difference is produced on the electrodes of a semiconductor when a magnetic flux is applied in a direction perpendicular to that of the flow of current. The voltage generated on the semiconductor is also called as Hall voltage. The value of this voltage is only a few mV, therefore it has to be amplified via operational amplifiers (Cviklovič, 2017).

The principle of the current sensor is based on a wire through which is the measured current flowing. The flowing current produces a magnetic field that is transferred to the semiconductor through a magnetic toroidal core. The core is made with a gap in which the Hall cell (semiconductor) that is measuring the magnetic flux is placed. This cell has to be supplied with a control current I_C , which allows the magnetic flux to produce voltage on the electrodes of the semiconductor. The principle of the Hall-effect current sensor is shown in Figure 4.

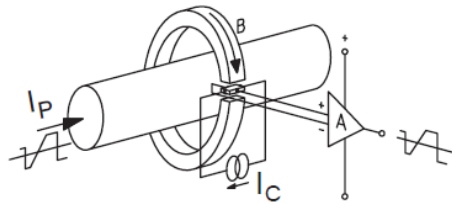


Fig. 4. Principle of the Hall-effect current sensor
Obr. 4. Princíp Hallovho snímača prúdu

The Hall-effect current sensor allows to measure direct and alternating current and it provides galvanic isolation of the measured object. The main pros of this sensor are: low price, small dimensions, low consumption and ability to measure currents up to 10 kA. Its cons are: temperature dependent amplifying drift, limits for current frequency and middle set up time (Cviklovič, 2017).

RESULTS

The design of the measuring device was based on the design of a measuring chain for data transmission from Hall-effect current sensors and the Keyence IV-500MA industrial camera. The block diagram of the designed measuring chain is shown in Figure 5.

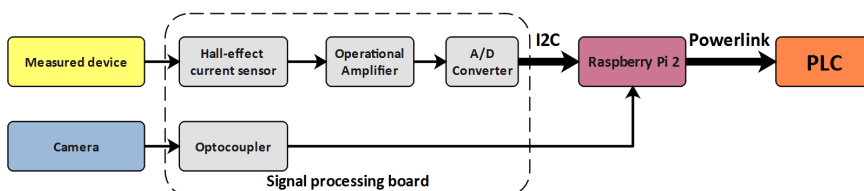


Fig. 5. Block diagram of the measuring chain
Obr. 5. Bloková schéma meracieho reťazca

The basic element of the measuring chain is the signal processing board that serves to process the signal from Hall-effect current sensors and the industrial camera. The used current sensors are ACS712 sensors in 5 A and 20 A versions. These sensors have a sensitivity of 185 mV/A (5A version) and 100 mV/A (20A version). The voltage at the output is at zero current $0.5 \times V_{cc}$, while the V_{cc} is supply voltage of 5 V. The given voltage offset appears to be undesirable for measurement purposes, so it needs to be shifted to 0V by operational amplifiers. The adjusted voltage from operational amplifier cannot be processed directly with the Raspberry Pi 2, because it does not contain an AD converter. For this reason, it was necessary to use an external AD converter that modulates the analogue signal from the operational amplifier to a digital signal that is easy to process. We chose an ADS1115 circuit from Texas Instruments as an AD converter. The ADS 1115 is a 4-channel 16-bit AD converter that communicates via I2C bus. This converter allows to process voltage signals in range of 0–4,096 V at a supply voltage of 5 V. Therefore, it is necessary to set the output voltage range to the same value after processing the signal from the Hall-effect sensors via the operational amplifiers. A comparison of the original and adjusted measuring ranges and sensitivities is shown in Table 1.

Table 1. Original and changed ranges and sensitivities
Tabuľka 1. Pôvodné a upravené rozsahy a citlivosti

ACS712	Original range ¹⁾ [V]	Original sensitivity ²⁾ [mV/A]	Adjusted range ³⁾ [V]	Adjusted sensitivity ⁴⁾ [mV/A]
5A	2.5-3.425	185	0-4.096V	819.2
20A	2.5-4.5	100		204.8

¹⁾Pôvodný rozsah, ²⁾Pôvodná citlivosť, ³⁾Upravený rozsah, ⁴⁾Upravená citlivosť

The adjustment of the measuring range was performed by a LM324 operational amplifier, which was used as an inverting amplifier in two serially connected blocks. The voltage offset shifting at zero current was achieved by an additional input branch in the summing amplifier circuit. The amplifier is shown in Figure 6.

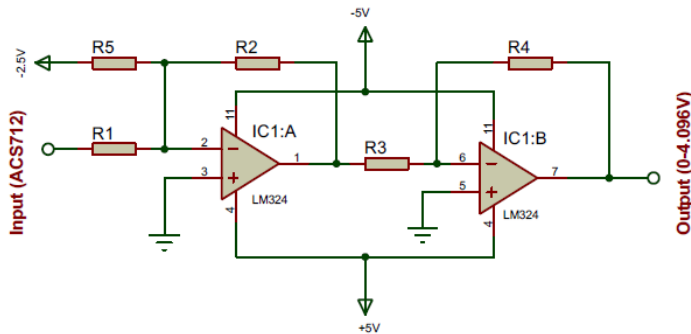


Fig. 6. Schematic of the operational amplifier
Obr. 6. Schéma zapojenia operačného zosilňovača

Figure 6 shows that to achieve the correct voltage range, it is necessary to provide a power supply of ± 5 V and a voltage of -2,5 V to the input of the summing amplifier. Sin-

ce the proposed device is intended for industrial applications where a +24 V DC voltage source is used, it is necessary to provide the needed voltage levels via step down (buck) converter. The used +24 V to +5 V step down converter is an available module based on LM2596 circuit, which works with 4 – 35 V input voltage, 1,23 – 30 V output voltage and provides maximally 3 A output current. To provide a -5V voltage level, it was necessary to use a LM2662 voltage inverter from Texas Instruments, which allows inverting voltage in 1,5 – 5 V range with maximal output current of 200 mA. The -2,5V voltage was provided by a voltage divider consisting of two resistors with a resistance of 1 kΩ. In addition to data from Hall-effect sensors, it was also necessary to process data from an industrial camera that was transmitted through four digital outputs (0 – 24 V). The voltage levels of these outputs had to be converted to a 3,3 V logic supported by the Raspberry Pi 2. The conversion of voltage levels was performed by PC817 optocouplers, which switched 3,3 V for specific GPIO pins.

The next step in the design was to set up the interface for the POWERLINK communication protocol. In the first phase, it was necessary to install the openPOWERLINK V2.1.1 open-source software package developed by Kalycito®. This package contains all the default objects specified by the POWERLINK communication protocol. Because the package does not contain objects to transfer 16-bit data, it has to be modified to be able to transmit the measured data from the AD converters. The modification was based on modifying the XDD file of the package. It was necessary to add objects into the XDD file that would be processed by the MN.

The objects can be added to the Manufacturer Specific Profile Area, where can be added specific objects depending on the current design requirements. This space allows defining objects with addresses from 0x2000 to 0x5FFF. To transfer the data from the camera, we did not need to add new objects, because we could use predefined UNSIGNED8 data type objects. The modification of the XDD file for the transmission of the 16-bit data is shown in Figure 7.

```
<!-- Manufacturer Specific Profile Area (0x2000 - 0x5FFF): may freely be used by the device manufacturer -->
<Object index="2000" name="ADConverterData" objectType="8" dataType="0005">
    <SubObject subIndex="00" name="NumberOfEntries" objectType="" dataType="0005" accessType="const" defaultValue="3" PDOmapping="no"/>
    <SubObject subIndex="01" name="ADC1" objectType="7" dataType="0003" accessType="rw" PDOmapping="TPDO"/>
    <SubObject subIndex="02" name="ADC2" objectType="7" dataType="0003" accessType="rw" PDOmapping="TPDO"/>
</Object>
```

Fig. 7. Modified XDD file
Obr. 7. Upravený XDD súbor

In the modified XDD file, an array type object (*objectType* = „8“) with a 0x2000 index named *ADConverterData* of the data type UNSIGNED8 (*dataType* = “0005”) was created. Under this subject, three subobjects, where the first created subobject with index 00 is called *NumberOfEntries*. This subobject defines the number of objects under the *ADConverterData* object array through *defaultValue* parameter. The subobject with index 01 is called as *ADC1* and it is responsible for the data transfer of the first AD conversion. The data type of this object was set up as INTEGER16 (*dataType*=”0003”) with the possibility to read and write (*accessType*=”rw”). It is also mapped for the PDO as a TPDO (object for data transfer for the PDO). Subobject with index 02 has same definition as object with index 01.

In addition to the XDD file for MN, it was also necessary to modify the Objdict.h file, which performs the same function as the XDD file, but this file, is used by the CN device. The way the Objdict.h file was modified is shown in Figure 8.

```
OBD_BEGIN_PART_MANUFACTURER ()
OBD_BEGIN_INDEX_RAM(0x2000, 0x04, FALSE)
    OBD_SUBINDEX_RAM_VAR(0x2000, 0x00, kObdTypeUInt8, kObdAccConst, tObdUnsigned8, NumberOfEntries, 0x04)
    OBD_SUBINDEX_RAM_USERDEF(0x2000, 0x01, kObdTypeUInt16, kObdAccVPR, tObdInteger16, ADC1, 0x00)
    OBD_SUBINDEX_RAM_USERDEF(0x2000, 0x02, kObdTypeUInt16, kObdAccVPR, tObdInteger16, ADC2, 0x00)
OBD_END_INDEX(0x2000)
```

Fig. 8. Modified Objdict.h file

Obr. 8. Upravený súbor Objdict.h

The modification of this file consists of adding a new main object *OBD_BEGIN_INDEX_RAM* with a 0x2000 index, which consists of three subobjects and its trigger is set up to *FALSE*. The trigger is always called only when a read or a write action was performed. Subobjects *OBD_BEGIN_INDEX_RAM_VAR* and *OBD_SUBINDEX_RAM_USERDEF* are connected with the subobjects *NumberOfEntries*, *ADC1* and *ADC2*, which definition is the same as in the XDD file, but it is necessary to keep the definition declared by the communication protocol.

After editing and loading the modified files into the openPOWERLINK package in the Raspberry Pi, it was possible to set the POWERLINK communication interface on the PLC to be able to receive data from the Raspberry Pi. The setup consisted of loading the XDD file and setting correct cycle time timings in μ s for the MN (Cycle time) and response time in μ s (Response timeout). The cycle time was set to 100,000 μ s and the response time was set to 15,000 μ s. After compiling and loading the configuration into the PLC, the configured devices are ready for future use. The photograph of the created measuring device is shown in Figure 9.

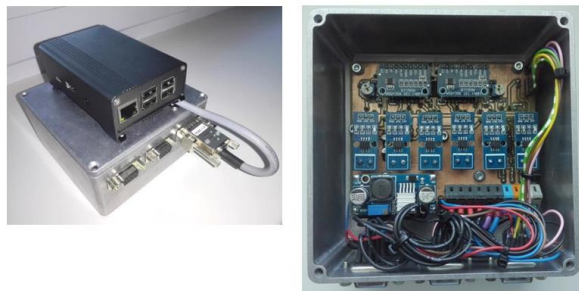


Fig. 9. Created openPOWERLINK measurement system

Obr. 9. Zhotovené openPOWERLINK meracie zariadenie

CONCLUSION

The aim of this project was to design an universal measuring system based on open-POWERLINK. The article describes one of the ways of how to design a measurement system based on modification of an existing open-source communication protocol to reduce

the costs of designing technological solutions. The designed device is currently located on a technological machine for processing plastics. This machine's current consumption is nowadays monitored by six Hall-effect current sensors and the production quality via the Keyence IV-500MA industrial camera. The analyzed method how to provide data transmission in an industrial environment with limited hardware configuration is a very effective solution, since it can be adapted to several applications where it is required to sense different physical quantities. At this time, the cycle time (transmitting speed) is limited by the Raspberry Pi's Ethernet interface to 100 ms. This timing limit can be decreased in the future by usage of another programmable platform with faster Ethernet interface.

LITERATURE

- CVIKLOVIČ, V. 2017. Aplikovaná elektronika a komunikačné štandardy. Nitra: Slovenská poľnohospodárska univerzita; 2017. ISBN 978-80-552-1647-8.
- GIRLING, G. 2016. Raspberry Pi 2 Manual: A practical guide to the revolutionary small computer. Haynes Publishing UK; 2016. ISBN 978-1-78-521073-0.
- Kalycito®, Introduction on how to get POWERLINK working on Raspberry PI 2. <https://www.kalycito.com/index.php/detailedhowto-run-openpowerlink-on-raspberry-pi2> [accessed February 2018].
- KNEZIC, M., ET AL. 2017. Theoretical and Experimental Evaluation of Ethernet Powerlink Poll-Response Chaining Mechanism. In *IEEE Transactions on Industrial Informatics*, vol. 13, no. 2, pp. 923-933; 2017. DOI: 10.1109/TII.2016.2634554.
- KUBACKI, A., ET AL. 2016. Controlling the Direction of Rotation of the Motor Using Brain Waves via Ethernet POWERLINK Protocol. In *Challenges in Automation, Robotics and Measurement Techniques: Proceedings of AUTOMATION-2016*, pp 81-88. Springer International Publishing; 2016. ISBN 978-3-31-929357-8.
- LINDNER, T., WYRWAŁ, D., KUBACKI, A. 2018. Autonomous stand for 3D printing and machine vision system. In *Advances in Intelligent Systems and Computing*, pp. 62-71; 2018. DOI: 10.1007/978-3-319-77179-3_6.
- LUVISOTTO, M., ET AL. 2017. Real-time wireless extensions of industrial ethernet networks. In *Proceedings - 2017 IEEE 15th International Conference on Industrial Informatics*, pp. 363-368; 2017. DOI: 10.1109/INDIN.2017.8104799.
- MOZDÍK, R., KOLEDÁ, P., VANČO, M. 2015. Analysis of wireless control of mechatronic CNC system by measuring feedback intensity and control signals. In *CER Comparative European Research 2015: proceedings / research track*. Issue 2 (2015), pp. 138-141. ISBN 978-0-9928772-8-6
- THOMESSE, J. P. 2005. Fieldbus Technology in Industrial Automation. In *Proceedings of the IEEE*, vol. 93, no. 6, pp. 1073-1101; 2005. DOI: 10.1109/JPROC.2005.849724.
- ZURAWSKI, R. 2014. Industrial Communication Technology Handbook, Second Edition, Taylor & Francis; 2014. ISBN 978-1-48-220732-3.

Corresponding author:

Patrik Kósa, tel. +421 911 267 832, e-mail: xkosa@is.uniag.sk

ASSESSMENT OF ADHESIVE PROPERTIES OF SUMMER AND WINTER TYRES UNDER SPECIFIED CONDITIONS

POSÚDENIE ADHÉZNYCH VLASTNOSTÍ LETNÝCH A ZIMNÝCH PNEUMATÍK ZA STANOVENÝCH PODMIENOK

Peter Kuchar¹, Marek Halenár¹, Jozef Nosian¹, Juraj Tulík¹,
Michal Holubek², Adam Fürstenzeller³

¹Department of Transport and Handling, Faculty of Engineering, Slovak University of Agriculture in Nitra, Tr. A. Hlinku 2, 949 76, Nitra, Slovakia, xkuchar@is.uniag.sk

²Department for Quality and Dependability of Machines, Faculty of Engineering, Czech University of Life Sciences, Kamýcka 129, 16500 Prague 6 – Suchdol, Czech Republic, holubekm@tf.czu.cz

³Department of Machine Design, Faculty of Engineering, Slovak University of Agriculture in Nitra, Tr. A. Hlinku 2, 949 76, Nitra, Slovakia, xfürstenzell@is.uniag.sk

ABSTRACT: The paper deals with the behaviour of different type of tires on the asphalt road in summer conditions, when the temperature reaches more than 20 °C. Observed parameters such as braking deceleration, braking distance together with time and vehicle speed were measured by using the XL-Meter_{tm} Pro Gamma decelerometer. The measurements were performed on the vehicle Peugeot 301 1.2 Vti with a maximum output power of 53 kW at 5000 rpm and operating weight 1165kg. The tested tyres used on the vehicle were Kleber Krisalp HP2 winter tyres and the 185/65 R15 88T GoodYear GT3 summer tyres. As measured speeds were proposed speeds 40, 60 and 100 km h⁻¹. The results in the submitted paper show importance of choosing the right type of tyres at different seasons during a year, due to the fact that under the stated conditions summer tyres showed significantly better attributes than winter tyres.

Key words: tyres, vehicle, braking deceleration, braking distance

ABSTRAKT: Príspevok sa zaoberá správaním rôznych druhov pneumatík na asfaltovej vozovke v letných podmienkach, kedy teplota dosahuje viac ako 20 °C. Sledované parametre, ako je brzdné spomalenie, brzná dráha spolu s časom a rýchlosťou vozidla boli merané pomocou decelerometrického prístroja XL-Meter_{tm} Pro Gamma. Merania prebiehali na vozidle Peugeot 301 1.2 Vti s maximálnym výkonom 53 kW pri 5000 min⁻¹ a prevádzkovou hmotnosťou 1165kg. Testovanými pneumatikami použitými na vozidle boli zimné pneumatiky značky Kleber Krisalp HP2 a letné pneumatiky GoodYear GT3 s rozmermi 185/65 R15 88T. Za merané rýchlosťi boli navrhnuté rýchlosťi 40, 60 a 100 km.h⁻¹. V príspevku uvedené výsledky ukazujú dôležitosť voľby správneho druhu pneumatík v rôznych ročných obdobiach vzhľadom na fakt, že za daných podmienok vykazovali letné pneumatiky významne lepšie hodnoty ako zimné pneumatiky.

Kľúčové slová: pneumatika, vozidlo, brzdné spomalenie, brzdná dráha

INTRODUCTION

Tires are very important for cars, which ensures the transmission of drive and side forces on the road. To achieve the actual properties of the tire, the tire goes a long way. The first cars used wooden wheels with a steel rim. The maximum speed of 20 km.h^{-1} was unfortunate and due to the lack of elasticity of the wheels, did not offer any comfort during the ride. From the historical point of view, it was the breakthrough year 1888, when the first tire was patented and 8 years later it was used for a car. (Sloboda, 2008; Abrahám, 2014)

During the improvement of the tire properties, was made tread on tires and were used cords together with the synthetic caoutchouc. Historic tires have come close to today's tires after 1948 and 1950 when were developed a radial and tubeless design. (Sloboda, 2008; Abrahám, 2014)

The modern automotive and rubber industry is making great progress. Over the past few decades, it has undergone a major transformation not only in the production technology but also in the development of new materials and product designs. Today the customer can choose from a large number of quality products, which are divided into the basic 3 groups according to the period of use. It is summer, winter and all-season tires. I distinguish with many parameters, but mainly with a mixture of rubber and decay. Tested types of tires have certain advantages and disadvantages and there exist recommendation to use these tires depending on environmental and road temperature. (Abrahám, 2011; Janoško, 2014a)

Therefore, the contribution deals with the braking capabilities of selected summer and winter tires from different manufacturers under summer temperature conditions, thus temperatures about 15°C and points to the importance of choosing the correct tire type. (Janoško, 2014c; Chrastina, 2014)

MATERIAL AND METHODS

The braking properties of the tires were measured on the Peugeot 301. The Peugeot 301 belongs to the lower middle class. The car has begun to produce it in 2013 and is still produced today. The car is powered by a 1199 cm^3 petrol engine with the highest engine output of 53 kW at 5000 revs. The vehicle was almost new and has a total of 5642 km. The vehicle is equipped with ABS anti-blocking system and electronic ESP stabilization system.

Table 1. Technical parameters of Peugeot 301 vehicle
Tabuľka 1. Technické parametre automobilu Peugeot 301

Kind of vehicle	Personal vehicle
Factory brand, type	Peugeot 301
Engine power	$53 \text{ kW} / 5000 \text{ min}^{-1}$
Cylinder displacement	1199 cm^3
Transmission / Number of speed	Manual / 5 speed
Body type	Sedan
Color	Dark gray metallic
Manufacturer	PSA PEUGEOT Slovakia - Trnava
Operating weight	1165 kg

For testing were used winter and summer tires. As summer tires were used Goodyear GT3 185/65 R15 88T and as winter tires were used Kleber Krisalp HP2 with dimensions 185/65 R15 88T. The tables show the basic parameters of the given tires.

Table 2. Technical parameters of Kleber Krisalp HP2 tires
Tabuľka 2. Technické parametre pneumatík Kleber Krisalp HP2

Manufacturer	Kleber	
Type	Krisalp HP2	
Dimension	185/65 R15	
Load and speed index	88T	
Tire pressure	Tread depth	
Left front wheel	250 kPa	8 mm
Right front wheel	250 kPa	8 mm
Left rear wheel	260 kPa	8 mm
Right rear wheel	260 kPa	8 mm

Table 3. Technical parameters of GoodYear GT3 tires
Tabuľka 3. Technické parametre pneumatík GoodYear GT3

Manufacturer	GoodYear	
Type	GT3	
Dimension	185/65 R15	
Load and speed index	88T	
Tire pressure	Tread depth	
Left front wheel	260 kPa	8 mm
Right front wheel	260 kPa	8 mm
Left rear wheel	260 kPa	8 mm
Right rear wheel	260 kPa	8 mm

To measure acceleration, resp. deceleration was used digital measuring instrument XL-Meter™ Pro Alpha. XL-Meter™ Pro Alpha is the third-generation device of the ultra-sophisticated XL Meter™ Pro range. XL Meter™ PRO Alpha allows to make a more accurate measurement of the longitudinal and transverse acceleration of the car on the road. Fast installation and easy use is one of the other benefits of this device. (Szabó, 2013; Hujo, 2016)

During an evaluating of data, the device will create graphical measurement of the measurement using the software. The software is available with the device. XL Meter™ for Alpha and has more language options and Slovak languages also. The device is mounted on the windscreens, which can be longitudinally fixed to the place where it was most comfortable. However, the device in the transverse direction must be placed horizontally. The numbers in the display indicate the position of the device – two zeroes indicate a horizontal position. (Janoško, 2015; Tkáč, 2016)

Table 4. Technical parameters of XL MeterTM PRO Alpha
 Tabuľka 4. Technické údaje zariadenia XL MeterTM PRO Alpha

Number of measurements	3 - 8
Storage capacity of measurements [s]	3 x 80 s - 5 x 40
Frequency of data collection [Hz]	25 - 200
Range [$m.s^{-2}$]	$\pm 13,0 - \pm 20,0$
Resolution [m/s^2]	0,005
LCD	16 x 2 LED
Dimensions (H x W x D) [mm]	50 x 97 x 110 mm



Fig. 1. XL MeterTM Pro Alpha
 Obr. 1. XL MeterTM Pro Alpha

To measure the traveled distance was used Rollmeter. This device is used to measure ground distances on communications or on terrain. The meter works with a measuring range of 0.1 to 9999 m with the smallest possible unit of 1 dm. When reverse gear, the device automatically registers the wheel counterclockwise, and subtracts the value. (Švec, 2013; Janoško, 2014b)



Fig. 2. Rollmeter
 Obr. 2. Rollmeter

The measurement was carried out on a reinforced, asphalt road road in the vicinity of the city of Nitra with a mild wind, an ambient temperature of 22 °C and a road temperature of 24 °C. The instrument was placed on the windscreen of a car. Subsequently, was setted a test section on which the vehicle was driven.

Vehicle braking has taken place from a few speeds:

- 40 km.h⁻¹,
- 60 km.h⁻¹,
- 100 km.h⁻¹.

After the braking process, it was necessary to draw and measure the braking distance of the vehicle by rollmeter and write it together with XL-Meter data into the table.

The measurement procedure was applied to both the tire sets and therefore the summer and winter tires.

RESULTS

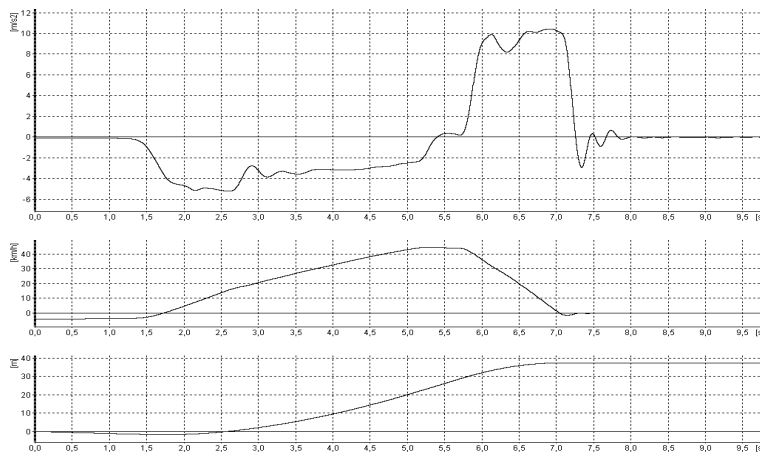
During the measurement, the braking performance of GoodYear GT3 tires and winter tires from Kleber Krisalpin HP2 was measured. The tires were new, almost unused with a depth of 8 mm. Measurements were made at vehicle speeds of 40, 60 and 100 km.h⁻¹.

On the basis of measured data, the braking distance and the data from the XL-Meter Pro Alpha, it was possible to review and compare the tire brake test under summer conditions at an ambient temperature at 22 °C and a road temperature at 24 °C. The results of the summer tire braking performance are recorded in Table 5 and shown in Figures 3–5.

Table 5. GoodYear GT3 summer tires measurement results

Tabuľka 5. Výsledky merania letných pneumatík GoodYear GT3

Vehicle type	Peugeot 301		
Tire type	Summer tires GoodYear GT3 185/65/R15 88T		
Measurement / Temperature	Summer / 22°C		
Prescribed initial speed [km.h ⁻¹]	40	60	100
Brake lane (road) [m]	9,6	17,8	31
Measured values from XL-Meter			
S ₀ [m]	9,7	17,7	44,2
V ₀ [km.h ⁻¹]	45,9	63,5	101,0
Tbr [s]	1,45	1,95	3,07
MFDD [m.s ⁻²]	9,2	9,3	9,8



$S_0: 9,74 \text{ [m]}$ $V_0: 45,69 \text{ [km/h]}$ $T_{br}: 1,45 \text{ [s]}$ $MFDD: 9,34 \text{ [m/s}^2\text{]}$

Fig. 3. Peugeot 301, $v_0 = 45,69 \text{ km.h}^{-1}$, temperature 22°C , GoodYear GT3
Obr. 3. Peugeot 301, $v_0 = 45,69 \text{ km.h}^{-1}$, teplota 22°C , GoodYear GT3



$S_0: 17,70 \text{ [m]}$ $V_0: 63,50 \text{ [km/h]}$ $T_{br}: 1,95 \text{ [s]}$ $MFDD: 9,55 \text{ [m/s}^2\text{]}$

Fig. 4. Peugeot 301, $v_0 = 63,50 \text{ km.h}^{-1}$, temperature 22°C , GoodYear GT3
Obr. 4. Peugeot 301, $v_0 = 63,50 \text{ km.h}^{-1}$, teplota 22°C , GoodYear GT3

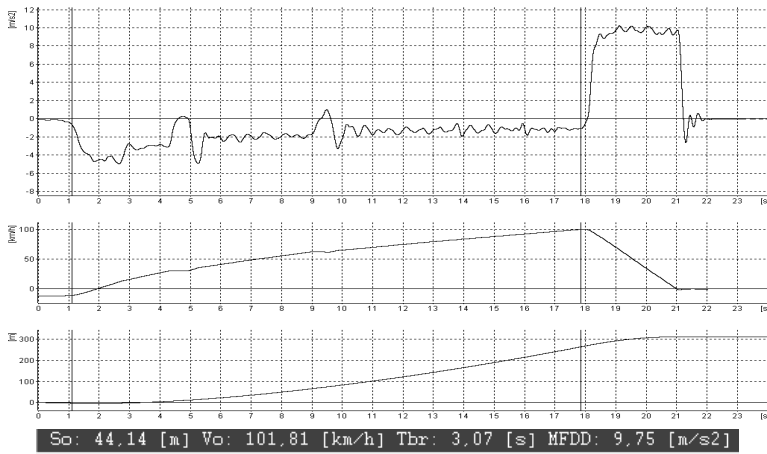


Fig. 5. Peugeot 301, $v_0 = 101.81 \text{ km.h}^{-1}$, temperature 22°C , GoodYear GT3

Obr. 5. Peugeot 301, $v_0 = 101.81 \text{ km.h}^{-1}$, teplota 22°C , GoodYear GT3

From the recorded values in Table 5, we can notice that the braking distance increases with increasing speed. Braking deceleration values (MFDD) increased from increasing speed. The measured values are very good and the GoodYear GT3 fulfills its purpose, transferring power to the pad.

After measuring the properties of a summer tire, followed a wheel change to winter Kleber Krisalp HP2 measuring 185/65 / R15 88T, and the control of inflation. Followed by further measurements, which were conducted under the same conditions, the same ambient temperature (22°C) and the ground temperature (24°C), which results are recorded and shown in Table 6 and Figures 6–8.

Table 6. Kleber Krisalp HP2 summer tires measurement results
Tabuľka 6. Výsledky merania zimných pneumatík Kleber Krisalp HP2

Vehicle type	Peugeot 301		
Tire type	Winter tires Kleber Krisalp HP2 185/65/R15 88T		
Measurement / Temperature	Summer / 22°C		
Prescribed initial speed [km.h^{-1}]	40	60	100
Brake lane (road) [m]	8,2	16,0	58,6
Measured values from XL-Meter			
$S_0 \text{ [m]}$	11,1	20,6	50,7
$V_0 \text{ [km.h}^{-1}\text{]}$	43,1	63,6	101,2
$T_{br} \text{ [s]}$	1,68	2,26	3,53
MFDD [m.s^{-2}]	8,0	8,2	8,2

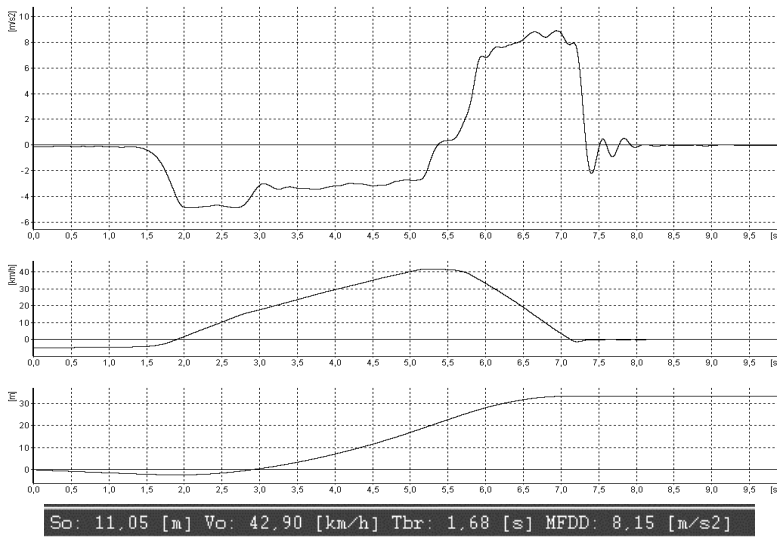


Fig. 6. Peugeot 301, $v_0 = 42,90 \text{ km.h}^{-1}$, temperature 22°C , Kleber Krisalp HP2
 Obr. 6. Peugeot 301, $v_0 = 42,90 \text{ km.h}^{-1}$, teplota 22°C , Kleber Krisalp HP2

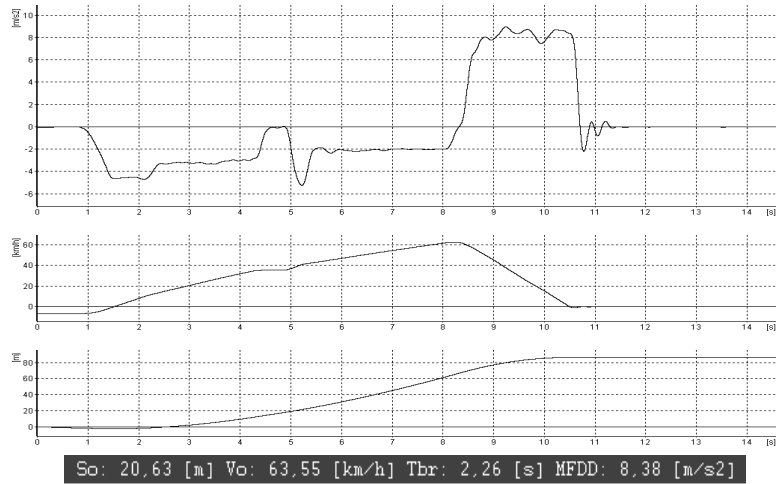


Fig. 7. Peugeot 301, $v_0 = 63,55 \text{ km.h}^{-1}$, temperature 22°C , Kleber Krisalp HP2
 Obr. 7. Peugeot 301, $v_0 = 63,55 \text{ km.h}^{-1}$, teplota 22°C , Kleber Krisalp HP2

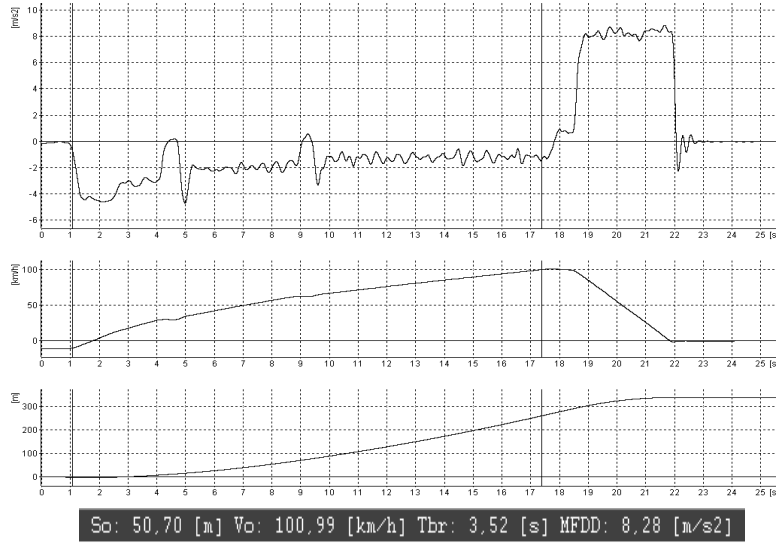


Fig. 8. Peugeot 301, $v_0 = 100,99 \text{ km.h}^{-1}$, temperature 22 °C, Kleber Krisalp HP2
 Obr. 8. Peugeot 301, $v_0 = 100,99 \text{ km.h}^{-1}$, teplota 22 °C, Kleber Krisalp HP2

Unlike summer tires, winter tires do not have sufficient braking effect on the road during summer. During comparing the summer tire braking distance of Table 5 and winter tires in Table 6, we see that winter tires have a braking distance of 100 km.h^{-1} by 1/3 longer and also winter tires have a lower deceleration than summer tires. The used mixture from which the winter tire was made was softer and thus more wear-free.

In the data from the table it is possible to see the difference between the measured braking distance using the roll meter and XL-Meter. Imprecision is attributed to the poor visibility of the vehicle brakes track from the overlapping with other braking traces and the fact that begin of braking tracks were poorly visible and identifiable due to the use of the vehicle with ABS system.

CONCLUSION

During the measurements, we focused on testing 15-inch summer and winter tires. The measurements were carried out on asphalt road near Nitra city at temperature 22 °C on selected 185/65/R15 88T tires. Summer tires were GoodYear GT3 and winter tires from Kleber Krisalp HP2. As measured velocities were determined speed 40,60 and 100 km.h^{-1} . The measurements were made on the Peugeot 301 1.2 Vti with a maximum output of 53 kW at 5000 rpm. Result of the work pointed out that the impact on driving safety have winter tires in the summer. It also pointed out that winter tires are not safe in the summer because of a low braking effect on the road above 15 °C, where the braking distance was evaluated from 100 km.h^{-1} to 1/3 longer braking distance. Irresponsibility of the driver at a late tire change, or the wear of the winter tires at the end of tire life may cause a threat to him and other road users.

LITERATURE

- ABRAHÁM, R., MAJDAN, R., ŠIMA, T., CHRASTINA, J., TULÍK, J. 2014. Increase in tractor drawbar pull using special wheels. *Agronomy Research* 12(1), pp 7–16. ISSN 1406-894X
- ABRAHÁM, R. HUJO, L. MAJDAN, R. JABLONICKÝ, J. 2011 Návrh na zlepšenie prenosu sily pneumatikou na pôdu. In: *Mobilné energetické prostriedky - Hydraulika - Životné prostredie - Ergonómia mobilných strojov*. Zvolen, 2011.
- CHRASTINA, J., JANOŠKO, I. Kangalov, P. 2014. Monitoring the operating parameters of municipal vehicles. Ruse : Angel Kanchev University of Ruse, ISBN 978-954-712-629-9, 108 p.
- HUJO, L., TKÁČ, Z., TULÍK, J., KOSIBA, J., UHRINOVÁ, D., JÁNOŠOVÁ, M. 2016. Monitoring of operation loading of three-point linkage during ploughing. In *Research in agricultural engineering* 62(1), pp 24–29. ISSN 1212-9151
- JANOŠKO, I., CHRASTINA, J. 2014a. Monitoring parameters of municipal vehicles. Nitra : Slovak University of Agriculture in Nitra, ISBN 978-80-552-1276-0, 113 p.
- JANOŠKO, I., LINDÁK, S., KUCHAR, Peter. 2015. Testing devices for optimization of parameters of small engines. In *Traktori i pogonske mašine*. ISSN 0354-9496, 2015, vol. 20, no. 1, s. 12–17.
- JANOŠKO, I., LINDÁK, S., KOSIBA, J. 2014b. Monitoring of the impact of operating personnel on the transportation efficiency in the intercity bus transport. *Naučni trudove* 53(1), pp 145–152. ISSN 1311-3321
- JANOŠKO, I., LINDÁK, S. POLONEC, T. 2014c. Technical-economic analysis of the logistics collection of waste in the city of Nitra. *Rural construction in European regions (II) – architecture, construction, technology, security and logistics*. SPU Nitra, Nitra, 2014c, pp. 139–146, ISBN 978-80-552-1242-5
- SLOBODA, A., FERENCEY V., HLAVŇA V., TKÁČ, Z. a kol. 2008. Konštrukcia kolesových a pásových vozidiel : teória, konštrukcia, riziká - 1. vyd. - Košice : Vienala, ISBN 978-80-89232-28-4, 547 p.
- SZABÓ M., MAJDAN R., TKÁČ Z., ČÁPORA R., HUJO L. 2013. Evaluation of fuel consumption in road freight transport. In *Acta technologica agriculturae* 16(1), pp 17–20. ISSN 1335-2555.
- ŠVEC, J. DUREC, J. CHRASTINA, J. TULÍK, J. 2013. Evaluation of inspected vehicles in reporting period at technical inspection and emission control station. In *Acta technologica agriculturae* 16(3), pp 57–60. ISSN 1335-2555.
- TKÁČ, Z., KOSIBA, J., JABLONICKÝ, J., ŠINSKÝ, V., SHCHUR, T. 2016. Tractor decelometric trials by application of the ecological hydraulic oil. In *Econtechmod* 5(3), pp. 171–176. ISSN 2084-5715.

Corresponding author:

Ing. Peter Kuchar, +421 37 641 4616, e-mail: xkuchar@is.uniag.sk

IMPORTANT CHANGES IN ISO 9001:2015 FROM ISO 9001:2008 AND THEIR IMPACT ON SUPPLIER COMPLAINTS MANAGEMENT

VÝZNAMNÉ ZMENY NORMY ISO 9001:2015 OPROTI ISO 9001:2008 A ICH DOPAD NA RIADENIE DODÁVATEĽSKÝCH REKLAMÁCIÍ

Adéla Melicharová

Department of Agriculture Machines, Faculty of Engineering, Czech University of Life Sciences Prague, Kamýcká 129, Praha 6, 16521, Prague, Czech Republic, e-mail: melicharovaa@tf.czu.cz

ABSTRACT: ISO 9001 is an international standard of the Quality Management System (QMS). ISO 9001 specifies the basic requirements for QMS. The latest version was published in September 2015 and is known as ISO 9001:2015. Organizations that are currently registered to ISO 9001:2008 must transition to the 2015 version until September 2018. ISO 9001:2015 brings some changes from the previous 2008 version. The paper attempts to provide knowledge on important changes and their impact on supplier complaints management in organization. One of the most important changes in ISO 9001:2015 versus ISO 9001:2008 is the increased focus on risk-based thinking which is also required to manage suppliers. The aim of this paper is to analyse the supplier claims in organization and to determine risk-based requirements for suppliers of the most problematic category of supplied products with regard to the ISO 9001:2015. For this purpose, organization XY was used as the case study. XY is located in the Czech Republic and is the molded plastic parts producer, including its decoration, assembling and final packaging process.

Key words: Quality Management System, ISO 9001:2015, risk-based thinking, complaint, supplier

ABSTRAKT: Medzinárodná norma ISO 9001 špecifikuje požiadavky na systém manažmentu kvality (QMS). Posledná verzia normy je ISO 9001:2015. Organizácie, ktoré sú v súčasnej dobe certifikované podľa normy ISO 9001:2008, museli prejsť na verziu 2015 do septembra 2018. Oproti predchádzajúcej verzii prináša ISO 9001:2015 významné zmeny. V článku je uvedený prehľad týchto zmien a ich dopad na riadenie dodávateľských reklamácií v organizácii. Jednou z hlavných zmien ISO 9001:2015 je zavedenie systematického prístupu k zvažovaniu rizík, ktorý je rovnako vyžadovaný pri riadení dodávateľov. Cieľom tohto článku je vyhodnotiť dodávateľské reklamácie v organizácii a určiť požiadavky na dodávateľov najproblematickejších kategórií dodávaných výrobkov s ohľadom na zvažovanie rizík. Za týmto účelom bola prevedená prípadová štúdia organizácie XY. Organizácia XY sídli v Českej republike a zaoberá sa výrobou lisovaných plastových dielov.

Kľúčové slová: systém manažmentu kvality, ISO 9001:2015, zvažovanie rizík, reklamácie, dodávateľ

INTRODUCTION

ISO 9001 is an International Standard of the Quality Management System (QMS). ISO 9001 specifies the basic requirements for a quality management system that an organization must fulfil to demonstrate its ability to consistently provide products and services that enhance customer satisfaction and meet applicable statutory and regulatory requirements (*ISO, 2015*). The first version of this standard was published in 1987. ISO 9001 underwent revisions in 1994, 2000 and again in 2008 (*Staněk, 2013*). The latest revision was published in September 2015 and is known as ISO 9001:2015 (*ISO, 2015*). This fifth edition cancels and replaces the fourth edition (ISO 9001:2008) (*EN ISO 9001:2015*). Organizations that are currently registered to ISO 9001:2008 must transition to the 2015 version until September 2018.

In 1993, when a system overview of certifications was for the first time introduced, 24 000 certificates were registered in 48 countries (*Staněk, 2013*). Now more than one million organizations from more than 160 countries have applied the ISO 9001 standard requirements to their quality management systems. A total of 1 106 356 valid certificates were reported for ISO 9001 (including 80 596 issued to the 2015 version) in 2016 (*ISO, 2017*).

ISO 9001 certification can have internal and external benefits. *Casadesús et al. (2000)* and *Boiral (2012)* reported the following benefits:

- Internal benefits: product and service quality improvement; decrease in incidents, rejections, and complaints; improved productivity and efficiency;
- External benefits: improved customer service (increased customer satisfaction and complaints reduction), fewer complaints with suppliers (improvement in supplier quality, less inspection) and marketing advantages.

The latest version ISO 9001:2015 brings some structural changes and changes in terms of content. It includes a revised clause sequence and the adaptation of the revised quality management principles and of new concepts (*ISO, 2015*). If ISO 9001:2008 emphasizes on continual improvement and customer satisfaction, ISO 9001:2015 puts more focus on risk-based thinking (*Sari et al., 2017*). The major changes are as follows:

- A high-level structure: the new structure is the most noticeable change to the standard. ISO 9001:2015 now follows the same overall structure as other ISO management system standards, making it easier for anyone using multiple management systems (*ISO, 2015*).
- The focus on risk-based thinking: it is a way of thinking that replaces preventive action and seeks to add some systematic evaluation of potential and actual issues with the aim of making processes more robust and capable (*Fonseca, 2015*). More information on how to adapt to this risk-based thinking can be found in *Ezrahovich et al. (2017)*.
- Increased involvement of the leadership team: leadership replaced the previous edition concept of management responsibility, requiring top management to engage and support the QMS (*Fonseca & Domingues, 2016*).
- A reinforced emphasis on the process approach and intended results with less emphasis on prescriptive requirements and on documentation (*Fonseca & Domingues, 2016*).
- The consideration of change management and knowledge management has been introduced (*Fonseca & Domingues, 2016*).
- Different terminology between ISO 9001:2008 and ISO 9001:2015 (*ISO, 2015*).

Table 1. The comparison of clauses between 2008 and 2015 versions of ISO 9001
 Tabuľka 1. Porovnanie kľauzulí medzi 2008 a 2015 ISO 9001

ISO 9001:2008	ISO 9001:2015
1. Scope	1. Scope
2. Normative References	2. Normative References
3. Terms and Definitions	3. Terms and Definitions
4. Quality Management System	4. Organizational context
5. Management Responsibility	5. Leadership
6. Resource Management	6. Planning
7. Product Realizations	7. Support
	8. Operation
8. Measurement, Analysis and Improvements	9. Performance Evaluation
	10. Improvement

More information about the comparison of the changes between the ISO 9001:2008 and ISO 9001:2015 is given in *Fonseca* (2015) and *Fonseca & Domingues* (2016). Table 1 shows the relationship between ISO 9001:2008 and those in the new ISO 9001: 2015. While the previous version has 8 clauses, the new version has 10 clauses.

Table 2 is a brief summary of a number of important changes to the terminology compared with ISO 9001:2008.

Table 2. Major differences in terminology between ISO 9001:2008 and ISO 9001:2015
 Tabuľka 2. Hlavné zmeny v terminológii medzi ISO 9001:2008 a ISO 9001:2015

ISO 9001:2008	ISO 9001:2015
Products	Products and services
Documentation, quality manual, documented procedures, records, instructions	Documented information
Work environment	Environment for the operation of processes
Monitoring and measuring equipment	Monitoring and measuring resources
Purchased product	Externally provided products and services
Supplier	External provider

One of the most significant changes in ISO 9001:2015 versus ISO 9001:2008 is the increased focus on risk-based thinking. It can contribute to eliminate complaints that are one of the biggest costs to be borne by the organization. Complaints with suppliers are very important because poor quality supplied products and services can have a huge negative impact on quality of the organization's production process and – even worse – on its customers.

ISO 9001:2015 requires the use of risk-based thinking to manage suppliers. The organization shall ensure that externally provided processes, products and services do not adversely affect the organization's ability to consistently deliver conforming products and services to its customers. The organization shall take into consideration the potential impact of the externally provided processes, products, and services on the organization's ability to consistently meet the customer and applicable statutory and regulatory requirements (*EN ISO 9001:2015*).

The aim of this paper is to: (i) analyse supplier claims in organization, (ii) identify the most problematic category of supplied products, and (iii) determine risk-based requirements for suppliers of this category with regard to the ISO 9001:2015.

MATERIAL AND METHODS

Organization XY was used as the case study in this paper. XY is located in the Czech Republic and is the molded plastic parts producer, including their decoration, assembling and final packaging process. XY is ISO 9001:2008 certified and will make the transition to the latest version of the standard in 2018.

The collected data were 2016 annual supplier claim report. This report presents data on XY's supplier claims in each category of the supplied products – cardboard, printed matter, plastic packaging, non-standard material, paints and granules. Claim frequency and claim costs were evaluated for each of these categories. Claim costs at XY are calculated according to (1). It is the sum of the material cost and manpower-hour costs including manual power hours and machine hours.

$$Cc = C_{Mat} + C_{MPH} \quad (1)$$

where Cc is claim cost [EUR],

C_{Mat} is material cost [EUR],

C_{MPH} is manpower-hour cost [EUR].

The collected data were analysed using the Pareto diagram to identify the most problematic supplied products in the XY claim process. The Pareto diagram is one of the seven basic quality tools and one of the most popular techniques for identifying the causes of quality problems. It is based on the Pareto principle, which states that 80% of the consequences stem from 20% of the causes. Formulated by the father of quality J. M. Juran and named after the famous Italian economist Vilfredo Pareto, this principle helps separate the „vital few“ from the „useful many“. This helps to focus on solving the right set of problems (*Nenadál et al., 2008*). Pareto diagram is having bar graphs and line graphs, where individual items are represented by a bar graph in order of decreasing frequency and the cumulative total is shown by a line graph (Lorenzo curve) (*Veber et al., 2007*).

RESULTS

A total of 82 claims were made with total claim cost of EUR 15 746 in 2016 at XY. Fig. 1 shows that cardboard and printed matter represent the most problematic categories of supplied products in terms of claim frequency. Conversely, claim frequency was minimal for plastic packaging, non-standard materials, paints and granules. Cardboard and printed matter are also the most problematic categories in terms of claim costs. Claim costs were low for paints and granules, and zero for plastic packaging and non-standard materials.

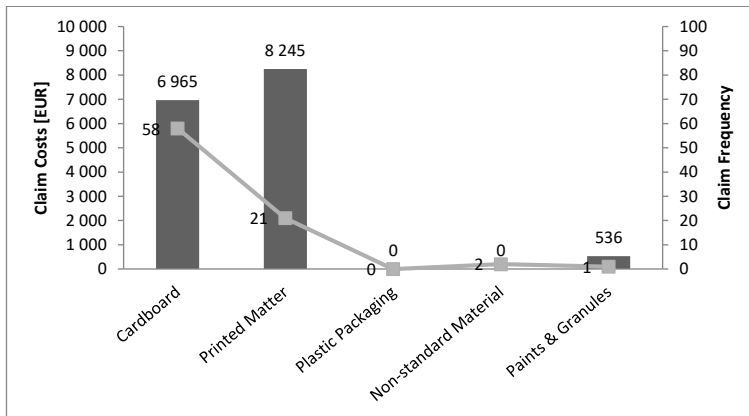


Fig. 1. Claim frequency and claim costs in each category of supplied products
Obr. 1 Frekvencia reklamácií a náklady na reklamácie v každej kategórii dodaných produktov

The same data are presented in Fig. 2 and Fig. 3. Pareto diagram of claim frequency can be found in Fig. 2. Pareto diagram of claim costs is given in Fig. 3. The criterion for identifying the „vital few“ was chosen at level 70%. Fig. 2 shows that the category of cardboard was identified as the „vital few“ in terms of claim frequency. This category accounts for 71% of the total claims.

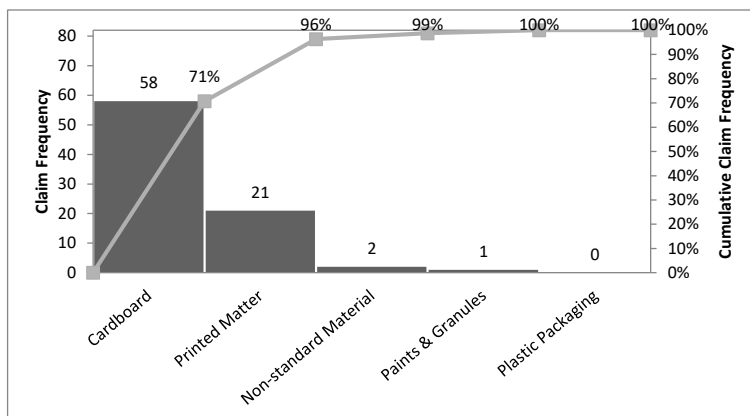


Fig. 2. Pareto diagram of claim frequency in each category of supplied products
Obr. 2. Pareto diagram frekvencie reklamácií v každej kategórii dodaných výrobkov

Pareto diagram of claim costs (Fig. 3) takes into account the economic aspect and constitutes another approach to identifying the „vital few“. Only one category of supplied products cannot be identified as the „vital few“ in terms of claim costs. 70% of claim costs are caused by category of printed matter (52% of total claim costs) and in part by category of cardboard (18% of total claim costs). These two categories account for 97% of the total claim costs.

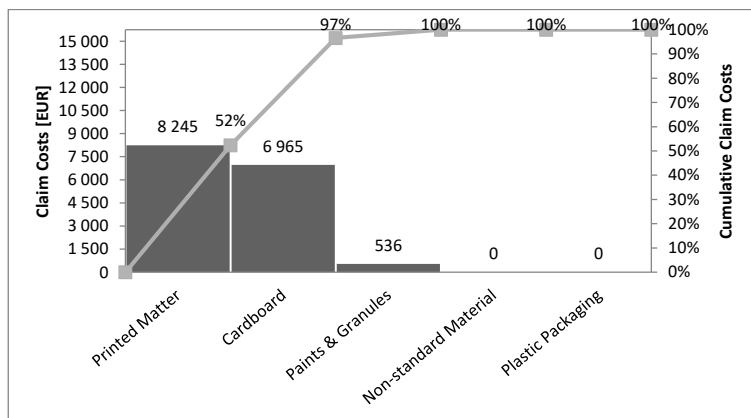


Fig. 3. Pareto diagram of claim costs in each category of supplied products
Obr. 3. Pareto diagram nákladov na poistné plnenia v každej kategórii dodaných výrobkov

It follows from the above that cardboard was identified as the most problematic category of the supplied products in terms of claim frequency. Printed matter and partly cardboard was identified as the most problematic category of the supplied products in terms of claim costs.

DISCUSSION

One of the most significant changes in ISO 9001:2015 versus ISO 9001:2008 is the increased focus on risk-based thinking. The new version ISO 9001:2015 also requires the use of risk-based thinking to manage suppliers. Since XY will make the transition to this version, it should increase the requirements for selected suppliers of the most problematic products – for suppliers of cardboard and printed matter. These suppliers cause XY the most frequent and costly claims. They are at the same time the highest risk of XY's production. For example, the following categories can be used:

- Strategic supplier – A supplier that provides a large number of products. There is currently no other supplier available to deliver the same kind of product.
- Supplier with poor rating – A supplier that has achieved a low level in regular Quality Supplier Evaluation.
- Supplier after big accident – A supplier that delivered nonconforming products and caused XY the necessity of recall and the impossibility of selling products (products blocked in distribution centres).

Table 3 shows example minimum requirements for selected supplier categories using a risk-based approach.

Table 3. Minimum risk-based supplier requirements
 Tabuľka 3. Minimálne požiadavky dodávateľov

Minimum requirements	Supplier Category		
	Strategic supplier	Supplier with poor rating	Supplier after big accident
QMS certification	ISO 9001	ISO 9001	ISO 9001
Receiving inspection	Permanent	Permanent	Temporary
Supplier audit	Once a year	Once a quarter	After the accident
FMEA	Before conclusion of the contract	Half-yearly	After the accident

XY should require these categories of suppliers to have their QMS based on the ISO 9001 standard to ensure that the supplied products consistently meet the quality requirements of XY, and that the quality of the products is consistently improved. At the same time, XY should introduce receiving inspection for these categories of suppliers, such as sampling based on performance. A permanent receiving inspection should be implemented by strategic suppliers and suppliers with poor rating. Suppliers after big accident would have implemented a temporary receiving inspection. Its duration would depend on the verification of the corrective action. Supplier audits should be conducted by the XY audit team at different time intervals or after big accident, depending on the supplier category. It is also very important that all three categories of suppliers use the FMEA for risk analysis. XY should require strategic suppliers to use the FMEA before conclusion of the contract. Suppliers with poor rating should use the FMEA half-yearly and the remaining supplier category after the accident. More information about the FMEA as a step-by-step approach for identifying all possible causes of failure is given in *Juran & Blanton Godfrey* (2000).

CONCLUSION

Organizations that are currently registered to ISO 9001:2008 must transition to the 2015 version until September 2018. One of the most significant changes to ISO 9001:2015 is the increased focus on risk-based thinking which is also required to manage suppliers. This paper showed how this requirement could be met and the example of implementation in the organization XY. Analysis of supplier claims and use of minimum risk-based requirements for selected supplier categories of the most problematic products can lead to a significant reduction in claims and claim costs. The method used in this paper is very well applicable in the QMS and supply relationship management.

LITERATURE

- BOIRAL, O. 2012. ISO 9000 and organizational effectiveness: A systematic review. *Quality Management Journal*, 19(3), pp. 16-37.
- CASADESÚS, M., HERAS, I., OCHOA, C. 2000. The benefits of the implementation of ISO 9000 normative: Empirical research in the Spanish companies. In: *Proceedings of International conference: Fifth world conference on production and operations management*. Sevilla, Spain.
- EN ISO 9001:2015. Quality management systems – Requirements.

- EZRAHOVICH, A.Y., VLADIMIRTSEV, A.V., LIVSHITZ, I.I., LONTSIKH, P.A., KARASEVA, V.A. 2017. Risk-based thinking of ISO 9001:2015 - The new methods, approaches and tools of risk management. In: *Proceedings of International conference: Quality Management, Transport and Information Security, Information Technologies*. October 26, St. Petersburg, Russian Federation, pp. 506-511.
- FONSECA, L. 2015. From Quality gurus and TQM to ISO 9001:2015: a review of several quality paths. *International Journal for Quality Research*, 9(1), pp. 167-180.
- FONSECA, L., DOMINGUES, J.P. 2016. ISO 9001:2015 edition- management, quality and value. *International Journal for Quality Research*, 11(1), pp. 149–158.
- ISO, 2015. *Moving from ISO 9001:2008 to ISO 9001:2015*. ISO, Geneva, Switzerland. ISBN 978-92-67-10646-5.
- ISO, 2017. *ISO Survey of certification systems to management system standards*. [online] [02.02.2018]. Available at: https://isotc.iso.org/livelink/livelink/fetch/-8853493/8853511/8853520/18808772/00._Executive_summary_2016_Survey.pdf?nodeid=19208898&vernum=-2
- JURAN, J.M., BLANTON GODFREY, A. 2000. *Juran's quality handbook*. Fifth edition. New York: McGraw-Hill. ISBN 0-07-034003-X.
- NENADÁL, J., NOSKIEVIČOVÁ, D., PETŘÍKOVÁ, R., PLURA, J., TOŠENOVSKÝ, J. 2008. Moderní management jakosti: principy, postupy, metody (*Modern quality management: principles, procedures, methods*). Praha: Management Press. ISBN 978-80-7261-186-7.
- SARI, Y., WIBISONO, E., WAHYUDI, R.D., LIO, Y. 2017. From ISO 9001:2008 to ISO 9001:2015: Significant changes and their impacts to aspiring organizations. In: *Proceedings of: International Conference on Informatics, Technology and Engineering*. August 24-25, Univ Surabaya, Indonesia.
- STANĚK, M. 2013. Mezinárodní norma ISO 9001: pohled do historie a budoucnosti (International Standard ISO 9001: a look into the past and the future). *Czech journal about quality: Perspektivy kvality*, 2(1), pp 46-48. ISSN 1805-6857.
- VEBER, J., HŮLOVÁ, M., KOŘÁNOVÁ, H., PLÁŠKOVÁ, A. 2007. Řízení jakosti a ochrana spotřebitele (*Quality management and consumer protection*). Praha: Grada Publishing. ISBN 978-80-247-1782-1.

Corresponding author:

Adéla Melicharová, e-mail: melicharovaa@tf.czu.cz

MONITORING OF THE HOUSEHOLDS' ENERGY CONSUMPTION AS INDICATOR OF LIFE QUALITY IN RURAL MICRO-REGIONS

MONITOROVANIE KVALITY ŽIVOTA MIKROREGIÓNOV VIDIEKA SO ZRETEĽOM NA SPOTREBU ENERGIE

Petra Procházková

Czech university of Life Sciences Prague, Department of vehicles and ground transport, Faculty of Engineering, Kamýcká 129, 165 00 Praha 6 – Suchdol, Czech Republic, prochazkovap@tf.czu.cz

ABSTRACT: The aim of paper is to introduce project that monitored households' energy consumption in selected rural micro-regions of the northern Bohemia. The public survey was carried out by a questionnaire method. The attention was payed to different energy sources to describe a fossil and alternative energy sources proportions. The obtained data characterise the quality of life in accordance with the selected criteria.

Key words: monitoring energy consumption; alternative source; “post-carbon” future;

ABSTRAKT: Cieľom príspevku je predstaviť projekt, ktorý sleduje spotrebu energie domácností vo vybraných vidieckych mikroregiónoch severných Čiech. Verejný prieskum bol vykonaný dotazníkovým výskumom. Pozornosť bola venovaná rôznym zdrojom energie k zmapovaniu pomery fosílnych a alternatívnych zdrojov energie. Získané údaje charakterizujú kvalitu života v súlade s vybranými kritériami.

Kľúčové slová: monitorovanie spotreby energie, alternatívne zdroje energie, „bezuhlíková“ budúcnosť

INTRODUCTION

To a certain degree, every human being affects his environment and the whole of humanity with their existence and activities, and in this manner, they also affect the Earth's climate system. The durability of this system is currently under threat but humanity can extend or shorten it with their possible actions. One of the possibilities is to slow down the speed of consumption of fossil energy resources and to replace them with other, non-fossil or low-carbon resources. The transfer to a “post-carbon” future is represented by innovation in energy supply from renewable (alternative) sources, for example, to communities within the country. A growing number of such communities is interested in to get to know

their complete energy demand. It is necessary to solve transfer's technical possibilities to the use of alternative energy resources in a complex manner but it must not be forgotten all social and cultural changes that are connected with the future low-carbon society. The aim of this changes is to decrease consumption of fossil fuels and to reduce greenhouse gases production (Vávra, 2012) (Neuvonen *et al.*, 2014) (Phillips *et al.*, 2014) (Dou *et al.*, 2016) (Maier, 2016).

A fundamental condition to carry out transformation to a low-carbon society is a clear intervention "from above" in form of regulations and functioning incentives. A change in the system is necessary: "but it is not possible to rely only on individual changes of behaviour". When we look at the carbon footprint of households in the Czech Republic, we can make some interesting observations. The greatest share of the footprint falls on emissions from heating and food consumption. Since a connection between the expressed pro-environmental opinions of the respondents and their real behaviour is different, this points out the influence of the infrastructure and the system, that include, for example, heat sources, and also the problematic relation between attitudes and behaviour (Vávra, 2012) (Hulme, 2008) (Jones *et al.*, 2012) (Dreborg, 1996) (Quist, 2006).

A safe, secured, sustainable and affordable energy is a condition of a full-value and quality life of citizens, competitive industry and fully functional society. Already now, an energy infrastructure is being built here, which will become a source of energy for households, industry and services in 2050, the buildings that people are going to use are also designed and constructed. At the same time, a model of energy production and use for the year of 2050 is being set up. The EU has bound itself that until 2050 it will decrease emissions of the greenhouse gasses by 80–90% in comparison to the values from 1990 within the necessary decrease of emissions in the developed countries as a whole. The impacts of this reality have been analysed in the "Roadmap for moving to a competitive low carbon economy in 2050". "Roadmap to a Single European Transport Area" focused on solutions for the transport field and on creation of a singular European transport area. In this energy roadmap drawn for the period until 2050, such tasks are being researched, that are based on fulfilment of the EU decarbonisation goal along with simultaneous provision of energy supplies and preserved competitiveness (Evropský parlament, 2016) (Grunfmann *et al.*, 2015) (Svenfelt *et al.*, 2011) (Jenssen *et al.*, 2010) (Urban *et al.*, 1988).

The prognosis implies, that until 2050, the emissions will be lowered by 40%, however, that is not sufficient to achieve the goal of decarbonisation of the EU. Behind all this, we can imagine the amount of changes and effort, which are going to have to be put forth for the emissions to be lowered and for the competitiveness and security of energetics to be preserved (Jenssen *et al.*, 2014) (Höjer *et al.*, 2000) (Svenfelt *et al.*, 2001).

MATERIAL AND METHODS

The main cause for concerns about changes is the impact of anthropogenic activities on the climate, that is, the phenomena named global warming. The methods of research in use thus far are predominantly sociological and they are dedicated to the viewpoint of households and individuals from communities in the countryside i.e. micro-regions. In each of these micro-regions, it is necessary, using the methodology of qualitative and quantitative solutions, to establish and analyse the real and prospective energy consumption, but also opinions and attitudes of the inhabitants in connection to changes in energy

consumption and thereby in connection to the decrease of emission production as well (Curtis *et al.*, 2016) (Robinson, 2016) (Svenfelt *et al.*, 2001) (Urban *et al.*, 1988).

Questionnaires were focused on the inquiry of different energy source structure that enables to describe the ratio of fossil and alternative energy sources. The obtained data were used to assess the quality of life according to the chosen criteria and the impact on the climate system. Due to the significant positive influence of alternative energy sources on the life of citizens, the alternative source will be recommended to selected micro regions.

The survey was conducted using printed questionnaires whose structure of questions is shown in Table 1. The first part of the questionnaire was devoted to the characteristics of households, consumption monitoring, used energy resource etc. In the second part, questions were asked to the respondents linked with their global warming awareness and their attitudes, as addressed citizens, to the use of alternative energy sources.

Data collection from the respondents was carried out in cooperation with the trained staff of the local action group Labské skály. Questionnaire survey was carried out in municipalities: Libouchec, Verneřice, Petrovice, Arnultovice, Velké Chvojno, Luční Chvojno, Žďár, Mnichov, Malečov and Březí. The 250 households with different structure and use of energy sources were addressed in total. Subsequently, the data were overwritten using MS Excel software.

Data processing expects to divide building according their age (operational life) i.e. into groups over 50 years, 30-49 years and building under 30 years. The data obtained should also provide information on the state of households, the means of transport used, the most frequent lengths of the respondents' journey and their objectives, the number of means of transport. In addition, information on the attitudes of the public to the transition to a low-carbon future, their awareness of the future and the current state of affairs should also be obtained.

RESULTS

Results of carried our survey (during July - August 2017) of monitored energy consumption in selected micro regions of the Northern Bohemia. The selected evaluation criteria are presented at the Fig. 1.

Structure of household
Household condition
Used of energy sources
Used renewable sources
Usage appliances
Usage of means of transport
Usage of public transport
Characteristics of respondents routs
Supplementary questions about global warming
Supplementary questions about renewable resource support

Fig. 1: Structure of questionnaire
Obr. 1: Struktura dotazníku

The most frequently represented objects in the studied region are more than 50 years old and in accordance with this fact is the state of their energetic character, see Figures 2 and 3.

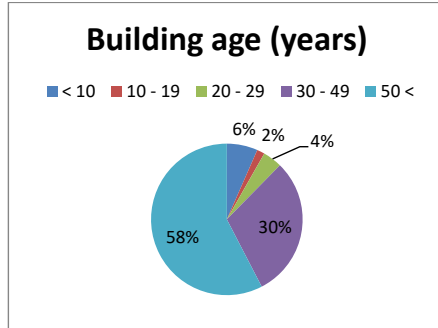


Fig. 2: Age of buildings
Obr. 2: Stáří objektů

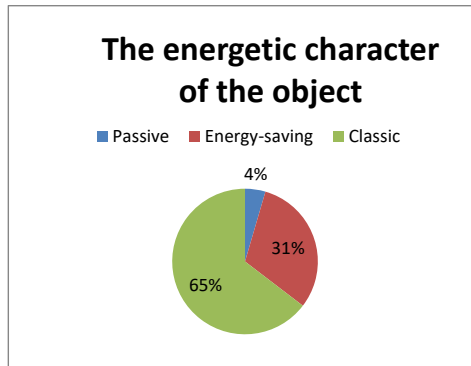


Fig. 3: The energetic character of the object
Obr. 3: Energický charakter objektu

According to the results of the survey, it was estimated that the state of the objects is standard in terms of energy savings and there are only 4% of passive buildings.

Furthermore, the energy consumption of individual commodities used for house heating and water heating was monitored. The questionnaire survey found out in what proportion the limit is represented Energy resources for water heating and heating in households: Gas, Coal, Coke, Wood, Pellets, Biomass and Electrical energy. The individual representation of the sources is shown in Figure 4.

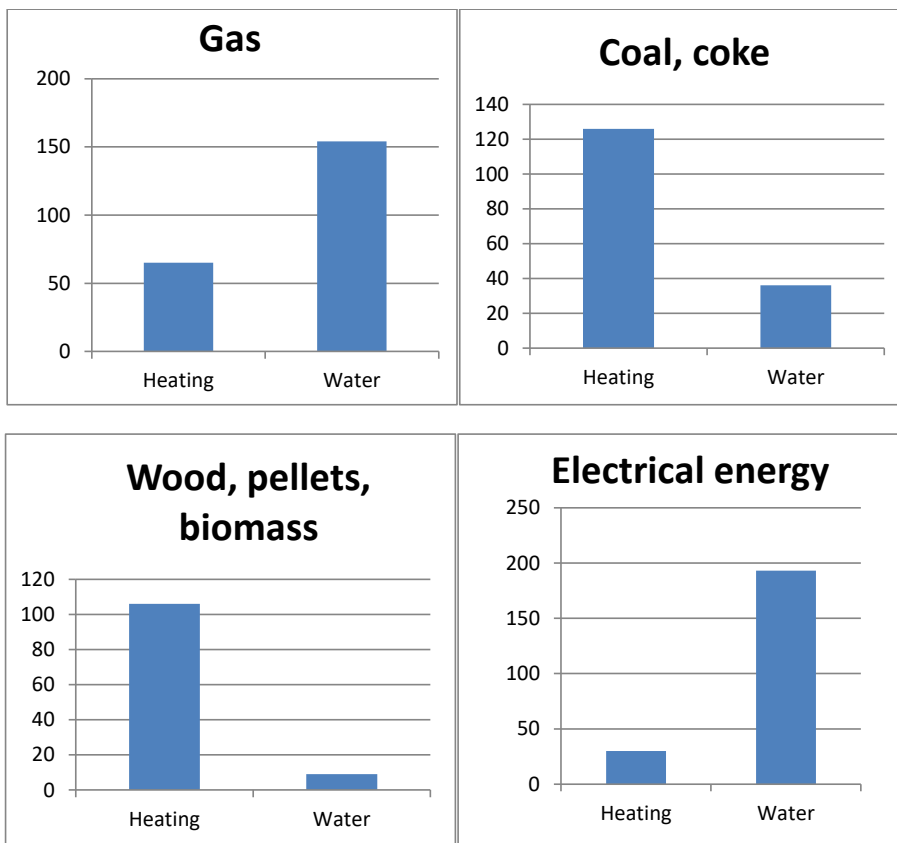
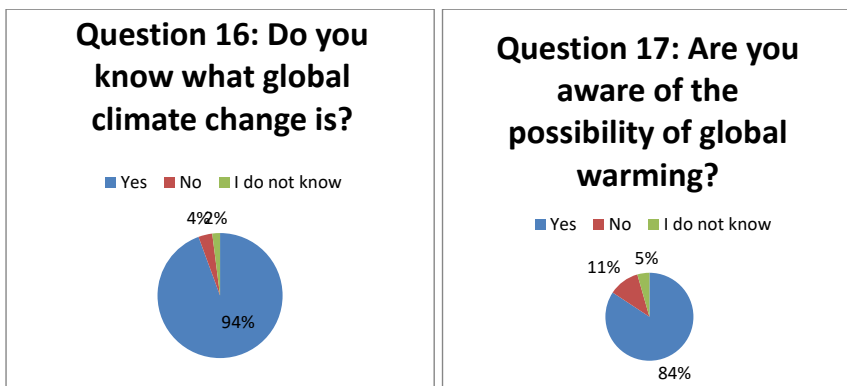


Fig. 4: Number of households use of energy resources for water heating and heating
Obr. 4: Počet domácností dle energetických zdrojů pro ohřev vody a vytápění domácností

In the third part of the questionnaire the respondents were asked about global warming and also about their attitudes towards alternative sources. The results are shown in Figure 5.



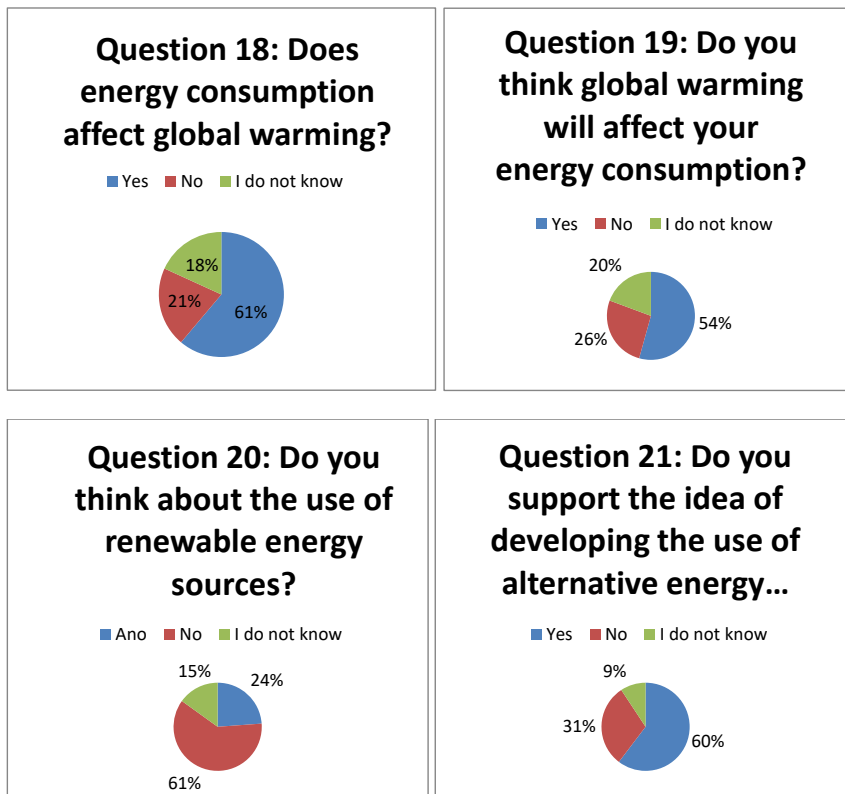


Fig. 5: Opinion poll
Obr. 5: Průzkum veřejného mínění

Individual household members are surveyed to report on the impact of the use of fossil resources on the environment and on their own consumption. Most respondents are in favor of the use of alternative sources, especially in the financing of municipalities.

The results show that in the surveyed regions it is 58% for buildings over 50 years old. Buildings aged 30-49 have 30% representation. According to these results, there are also energy states of the buildings where the passive house is represented by only 4%. Hot water is most often heated by gas and electricity. For heating, most respondents use carbonaceous fuels and gas. Regarding the use of renewable resources, their share is very small besides wood and pellets. On the other hand, respondents do not prevent their use and support them, which is a good ground for municipal intervention and central implementation. The results in individual graphs can be affected by ignorance of the possibilities of using alternative energy sources as well as by the own consumption of the population. Another limiting factor is certainly the possibility of financial investment in the purchase of new sources or the possible reduction of the energy intensity of the building by thermal insulation etc. However, the overall state of the municipalities can be solved centrally and thus help to reduce the production of carbon emissions.

DISCUSSION

On one hand the results of the questionnaire survey show the buildings in individual micro-regions need to reduce the energy demands. Although the respondents stated the use of gas as the most common source of house heating and water heating, solid fuel additional heating is a frequent alternative.

On the other hand public is informed about the impacts of global warning and the importance and they are not against the use of alternative sources of energy within the municipal development.

CONCLUSION

The obtained data prove the quality of life in accordance with the selected criteria. It is possible to assess their influence the on the climate system. The results can show the complete view of energy consumption in the selected micro-regions of the Northern Bohemia and its substitution effects by alternative sources. These survey results can create the basis of planning and designing of an alternative energy resources for a specific area. Research results can enable and it is possible to predict the energy consumption in future.

ACKNOWLEDGMENT

Contribution has been prepared within the solving of scientific grant project IGA 2017: 31150/1312/3122 "Monitoring of the life quality of the rural micro-regions with regard to energy consumption."

LITERATURE

- CURTIS, C., RENNE, J. 2016. Transit Oriented Development: Making It Happen.
- DOU, Y., LUO, X., DONG, L., WU, CT., LIANG, HW., REN, JZ. 2016. An Empirical Study on Transit-oriented Low-carbon Urban Land Use Planning: Exploratory Spatial Data Analysis (ESDA) on Shanghai, China. *Habitat International*. 2016, vol. 53 s. 379–389. ISSN:0197-3975.
- DREBORG, K., H. 1996. Essence of Backcasting. *Futures*. 1996, vol. 28, no. 9 s. 813–828. ISSN:0016-3287
- Evropský parlament. Communication From The Commission To The European Parliament, The Council, The European Economic And Social Commi Ttee And The Committee Of The Regions: A Roadmap for moving to a competitive low carbon economy in 2050. www.europarl.europa.eu [online]. ©2011 [cit. 2016-11-30]. Available from: http://www.europarl.europa.eu/meetdocs/2009_2014/documents/com/com_com %28 011%290112/_com_com%282011%290112_en.pdf
- GRUNFMANN, P., EHLERS, M. 2015. Determinants of Courses of Action in Bioenergy Villages Responding to Changes in Renewable Heat Utilization Policy. *Utilities Policy*. 2015, vol. 41 s. 183–192. ISSN:0957-1787.
- HÖJER, M., MATTSSON, L. 2000. Determinism and Backcasting in Future Studies. *Futures*. 2000, vol. 32, no. 7 s. 613-634. ISSN:0016-3287
- HULME, M. 2008. Geographical Work at the Boundaries of Climate Change. *Transactions of the Institute of British Geographers*. 2008, vol. 33, no. 1 s. 5-11.ISSN:0020-2754.

- JENSSSEN, T., KÖNIG, A., ELTROP, L. 2014. Bioenergy Villages in Germany: Bringing a Low Carbon Energy Supply for Rural Areas into Practice. *Renewable Energy*. 2014, vol. 61 s. 74–80. ISSN:0960-1481.
- JENSSSEN, T. 2010. The Good, the Bad, and the Ugly: Acceptance and Opposition as Keys to Bio-energy Technologies. *Journal of Urban Technology*. 2010, vol. 17, no. 2 s. 99-115. ISSN:1063-0732.
- JONES, R., ROBINSON, J., TURNER, J. 2012. Introduction.Between Absence and Presence: Geographies of Hiding, Invisibility and Silence. *Space and Polity*. 2012, vol. 16, no. 3 s. 257-263. ISSN:1356-2576.
- MAIER, S. 2016. Smart Energy Systems for Smart City Districts: Case Study Reininghaus District. *Energy, Sustainability and Society*. 2016, vol. 6, no. 1 s. 1–20. ISSN:2192-0567.
- NEUVONEN, A., KASKINEN, T., LEPPANEN, J., LAHTEENOJA, S., MOKKA, R., RITOLA, M. 2014. Low-carbon Futures and Sustainable Lifestyles: A Backcasting Scenario Approach. *FUTURES*. 2014, vol. 58 s. 66–76. ISSN:0016-3287.
- PHILLIPS, M., DICKIE, J. Narratives of Transition/non-transition Towards Low Carbon Futures Within English Rural Communities. *Journal of Rural Studies*. 2014, vol. 34 s. 79–95. ISSN:0743-0167.
- QUIST, J., VERGRAGT, P. 2006. Past and Future of Backcasting: The Shift to Stakeholder Participation and a Proposal for a Methodological Framework. *Futures*. 2006, vol. 38, no. 9 s. 1027-1045. ISSN:0016-3287.
- ROBINSON, J. 1982. Energy backcasting A proposed method of policy analysis. *Energy Policy* [online]. 1982, 10(4), 337-344 [cit. 2016-11-30]. DOI: 10.1016/0301-4215(82)90048-ISSN 03014215. Available from: <http://linkinghub.elsevier.com/retrieve/pii/0301421582900489>
- SVENFELT, Å., ENGSTRÖM, R., SVANE, Ö. 2011. Decreasing Energy Use in Buildings by 50% by 2050 – a Backcasting Study Using Stakeholder Groups. *Technological Forecasting & Social Change*. 2011, vol. 78, no. 5 s. 785–796. ISSN:0040-1625.
- URBAN, G., L., VON HIPPEL, E. 1988 Lead User Analyses for the Development of New Industrial Products. *Management Science*. 1988, vol. 34, no. 5 s. 569-582. ISSN:0025-1909.
- SVENFELT, Å., ENGSTRÖM, R., SVANE, Ö. 2011 Decreasing Energy Use in Buildings by 50% by 2050 — a Backcasting Study Using Stakeholder Groups. *Technological Forecasting & Social Change*. 2011, vol. 78, no. 5 s. 785–796. ISSN:0040-1625. 796. ISSN:0040-1625.
- VÁVRA, J. 2012. Zrození „post-uhlíkové“ společnosti? Kulturní změna očima lokální komunity. Praha, 2012. Disertace. Univerzita Karlova v Praze, Filozofická fakulta, Katedra teorie kultury (kulturologie). Vedoucí práce PhDr. Miloslav Lapka, CSc.

CHIPLESS CUTTING OF WOOD – DELIMBING KNIVES

BEZTRIESKOVÉ DELENIE DREVA – ODVETVOVACIE NOŽE

Ján Melicherčík, Jozef Krilek

Technická Univerzita vo Zvolene, Katedra environmentálnej a lesníckej techniky, Fakulta environmentálnej a výrobnej techniky, Študentská ulica 26, 960 01, Zvolen, Slovenská republika
jammelichercik88@gmail.com, jkriek@gmail.com

ABSTRACT: The article is aimed at comparing the course of the sector in terms of cutting force, cutting speed and knife geometry in the process of chipless cutting of wood. To address these problems, an experimental system has been put in place to monitor the cutting process under laboratory conditions and measure the cutting forces and cutting speeds, indicating the energy intensity of the processing process with respect to the quality of the unwinding process. By evaluating the analysis, was obtained theoretical knowledges through which was able to compared the factors that influence the process of delimiters. The cutting resistance of the tool when it enters the wood plays a significant influence on the delimiting process. The first measurements have shown us that the cutting force and cutting speed cutting speed for cutting spruce samples of wood. When measurements were used 3 types of knives with different geometries. The quality of a chipless shield timber other than the thickness of the delimiting knife and the cutting speed, which results in the optimal speed in the 2 cm.s^{-1} pneumatic chipless of wood.

Key words: cutting force, cutting speed, branch diameter, geometry knife.

ABSTRAKT: Článok je zameraný na porovnanie priebehu odvetvovania s ohľadom na reznú silu, reznú rýchlosť a geometriu noža pri procese beztrieskového delenia dreva – odvetvovania. Pre riešenie týchto problémov bol postavený experimentálny stend, ktorý dovoľuje sledovať proces rezania vetiev v laboratórnych podmienkach a merať pritom rezné sily a rezné rýchlosť, z čoho vyplýva energetická náročnosť procesu rezania s ohľadom na kvalitu odvetvovacieho procesu. Vyhodnotením analýzy sa zistili teoretické znalosti, vďaka ktorým bolo možné porovnať faktory ovplyvňujúce proces odvetvovania. Výrazný vplyv pri odvetvovanom procese zohráva rezný odpór nástroja pri jeho vnikaní do dreva. Prvé merania nám ukázali, aká je vhodná rezná sila a rezná rýchlosť pri odvetvovaní smrekovej vzorky dreva. Pri meraní sa používali 3 druhy nožov s rôznou geometriou. Na kvalitu beztrieskového delenia dreva ma okrem hrúbky odvetvovacieho noža aj rezná rýchlosť, na základe čoho sa javí najoptimálnejšia rýchlosť pri pneumatickom delení dreva 2 cm.s^{-1} .

Kľúčové slová: rezná sila, rezná rýchlosť, priemer vety, geometria noža

INTRODUCTION

The process chipless cutting of wood is a problem characterized by a number of input and output factors that are interconnected. Qualitative and quantitative indicators in this process are cutting force, cutting speed, cutting quality, cutting edge resistance to wear. The basic analysis is found in thesis (Kováč 2006). Initial measurements were carried out on an experimental stand, which consisted of a straight-ahead hydromotor. On the hydraulic motor, the blade with different geometry was fastened by means of a coupling fork. The forest harvesting is the process chipless cutting of wood is used mainly in the processing and dilution of wood by Harvester. This method of wood splitting is also applied to multi-operation machines (USA, Canada). Current, in the forestry industry, different kinds of multi-operation machines are applied to this work for the dilution or processing of wood. Their platform and functionality makes it possible to process wood even under available conditions (Pentek et.al., 2008) and (Wiesik 2015).The biggest problem with the application chipless cutting of wood in forestry about of timber harvesting is the frequent wear of the cutting device (Dvořák 2008). Incorrect cutting edge angle and partial tool deformation cause a poor woodcutting process. For this reason, wood is pulverized and longitudinal cracks result in high shear forces resulting in a considerable load on the mechanism.

From analyzes and publications abroad or at our department it was found that the greatest influence on the cutting resistance upon entering the wood has the thickness of the tool. The higher the thickness of the tool, the higher the energy consumption and the better the cutting surface quality (Mikleš 2009).

The cutting tool in the wood processing industry is a delimiting knife. Its geometry may be different and the design may have different shapes of cutting edge and blade angle. In this experiment, a wedge-shaped wedge is used, the shape of which is identical to the wedge with the angle of the cutting edge β , and the back angle $\alpha = 0$ where the angle $\delta = \beta$. The results of the chipless cutting of wood research showed that the cutting force at the entrance of the knife into the wood initially increased linearly and then dropped to zero. The maximum force F_c corresponds to the blade penetration depth of 0,55 to 0,80% of the cross sectional area. In the chipless cutting od wood by a wedge knife in a direction that does not agree with the direction of the wood fibers, considerable cutting forces are created. One of the specific cases of this method is the power cutting of branches. Therefore, sometimes a process of unthreading wood splitting with a wedge knife in a direction that is not identical to the direction of the fiber is called force cutting. In the case of power cutting of branches, knives of a complicated structure are used. The special feature of knives designed for cutting the branches by the force method is the combination of effective cutting with copying ability of knives in the process. The magnitude of the cutting force acting in the direction of the velocity vector is the result of all the components of the force of resistance acting on the different parts of the knife forming its cutting profile (forehead, back, cutting edge), (Mikleš, J. and Mikleš, M. 2015). The basic theory of the analytical calculation of the forces in the branch process was built by (Zacharenkov 1963, 1964).

Chipless cutting is characterized, in particular, by the fact that, up to the moment of removal of the branch from the forehead knife , it penetrates the wood only to the detriment of compressing the wood and pushing it out of the cutting zone in a volume equal to that of the protruding portion of the knife. This is illustrated by the fact that the branch has

a long enough length is characterized by such great resistance to shearing along the fibers, that the vertical force F_{Q1} is not able to overcome it. Therefore chip is not formed and subsequently observed a characteristic decrease cutting resistance. The cutting resistance is constantly increasing, reaching the maximum at the moment when the over-cut branch begins to separate from the forehead knife, after which the opposite process takes place. The nature of the growth and decrease of the cutting resistance must ideally be the same. The conclusions follow that the maximum force acting from the wood on the forehead of the knife must be counted out based on the condition of energy consumption for pressing the wood. Here we assume that the relative pressure, caused by the cut-off branch on the forehead is in direct dependence on the volume of wood extruded by the forehead in the cutting process.

Measuring pressure on the entire contact area with the forehead knife being evenly distributed, which is most likely to at chipless cutting. The principle is that in the given method the over-cut part of the branch does not leave the forehead knife but is attached to it until the condition is maintained and the relationship applies:

$$F_{Q1(a-z)} \leq \frac{1}{32} \cdot \pi \cdot (a - z)^2 \cdot b \cdot \sigma_{OH} \quad [N] \quad (1)$$

F_{Q1} measuring pressure wood [N],

a longer axis slit branch [mm],

z depth of knife penetration [mm],

b shorter axis slit branch [mm],

σ_{OH} timber strength of the branch along the fibers [MPa],

Subsequently, the calculation of the maximum force F_{S1} and its components can be made, based on the condition that the uniform pressure distribution on the knife forehead is maintained.

When calculating the forces F_{S1} , F_{Q1} and F_{P1} , only the deformations of the wood pressing, caused by the front edge of the knife. Then the normal force F_{N1} , acting on the knife's forehead, can be determined from the following relationship:

$$F_{N1} = q \cdot V_1 \quad [N] \quad (2)$$

Where:

q the specific compression force, per unit of volume of the compressed wood [$N \cdot mm^{-3}$],

V_1 volume of wood, knife – crush out [mm^3]

MATERIAL AND METHODS

In the experimental solution, we perform a comparison chipless cutting wood process without cutting force, cutting speed and knife geometry when cutting freely the cutting wood process. To solve article problems, an experimental machine has been developed which allows the cutting process to be monitored in laboratory conditions and to measure

the cutting forces resulting in the energy demand of the cutting process with respect to the quality of the delimiting process. The experimental device (1) is controlled by a direct pneumatic cylinder (6). For cutting, knives with different geometric parameters are used in Table. 1. Delimiting knives (7) are produced with STN 19 083. Wood spruce are branched sections of soil where the diameter of selected branches ranged from 10 to 70 mm. The relative humidity of wood w_{rel} % was determined by gravimetric method according to STN 49 0108. All knives achieve a hardened hardness of 52 - 56 HRC. They will be treated with surface roughness $R_a = 0.8 \mu\text{m}$. In the experiment, we varied pressure compressed airline in the pneumatic cylinder to be given to determine the optimum cutting speed and cutting force. The cutting speed was recorded by the acceleration sensor (4) and the cutting force using a tensometric sensor from DMP 331. The air to the pneumatic cylinder was supplied by the Orlik compressor. The pressure in the reservoir was controlled by a barometer (5). The air is conveyed to the hose of the air to the desired pressure (2).

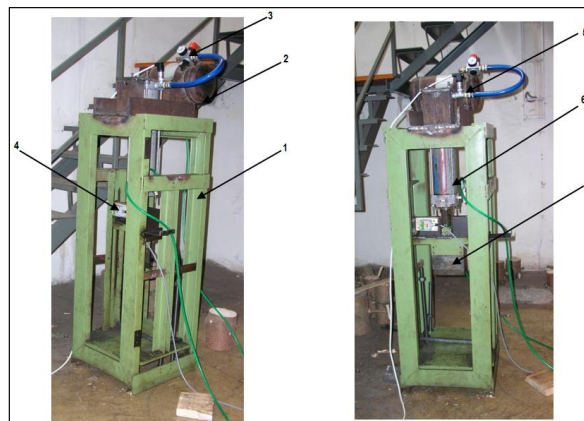


Fig. 1 Experimental device for delimiting the branched part of the tree
Obr.1 Experimentálne zariadenie na odvetvovanie zavetvenej časti stromu

$$F_{R_{MAX}} = a_1 \cdot D^2 \quad [\text{N}] \quad (3)$$

Where: a_1 - the coefficient of proportionality depends on the parameters of the knife, the wood and the angle of ingrowth of the branches

This relationship can be said to be that $F_{R_{MAX}}$ is directly proportional to the cutting surface of branch S :

$$F_{R_{MAX}} = k \cdot S \quad [\text{N}] \quad (4)$$

Where:

$k = F_{sp_{MAX}}$ the proportionality ratio corresponding to the maximum nominal cutting force, which includes the influence of the geometric characteristics of the knife $[\text{N} \cdot \text{mm}^{-2}]$,

S cutting surface of the branch [N.mm⁻³],

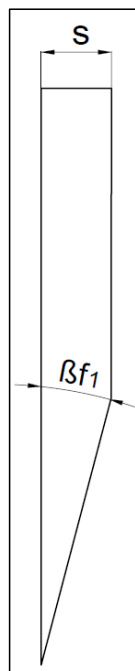


Fig. 2. The geometry of the cutting wedge delimiting knife
 Obr. 2 Geometria rezného klina odvetvovacieho noža
 s – thickness of the knife, βf_1 – side angle of the cutting wedge,

Table 1. Technical parameters of knives intended for experimental tests
 Tabuľka 1. Technické parametre nožov určených pre experimentálne skúšky

Knife number.	δ – cutting angle (°)	α – knife of back angle (°)	s – knife thickness(mm)	r – radius cutting edge (mm)
1	20	7	15	0,012–0,025
2	15	4	15	0,012–0,025
3	20	4	15	0,012–0,025

RESULTS

The main task of the experiment is to determine the optimum cutting speed and cutting force parameters in the process of repositioning on the experimental device. The deflation process is carried out by means of an air cylinder and a flat blade. In the measurements, woods with a diameter of between 10 and 70 millimeters were used. The sample wood was a spruce with a relative humidity of w_{rel} 30%.

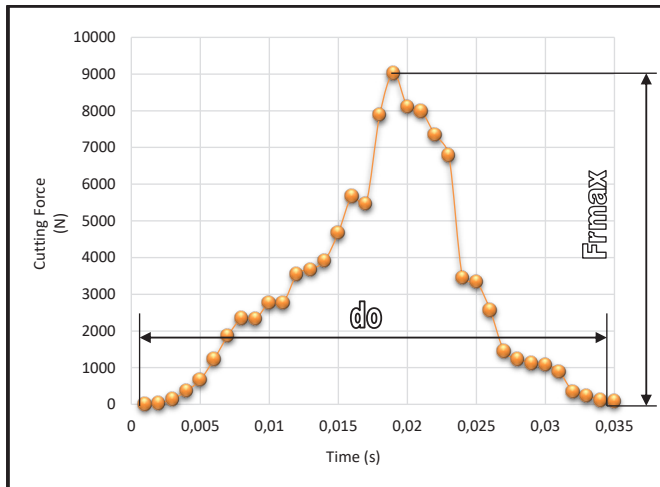


Fig. 3. The course of cutting force when delimiting branch mean d_0
Obr. 3 Závislosť reznej sily od času počas odvetvovania vety do priemeru d_0

The dependence of the cutting force on the delimiting process is limiting course. The forces required in the experiment were influenced by the diameter of the wood, the resistance of the wood and the geometry of the knife. In the determination of the maximum cutting force, knife with the best geometry was selected $\delta = 20^\circ$, $\alpha = 4^\circ$, $h = 2$ mm, $s = 15$ mm. The maximum cutting force recorded in the experiment is 9023 N.

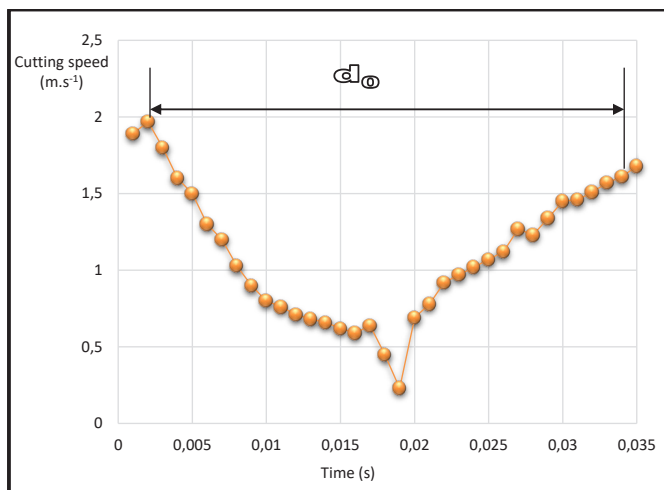


Fig. 4. The course of cutting speed when delimiting branch mean d_0
Obr. 4 Závislosť reznej rýchlosť od času pri odvetvovaní vety do priemeru d_0

The cutting speed dependence on the deflation process is plotted parabolically. The speeds required in the experiment were influenced by the pressurized air pressure in the pneumatic train, the wood resistance, and the knife geometry. In the determination of cutting speed, knife with the best geometry was selected $\delta = 20^\circ$, $\alpha = 4^\circ$, $h = 2 \text{ mm}$, $s = 15 \text{ mm}$. From the first experimental measurements, we determined the optimal cutting speed of the knife $2,0 \text{ m.s}^{-1}$.

DISCUSSION

Chipless cutting of wood is a theme that is closely related to forest management. Different researches and analyzes deal with this theme and theme (Hatton et al., 2015, Cacot et.al., 2016, Krilek 2016). In this article, the maximum cutting force and cutting rate required for cutting the bent part of the tree was determined using experimental measurements. By experimental measurement, it has been found that the great influence on the cutting force and the cutting speed has the resistance of the wood and its moisture. It also affects the branch and the sample tree diameter. The branch diameters used in the experiment ranged from $10 - 70 \text{ mm}$ and the humidity of the wood was wrel $21 - 46\%$ (Philipp D., et al., 2015). Another factor influencing the measurement was the geometry of the cutting knife, which is devoted to different studies (McEwan et al., 2016, Gerasimov et al., 2013). Based on analyzes (Mikleš 2009), three branch knives with different geometry were used. These, the most appropriate was chosen and used to determine a maximum cutting force of $9023N$ and a cutting speed of 2.0 m.s^{-1} . The greatest influence on the cutting force is the choice of the correct geometry of the cutting knives, it is characterized by different sizes of max. of the cutting force in the examined knives, and we confirmed the correctness of the best knife geometry selection with the following parameters $\delta = 20^\circ$, $\alpha = 4^\circ$, $h = 2 \text{ mm}$, $s = 15 \text{ mm}$. When delimiting with different geometry of a knife, the sphere does not change the character of the course and the change does not occur even when selecting another branch thickness. In the experiment there was also a change in the angle of neurite branch. If the blade is constantly penetrated into the wood where the cutting angle is increasing, the average value of the fiber deformation in the direction of the blade face is increased. This flag were causing increasing deformation forces. Assumed in the literature that refer to loads, they divide the process of deformation into two regions, the area of incomplete elasticity $\sigma < \sigma_m$ a and the area of plastic flow at $\sigma \geq \sigma_m$, (Mikleš and Marko 1992). In the first area there is a load on the body so that the deformation is reversible after unloading. Principally composed of Hooke's law. After deformation relief, it does not disappear but causes permanent body change. Plasticity is accomplished by the movement of dislocations.

CONCLUSION

The aim of this contribution was to determine the maximum cutting force and cutting speed in the process of repositioning on the experimental facility in the premises of TU Zvolen. The issue of wood processing in forest management is current. Therefore, it is necessary to devote itself to its deeper and subsequent research to monitor the forces determined from the initial measurements, how they will act on the cutting knife and

eliminate the device errors. From the first analyzes, we know that the force required for tree delimiting is about 9 kN at the cutting speed of movement of the knife 2,0 m.s⁻¹. This finding ensures the perfect tree delimiting without damaging the wood by pulling the wood or the rest of the branch.

LITERATURE

- CACOT, E., FAUROUX, J.; PEUCH, D., BOUVET, A., CHAKROUN, M. 2016: *New delimiting tool for harwood trees: feedback on new ribbed knives after one year experince*. In: *Formec 2016, From Theory to Practice: Challenges for Forest Engineering*; 49th Symposium on Forest Mechanization, Warsaw, Poland 2016: 37-43. ISBN 978-83-943889-9-7
- DVOŘÁK, J. *Performance of the Small Tracked Harvesters in Spruce Stands*. Nauka za gorata - Forest Science, 2008, roč. 44, č. 3, s. 77 - 85. ISSN: 0861-007X.
- GERASIMOV, Y., SOKOLOV, A. 2013 : Ergonomic evalutaion and comparison of wood harvesting system. Applied Ergonomics (2013) s - 1-21. ISSN: 0003-6870
- HATTON, B., POT, G., BOUZGARROU, B. CH., GAGNOL, V.; GOGU, G. 2015: *Experimental determination of delimiting forces and deformations in hardwood harvesting*, Croatian journal of forest engineering. ISSN 1845-5719, 2015, vol. 36, no. 1, pp. 43-53.
- KOVÁČ, J. 2006. Environmental analysis of working aspects in the harvester technologies. - VEGA 1/3534/06. In the Colloquium on Grant Assignment No. 1/3534/06: Proceedings. - Zvolen: Technical University in Zvolen, 2006. ISBN 80-228-1692-2. - S. 28-36.
- KRILEK, J., KOVÁČ, J., KRIŠTOF, K., JOBBÁGY, J., SPIRIDONOV, S., V. 2016: *Analýza rezných sil na odvetvovacích nožoch harvestorovej hlavy = Analysis of delimiting forces on the delimiting knives of the harvester head* / - VEGA 1/0826/15. In Kolokvium ku grantovej úlohe č. 1/0826/15 [elektronický zdroj] : vedecký recenzovaný zborník - Zvolen : Technická univerzita vo Zvolene, 2016. - ISBN 978-80-228-2920-5. - S. 55-65
- MCEWAN A., BRINK, M., SPINELLI, R. 2016 : Factors affecting the productivity and work quality of chain flail delimiting and debarking, The Finnish Society of Forest Science, ISSN-L 0037-5330 | ISSN 2242-4075
- MIKLEŠ, J., MIKLEŠ, M. 2015. Determination of the technical parameters of delimiting head the viewpoint of their number and their shape. *Acta facultatis technicae: Scientific journal of the Faculty of Environmental and Production Technology*. Elected: Technical University in Zvolen, 2015, 20 (2), 97-108. ISSN 1336-447
- MIKLEŠ, M. 2009. *Studying the geometry of the cutting head knives*. Acta Facultatis Technicae, XIV, 2009 (2) : p. 121 – 129, ISSN 1136 – 4472
- MIKLEŠ, M., MARKO, J. 1993. Teória a stavba lesných strojov I. Zvolen, ES TU, 1993, ISBN 80-228-0204-2 ,243s.
- PENTEK T., PORŠINSKY T., ŠUŠNJAR, M., STANKIĆ, I., NEVEČEREL, H., ŠPORČIĆ, M. 2008. *Environmentally Sound Harvesting Technologies on the Area of Northern Velebit – Functional Terrain Classification*. Periodicum Bilogorum 110 (2): 127-135. WOS Accession Number: 000258415000003
- PHILIPP, D., FRANKE, S., FRANKE, B., GAMPER, A., WINTER, S. 2015. *Methods to determine wood moisture content and their applicability in monitoring concepts*. Journal of Civil Structural Health Monitoring 2015. s 115-127, ISSN 2190-5452
- WIESIK, J. et.al. 2015 . Urzadzenia techniczne w produkcji lesnej, Wydawnictwo SGGW Warszawa 2015, 591 p., ISBN 978 – 83 – 7583 – 574 – 8
- ZACHARENKOV, F. E. 1963. *Analitičeskij sposob razčeta maksiman'nogo soprotivenija rezanija pri silovom metode obrezky sučjev*. Lesnoj žurnal No. 3, Archangelsk, 1963, s. 68 – 76.

This article was written within IPA project no. 13/2017 “Research of woodless cutting of wood using cutting blades”.

This article was written within VEGA project 1/0826/15 “Research of Cutting Mechanisms in Wood Processing Process”.

This article was supported by the Slovak “Research and Development Agency under the contract No. APVV-16-0194“.

Corresponding author:

Ing. Melicherčík Ján

tel. č. : +421 908 342 059

e-mail: janmelichercik88@gmail.com

LOCATION OF VEHICLE REGISTRATION PLATES IN REAL SCENE IMAGES

LOKALIZÁCIA EVIDENČNÝCH ČÍSIEL VOZIDIEL V REÁLNYCH OBRAZOCH

Ladislav Karrach, Elena Pivarčiová

Katedra výrobnej a automatizačnej techniky, Fakulta environmentálnej a výrobnej techniky, Technická univerzita Zvolen, Študentská 26, 960 53 Zvolen, karrach@seznam.sk, pivarciova@tuzvo.sk

ABSTRACT: The objective of the method proposed in following paper is to locate the Vehicle Registration Plate within the image taken by camera from real world. We understand this aim as the first necessary step to the total recognition of the vehicle registration number. We consider the vehicle registration plate as a series of 7 characters placed in a row. The designed method is based on adaptive thresholding, connection of neighbouring foreground points into continuous regions and on a searching of 7 regions which are of roughly the same size and are placed in the image approximately in the same Y-position. This method has been tested using a database of 50 Slovak vehicle registration plates and results achieved have shown satisfactory performance.

Key words: Vehicle Registration Plate, Morphological operations, Adaptive Thresholding

ABSTRAKT: Cieľom metódy navrhnutej v nasledujúcom článku je nájsť evidenčné číslo vozidla v obraze, ktorý bol získaný kamerou z reálneho prostredia. Tento cieľ chápeme ako prvý nevyhnutný krok k úplnému rozpoznaniu evidenčného čísla vozidla. Pre účely lokalizácie uvažujeme o evidenčnej tabuľke vozidla ako o sérii 7 znakov umiestnených v rade vedľa seba. Navrhnutá metóda je založená na adaptívnom prahovaní, spájanie susedných bodov popredia do súvislých oblastí a na hľadaní siedmich oblastí, ktoré majú zhruba rovnakú veľkosť a sú umiestnené v obraze približne v rovnakej Y-pozícii. Táto metóda bola testovaná na databáze 50 slovenských evidenčných čísel vozidiel a dosiahnuté výsledky preukázali uspokojivý výkon.

Kľúčové slová: evidenčné číslo vozidla, morfologické operácie, adaptívne prahovanie

INTRODUCTION

The recognition methods find still bigger use in various branches such as manufacturing, robotics, medicine, quality control, cartography, processing of satellite images etc. Their aim is to create an autonomous system, which does not need presence of man respectively they try to make analyse of image data easier. The main benefit is speed and efficiency of processing.

The recognition of Vehicle Registration Plate (VRP) is one of the classical tasks in recognition of text in real scene images. All vehicles which are in operation on public roads in Slovakia must have the Vehicle Registration Number (VRN), which is formed by letters and digits. The vehicle registration plate (VRP) replaced the previous plates with State Registration Number (SRN).

The recognition of VRP could be applied in various systems. You can find it in transportation e.g. in speed control, in tracing of traffic offences, monitoring of traffic density, parking systems, tolling systems, tracking of stolen cars etc. However, the algorithms and various ways of solving the problem of VRP recognition can be generalized and used in wide variety of other fields of life where the text recognition is required, such as manufacturing, indexation of texts in image database, automatic warnings in monitored processes, translating of foreign language texts, aids for visually impaired people etc.

We can divide the process of the recognition of VRP in two steps, first step is location finding of VRP in the whole image among many other objects, and the second step is the following detection of the individual characters, which form the VRP and their final recognition as a text. In this article we deal with the first phase of recognition of VRP – that means we solve the problem of finding the area which probably contains the VRP.

RELATED WORK

There were many papers published in the past on these problems (Abolghasemi & Ahmadyfard, 2009; Zhai et al., 2010; Mahini et al., 2006). Those works are based on the characteristic features of VRP such as geometrical shape (rectangle with certain aspect ratio), position (horizontal with upper and bottom edge of the image), the colour pattern of VRP (black characters on the white background i.e. similarity of colour intensities in RGB colour model), strong contrast of the characters against the background of the VRP (in case of standard Slovak VRP, the black lettering on the white background), minimal and maximal number of characters in VRP and so on. We present a brief overview of some frequently used approaches:

- **Edge detection:** is based on the assumption that individual characters of VRP are significantly contrasted against the background and so, on their rims you can find the significant edges. Applying the edge operator (e.g. the vertical Sobel operator) we are looking for regions with high density of the edge points.
- **Morphological operations:** by this method we suppose that the characters of VRP make up the relative small dark areas respectively that the gaps between the characters make up relative small white areas. When using the appropriate large structural element we are able to identify these areas. The size of structural element is critical for application of these methods and that is why we have to expect a certain specific size of VRP. If we are not able to make such guess we can use the iterative process whereby the image is gradually decreased and the location process is repeated.
 - **Morphological operation Bottom-Hat** is defined as subtraction of the original image from morphological closing (dilation followed by erosion). It highlights the details and elements which have size smaller than size of the structuring element

and they are darker (dark characters of VRP) compared to surrounding (white background). Morphological operation Bottom-Hat is defined as:

$$((F \oplus S) \ominus S) - I \quad (1)$$

where \oplus denotes dilation and \ominus denotes erosion operation.

Structuring element must be chosen bigger than stroke width of a character.

- **Morphological operation Top-Hat** is defined as subtraction of the morphological opening (erosion followed by dilation) from the original image. It highlights the details and elements which have size smaller than size of the structuring element and they are lighter (white spaces between the dark characters of VRP) compared to surrounding. Morphological operation Top-Hat is defined as:

$$I - ((F \ominus S) \oplus S) \quad (2)$$

Distance between the characters must not be bigger than the width of structuring element.

MATERIAL AND METHODS

We proposed and verified a method for position finding of VRP. All the parameters (sizes, tolerances) mentioned in the following text were set empirically from the testing set of VRP samples.

The location finding is based on the assumption that single characters of VRP make up together the distinct continuous areas of the foreground points of the same height and those continuous areas are in the roughly the same Y-position in the image and they are not far from each other than the given constant.

Image pre-processing

- Change of the size: because of the better efficiency of processing we decrease the images wider than 1600 points to the width defined by integer ratio width/800
- If image metadata (EXIF) contains the information about orientation of the image, we turn the image due to this information
- Colour conversion: we transform the colour (RGB) image to 8-bit gray scale image. Working with this method we do not make use of colour characteristic of VRP, but only the fact that characters making up the VRP are darker than the background.

Image segmentation

The goal of segmentation is the separation of the foreground points (black characters of VRP) from the background points (white background of VRP). There is a problem with the global thresholding using the fixed threshold, when the VRP are not uniformly illuminated. In the same way, the automatic setting of the threshold, e.g. by Otsu method

also does not lead to good results, as the image contains beside VRP also wide surrounding objects with many disturbing image information.

The better results we can achieve by adaptive thresholding. In the Fig.1, there are several not uniformly illuminated VRPs. In the Fig.2 are shown the VRPs after transformation into a gray-scaled image. The comparison of global thresholding using various thresholds you can see in the Fig.3. In the Fig. 4, there are shown the adaptive thresholding with window size 30 and delta 10 (Bradley & Roth, 2007).



Fig. 1 Non-uniformly illuminated VRP
Obr. 1 Nerovnomerne osvetlené EČV



Fig. 2 Gray-scaled VRP
Obr. 2 Šedotónové obrazy EČV

$t=100$



$t=130$



$t=160$



Fig. 3 Global thresholding
Obr. 3 Globálne prahovanie

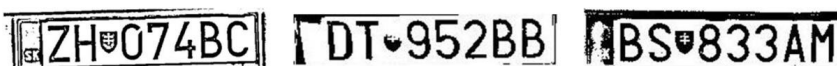


Fig. 4 Adaptive thresholding
Obr. 4 Lokálne prahovanie

When applying thresholding we get a binary image, where the black points represent the points of the foreground and the white points the background.

Forming of blobs by connecting points into continuous regions

In further progress we apply the 2-pass algorithm of connecting the neighbouring points into the continuous regions (Rosenfeld & Pfaltz, 1966). When we add a new point into region or when we connect the equivalent regions we update the region descriptors:

- area of the region (number of points in the region)
- dimensions (outer boundary rectangle of the region)
- number of holes

The Fig.5 shows the individual continuous regions which represent individual characters of VRP are colour-differentiated.



Fig. 5 The marked continuous regions
Obr. 5 Označované spojité oblasti

The selection of VRP character candidates

We are looking for such continuous regions which could be the characters of VRP. To declare the region to be candidate for further processing, the region has to fulfil the following conditions:

- Minimum and maximum size (width in $<5, 160>$, height in $<20, 210>$)
- Aspect ratio height to width in $<1.3, 7.6>$
- Maximum of 3 holes

We sort the satisfactory regions by Y-coordinate of the upper bound of the bounding box and we search in the list of sorted regions. We look for regions, which have ± 4 points in the same Y-position (we assume that characters making up the VRP are approximately of the same height and in a line) and the gap between them is from 2 to 40 points. If we find at least 7 such regions (we suppose that VRP consist of 7 characters) we have to test their specific features. We check if the height of the characters is ± 4 points (we suppose that all the characters are of the same height) and we check if the ratio width to height of the bounding box is from 4.5 to 6.25. If such testing gives positive result, we can declare the region as a candidate to be VRP.

(This algorithm expects that the VRP is a standard type of Slovak VRP for vehicle, with dimension 52×11 cm and that its position is approximately horizontal)

RESULTS

We have tested the above proposed method on a testing set of 50 photos of Slovak VRPs of standard dimensions 52×11 . The photos were taken from medium distance so that the VRP width made up from 10 to 50 % of the full width of the image (recognition algorithm was not tuned for detailed VRP pictures).

The testing set contained the photos which were taken at twilight, with partly overshadowed VRP or VRP, which were covered with safety strips. Samples of the photos are in Fig. 6.



Fig. 6 Samples of testing photos
 ideal contrasted
 low contrast
 overshadowed VRP
 VRP with safety strips

Obr. 6 Ukážky testovacích fotiek
 ideálny kontrast
 nízky kontrast
 zatienené EČV
 EČV s pojistnými páskami

With our method we achieve 86 % detection rate, when in 43 out of 50 VRP, the location was successfully found.

DISCUSSION

The proposed method expects the horizontal position and standard dimension of VRP. Our opinion is that this is not a limiting factor for most applications, like parking and security systems, where car must stop at certain place (before the gate) and the camera has a fixed position.

Problem for correct segmentation could make safety strips, running across the VRP, which causes wrong segmentation as shown in Fig. 7.



Fig. 7 VRP with safety strips
 Obr. 7 EČV s pojistnými páskami

If the width of safety strip is smaller than stroke width of character we can use morphological operation – conditional erosion in gray scale image. In the first step we dilate ima-

ge by structuring element “the horizontal line” of the strip width (all groups of black points with smaller width than width of structuring element will disappear) and in following step we erode image with same structuring element, but we recover only those black points which exists in original image.



Fig. 8 VRP after conditional erosion
Obr. 8 EČV po podmienenej erózii

The weak point of this approach is that for very small characters those characters themselves will be removed. It is difficult to set appropriate width of structuring element beforehand.

For this case the simplified method will remove up to X black points in the row only when they are surrounded by at least Y white points. This way we can make the segmentation better, but the remains of strips are still present and they deform characters.



Fig. 9 VRP after partial removal of strips
Obr. 9 EČV po odstránení časti poistných pások

CONCLUSION

In this article we describe the possibility of VRP location finding in image, which could be followed by recognition of individual VRP characters. The methods of image processing and text recognition could be adopted for various purposes as above mentioned traffic security, car monitoring, parking systems etc.

Automated text recognition and object identification in the image could be also used for recognition of traffic signs, recognition of objects in robotics systems or in equipment for visually impaired persons.

In manufacturing, object recognition can be used in robotic lines, for identification of components and their identification numbers. This identifiers could be linked to database of the components, where are full information available about the components, needed for adjoined processes like purchase, storing or selling.

LITERATURE

- ABOLGHASEMI V., AHMADYFARD A., 2009. An edge-based color-aided method for license plate detection. *Image and Vision Computing*. 27, p. 1134-1142.
BLÁZSOVITS G., 2006. DIP - Digital Image Processing: Interaktívna učebnica spracovania obrazu. [online] [cit. 2016-05-08]. Available in: <<http://dip.sccg.sk>>

- BRADLEY D., ROTH G., 2007. Adaptive thresholding using the integral image. *Journal of Graphics Tools*
- FISHER R., PERKINS S., WALKER A., WOLFART E., 2004. Hypermedia Image Processing Reference. [online] [cit. 2017-09-26]. Available in: <homepages.inf.ed.ac.uk/rbf/HIPR2/>
- MAHINI H., KASAEI S., DORRI F., DORRI F., 2006. An Efficient Features - Based License Plate Localization Method. 2. 841-844. 10.1109/ICPR.2006.239.
- KARRACH L., PIVARČIOVÁ E., 2017. Data Matrix code location marked with laser on surface of metal tools. *Acta Facultatis Technicae XXII*, 2017 (2): 29–38, ISSN 1336-4472
- KHAN A. M., SHARIF M., JAVED M. Y., AKRAM T., YASMIN M., SABA T., 2017. License number plate recognition system using entropy-based features selection approach with SVM. *IET Image Processing*, Volume 12, Issue 2, p. 200 –209
- KOLEDÁ P., NAŠČÁK L., 2011. Skeletization algorithms. In: *Acta Facultatis Technicae*, Zvolen: Technická univerzita vo Zvolene, XVI 2/2011, p. 73–82, ISSN 1336-4472
- NEUMANN L., MATAS J., 2015. Efficient Scene text localization and recognition with local character refinement. [online]. Available in: <<https://arxiv.org/pdf/1504.03522.pdf>>
- PIVARČIOVÁ E., 2016. IDENTIFICATION OF IMAGE OBJECTS AND ITS APPLICATION IN THE MANUFACTURING TECHNOLOGY. In: *Acta Facultatis Technicae*, Zvolen: Technická univerzita vo Zvolene, XXI 1/2016, p. 91–98, ISSN 1336-4472
- ROSENFELD A., PFALTZ J., 1966. Sequential operations in digital image processing. [online] [cit 2017-07-11]. Available in: <<http://www.cse.msu.edu/~stockman/Book/2002/Chapters/ch3.pdf>>.
- ŠIKUDOVÁ E., ČERNEKOVÁ Z., BENEŠOVÁ W., HALADOVÁ Z., KUČEROVÁ J., 2013. Počítačové videnie Detekcia a rozpoznávanie objektov. [online] [cit 2017-07-11]. Available in: <<http://vgg.fiiit.stuba.sk/kniha/>>.
- TRKAL O., 2016. Rozpoznávaní EČV. [online] [cit. 2018-04-22]. Available in: <https://www.vutbr.cz/www_base/zav_prace_soubor_verejne.php?file_id=124167>.
- YAO B., HE L., KANG S., CHAO Y., ZHAO X., 2015. A novel bit-quad-based Euler number computing algorithm. *SpringerPlus* 4(1).
- ZHAI X., BENSSALI F., RAMALINGAM S., 2010. License Plate Localisation based on Morphological Operations. *Control Automation Robotics & Vision (ICARCV)*, 2010 11th International Conference: 7 – 10 Dec. 2010.

Corresponding author:

doc. Mgr. Elena Pivarčiová, PhD., 045 5206 477, pivarciova@tuzvo.sk

ENERGY AND TRANSPORT INFRASTRUCTURE IN LOW POPULATION AREAS, TECHNICAL POSSIBILITIES OF CHARGING STATION FOR ELECTRIC VEHICLES IN THESE AREAS

ENERGETICKÁ A DOPRAVNÁ INFRAŠTRUKTÚRA V OBLASTIACH S NÍZKOU HUSTOTOU OBÝVATEĽSTVA, TECHNICKÉ MOŽNOSTI DOBÍJACÍCH STANÍC ELEKTROMOBILOV V TÝCHTO OBLASTIACH

Miroslav Krumbholc

*Department of Vehicles and Ground Transport, Department of Physics, Faculty of Engineering,
Czech University of Life Sciences, Kamýcká 129, Prague, 165 21, Czech Republic, krumbholc@
tf.czu.cz*

ABSTRACT: The article presents the possibilities and the extent of utilization of alternative energy sources (photovoltaics, biogas, wind, water) as adequate substitutes for traditional non-renewable resources in rural areas.

Subsequently, the thesis examines the possibilities of electromobility in areas with lower density of dwelling in connection with the location of fast-charging stations for electromobiles with a survey of density, directions and gradient areas of transport, as well as the supporting infrastructure of fast-charging stations.

Key words: electrovehicles, population density, environment, distribution system of electricity, survey of living conditions, renewable sources

ABSTRAKT: Článok predstavuje možnosti a rozsah využitia alternatívnych zdrojov energie (fotovoltaika, bioplyn, vietor, voda) ako primerané náhrady za tradičné neobnoviteľné zdroje vo vidieckych oblastiach. Následne práce skúma možnosti elektromobilu v oblastiach s nižšou hustotou obydlí v súvislosti s umiestnením rýchlonabíjacích staníc pre elektromobily s prieskumom hustoty, smerov a spádových oblastí dopravy, ako aj s podpornou infraštruktúrou nabíjacích staníc.

Kľúčové slová: elektromobil, hustota obyvateľstva, životné prostredie, distribučná sústava elektriny, prieskum životných podmienok, obnoviteľné zdroje

INTRODUCTION

Currently in the Central European region and the Czech Republic is infrastructure for massive development of electromobility at a very low level. Infrastructure refers to recharging stations, service and support centers for electrovehicles. The study on which this article is based provides guidance on how to remedy that condition at the time units of years. Developed world states are creating global agreements to reduce SO₂, CO₂ and NO_x emissions. Agreements the Kyoto Protocol and the Paris Agreement, in particular the Paris Agreement, commit states to reduce emissions of gases that cause adverse global and local climate change.

The European Council has adopted a common platform that encourages municipalities and cities to save energy, increase its production from renewable sources, and reduce dependence on fossil fuel imports and combustion. Typically, energy consumption and prices depend on local availability of resources. Separately developed energy supply options that meet these requirements vary by region and may vary within a large city. (Maier, 2016) An increasing number of municipalities want to cover their entire energy use by using their own renewable resources. (Jensen et al., 2017) Microregions in Austria are succeeding in reducing energy dependence on energy supplies from the external distribution system. They assess the possibilities and trade-offs between the costs and benefits of increasing the energy self-sufficiency of a small rural area. (Karchin, Geldermann, 2015) Energy projects are linked to the environmental impacts that can bring pros & cons to other economic activities. Therefore, the development of renewable resources must also be assessed on the basis of the preferences of life in rural areas. Part of the process is the need to assess the impacts on local transport and the economy. (Schmidt et al., 2012) Availability of the potential of renewable energy sources and high-efficiency technologies are two main reasons for expanding low-carbon energy supply. Creating a mathematical model that optimizes local power generation and distribution to customers must take into account parameters such as the availability of renewable energy sources, the number of customers for electricity and heat, system losses, economic appreciation or investment return assessment and a healthier environment. The mathematical model assesses availability or build, location and type of renewable resource with respect to the lowest cost of electricity and heat supply. The development of renewable energy sources, such as wind and hydroelectric power plants, brings about interference with landscape and nature. Energy projects are associated with environmental impacts that can cause damage or the decline of other economic activities. This activity is also tourism. Therefore, the development of renewable resources must also be assessed on the basis of the preferences of life in the village and the city. Surveys in the areas must be the acceptability of the type of renewable resources and their use in energy supply and transport. (Wappelhorst et al., 2014) Traffic from rural areas by automotive transport with internal combustion engines versus electrified vehicles faces problems of costs and driving distances. (Chen, Song, 2015) There are many innovative concepts and technologies that address the needs of energy supply and need to provide a comprehensive methodology for planning and evaluating the development of “smart” energy systems that will lead to a complex power supply of technological networks from various sources that minimize the influence to the environment. (Ramirez-Diaz et al., 2016) Effective and lasting reduction of negative impacts on

the environment in rural areas is a recommendation to expand the use of renewable electricity and heat. An increasing number of municipalities want to cover their entire energy use by using biomass. However, it is important to analyze the costs of land use and energy. (Bergmanna et al., 2008)

MATERIAL AND METHODS

The process of planning the development of energy and transport infrastructure in a particular geographical area is complex and lengthy. Optimizing energy technologies, networks, and scenarios resulting from the use of certain methods help to create an energy mix framework. Processed surveys and new scientific knowledge will be used to create smart solutions in the energy supply sector and as an integral part of stakeholder discussion (investors, municipalities and regions, suppliers, state institutions and last but not least, buyers) to implement their own plan through city development its parts, villages or areas.

The questionnaire survey was carried out in the areas with names MAS Vyhlídky and MAS Labské skály, which found, among other things, the number and type of vehicles, the kilometres per week, the system of heating the buildings. We tested driving with an electric vehicle and a vehicle with an internal combustion engine in identical routes and under the same conditions (time, climatic conditions, traffic situation). The routes were chosen as the usual and most common ones that were found in questionnaire surveys. The project solves the possibilities of electromobility in areas with lower density of dwellings in connection with the possibilities of recharging of electric vehicles in the mentioned areas. Secondary research addresses air pollution by emissions from local sources and transport and provides an optimal recommendation to remedy the situation. Thermovision measurement was performed in ideal design conditions for objects and with different types of heating systems in the area MAS Vyhlídky. Technical values were identified and measurements were done in the electricity distribution system in the area MAS Vyhlídky.

Proposal of methodology for the development of the studied area with regard to the consumption and supply of energy in buildings and in transport. The methodology for expanding electromobility is associated with a supportive infrastructure - comfort, the cost of electric vehicles, the cost of recharging and the reduction of transport emissions. The installation of renewable resources is confronted with the reduction of emissions from local heating, as well as the possibility of reducing losses in the energy system. There must be a wider dimension in relation to the site plan (possible restrictions on heritage conservation, nature reserves, protected landscape areas or national parks, etc.).

The whole of this development methodology has proven to be ideal and optimal in the area and time.

RESULTS

The measurement results from rides are very large, as well as from questionnaire survey. The measured values were fuel consumption, amount of carbon oxides, amount of solids in the exhaust for car with internal combustion engine. The measured value was mainly energy consumption of electric vehicle. This main index is further developed in

connection with the recharging of the electric device and the adjustment of this consumption with the energy mix in the Czech Republic and Europe. Comparison of emissions from industrial power generation to recharge a certain number of electric vehicles and emissions produced by a certain number of vehicles with internal combustion engines. Questionnaire survey has brought the number of people in the household, the number and type of motor vehicles, the average weekly number of kilometres, including the target location, the nature of the subject (from the standpoint of energy intensity), the age of the building, the used fuel and energy sources, the knowledge of the inhabitants about the environment, and other details.

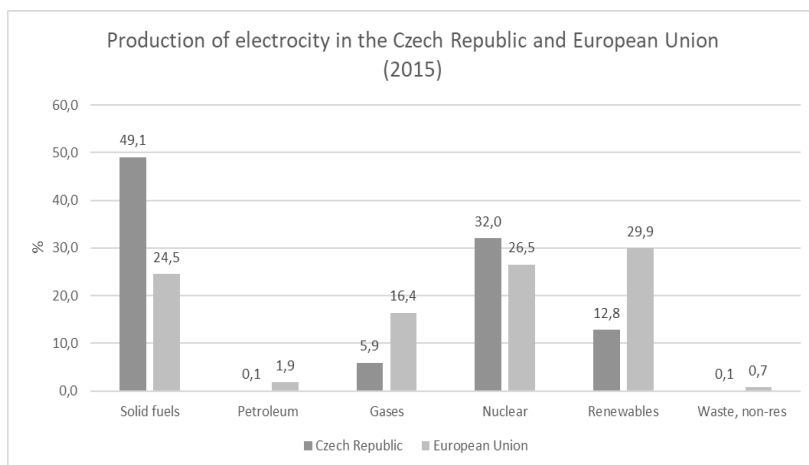


Fig. 1. Production of electricity in the Czech Republic and European Union (2015)
Obr. 1. Produkcia elektrickej energie v Českej republike a Európskej únii (2015)

The car of Skoda Citigo with Natural Gas 95 petrol spark ignition engine produced 10.9 kg of CO₂ per 100 km. Vehicle WV e-up! with an electric drive consumed 11.7 kWh per 100 km. When converting to the energy mix of the Czech Republic, 6.8 kg of CO₂ is produced to produce this amount of energy, and if we move on, only 4.4 kg of CO₂ is produced when converting to the EU energy mix. The maximum charging current taken from the fast charging station on the DC side has reached values of up to 100 A in so-called smart charging when the electric car control system communicates with the charging station via the charging connector.

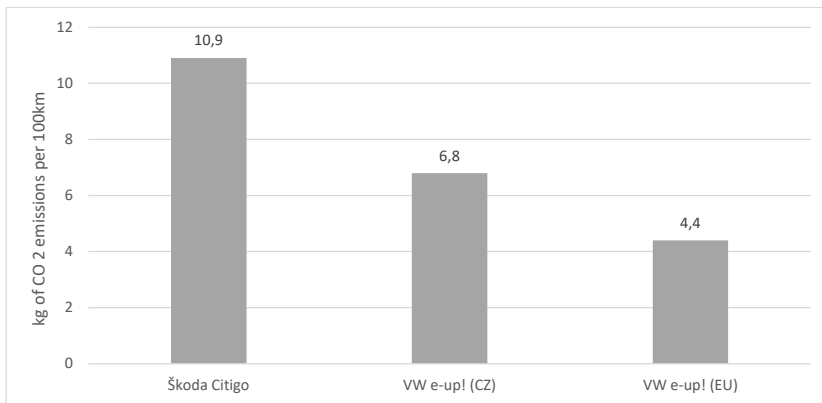


Fig. 2. The CO₂ emissions of the Škoda Citigo to 100 km and the converted CO₂ emissions of the electrovehicle WV e-up! for the energy mix of the Czech Republic and the European Union
Obr 2. Produkcia emisií CO₂ vozidla Škoda Citigo na prejdenie 100 km a prepočítané emisie CO₂ vozidla WV e-up! na energetický mix Českej republiky a Európskej únie

For calculations of CO₂ production per kilowatt-hour produced values from each source type were calculated from the average of 20 sources per source which excludes a significant statistical error.

On Tuesday, February 27, 2018, the maximum load in the winter of 2017/2018 was the Czech Republic's electricity system. Parameter monitoring has found that in the area of Mělník – Kokořínsko it is not possible to engage in bigger electricity consumption in the current state - in our case, the fast charging station for electric vehicles and these electric devices cannot be recharged from the mains from the socket 16 A in winter. The reason for this is the lack of transmission capacities in the distribution system and the calculations confirmed a strong and uncontrolled voltage degradation in the event of a further increase in the load of the distribution system with the possibility of damaging the equipment of the distribution system operator as well as electric appliances for the customers of electric energy. In the Mělník substation two transformers are installed in the area from which the surveyed areas are delivered. They do not work in parallel in the basic circuits and each feeds their power supply area on the secondary side.

DISCUSSION

Over the next few years, national and European interests will increase the number of electric vehicles in areas with lower population density, and the related infrastructure, especially energy and service, will have to be adapted to this trend. Power grid operators are unable and will not be able to cover the increase in electricity consumption for charging electric appliances without significant investments in the energy grid [HV (high voltage) – 110kV, HV – 22kV and LV (low voltage) – 400/230V lines, HV – 110kV/22kV and HV/LV – 22kV/400-230V transformations]. Energy production and its consumption must be close together because of low losses and the ability to respond faster to changing condi-

tions (eg climate). The impossibility to produce energy from renewable sources is quantified by the relevant functions and devices in the distribution system, and the forecasts and probabilities of production, consumption and external influences have to be incorporated into the planning model. The results offer planning and evaluation in several areas, improving living conditions, gaining profits, reducing emissions, minimizing energy loss, increasing stability and improving system security.

Local electrification systems can operate either synchronously connected to the parent system or can be disconnected and operated separately. Switching between these modes may cause intermittent or overcurrent oscillations on the remote island side and compromise device safety or system stability. With the energy self-sufficiency project of the entire territory, a way of automatically managing a seamless transition between island mode operation and the connected operating mode with the surrounding system must be designed.

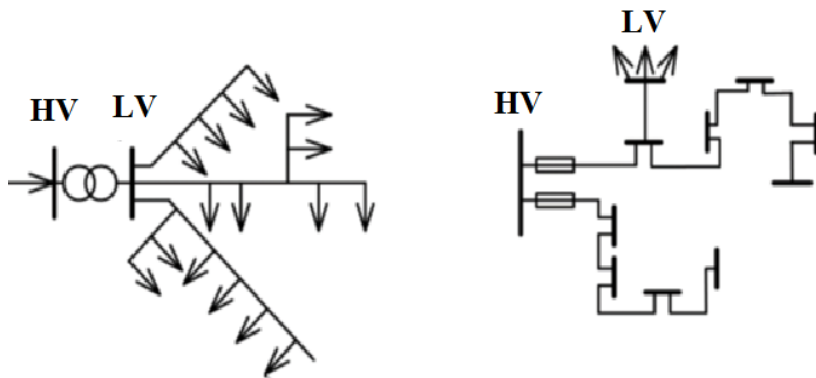


Fig. 3. Radial connection of the distribution system
Obr. 3. Radiálne (lúčové) zapojenie distribučnej sústavy

CONCLUSION

The project evaluates the environmental benefits of electric vehicles. This project recommends to these sites how to use available renewable and affordable sources with the possible accumulation of surplus and energy supply in order to avoid massive investment in energy infrastructure, which would mean a gradual and lasting increase in electricity for the final customer. Process determination – an algorithm that proposes a project variant suitable for implementing the region's energy self-sufficiency and determining an optimal energy mix for a given area and time based on the projected future energy consumption based on energy survey inputs, traffic measurements, questionnaire survey, environmental impact, optimization transport, territorial development, employment and other appropriate or necessary opportunities.

REFERENCES

- MAIER, S. 2016. Smart energy systems for smart city districts: case study Reininghaus District, *Energy, Sustainability and Society*, 2016, 6 – 23 p.
- JENSSSEN T., KÖNIG A., ELTROP L. 2014. Bioenergy villages in Germany: Bringing a low carbon energy supply for rural areas into practice, *Renewable Energy*, 2014, 61, 74 – 80 p.
- KARSCHIN I., GELDERMANN J. 2015. Efficient cogeneration and district heating systems in bioenergy villages: an optimization approach, *Journal of Cleaner Production*, 2015, 104, 305 – 314 p.
- SCHMIDT J., SCHÖNHART M., BIBERACHER M., GUGGENBERGER T., HAUSL S., KALT G., LEDUC S., SCHARLINGER I., SCHMID E. 2012. Regional energy autarky: Potentials, costs and consequences for an Austrian region, *Energy Policy*, 2012, 47, 211 – 221 p.
- WAPPELHORST S. et al. 2014. Potential of electric carsharing in urban and rural areas *Transportation Research Procedia* 4, 2014, 374 – 386 p.
- CHEN J., SONG X. 2015. Economics of energy storage technology in active distribution networks, *J. Mod. Power Syst. Clean Energy*, 2015, 3(4), 583 – 588 p.
- RAMIREZ-DIAZ A., RAMOS-REAL F. J., MARRERO G. A. 2016. Complementarity of electric vehicles and pumped-hydro as energy storage in small isolated energy systems: case of La Palma, Canary Islands, *J. Mod. Power Syst. Clean Energy*, 2016, 4, 604 – 614 p.
- BERGMMANNA A., COLOMBOB S., HANLEY N. 2008. Rural versus urban preferences for renewable energy developments, *Ecological Economics*, 2008, 65, 616 – 625 p.
- MARČEV D., RŮŽIČKA M., LUKEŠ M., KOTEK M. 2015. Energy consumption of commuting from suburban areas, *Agronomy Research* 2015, vol.13, n.2, pp. 596 – 603.
- LUKEŠ M., KOTEK M., RŮŽIČKA M. 2015. Comparison of transport systems in rural and suburbanized areas with regards to energy consumption and travel speed, *Engineering for Rural Development* 2015, ISSN 1691-5976, pp. 342 – 347.
- <https://ec.europa.eu/energy/en/data-analysis/energy-statistical-pocketbook> PDF ISBN 978-92-79-70449-9 ISSN 2363-247X doi:10.2833/80717 MJ-AB-17-001-EN-N
- http://ec.europa.eu/clima/citizens/eu_cs New governance to deliver on objectives of the energy union 30. 11. 2016

Contribution has been prepared within the solving of scientific grant project IGA 2017: 31150/1312/3121 – Energy consumption for the transport of rural households – perspectives of electromobility

Corresponding author:

Miroslav Krumbholc, krumbholc@tf.czu.cz, Department of Vehicles and Ground Transport, Department of Physics, Czech University of Life Sciences Prague, Kamýcká 129, Praha 6, Prague, 165 21

ANALYSIS OF ROLLING RESISTANCE OF TYRES FOR AGRICULTURAL AND FORESTRY MACHINES ON PAVED SURFACES

ANALÝZA VALIVÉHO ODPORU PNEUMATÍK AGROLESNÍCKYCH STROJOV NA SPEVNENEJ PODLOŽKE

Michal Berák, Ján Kováč, Milan Helexa

*Fakulta environmentálnej a výrobnej techniky, Technická univerzita vo Zvolene, T.G.Masaryka 24,
960 53 Zvolen, e-mail: xberak@is.tuzvo.sk, kovac@tuzvo.sk, helexa@tuzvo.sk*

ABSTRACT: The main objective of rolling resistance analysis for agricultural machines and equipment on a reinforced surfaces is to compare different combinations of rolling resistance at different tire loads with different inflation pressures. This is accomplished by measuring the pulling force on a device which is then stored on a computer using software. Subsequently, Excel and Statistics are used to chart and graph the data and draw conclusions.

Key words: tyre rolling, rolling resistance, analysis, agricultural tyres

ABSTRAKT: Hlavným cieľom analýzy merania valivého odporu pneumatík pre agrolesnícke stroje a zariadenia na spevnenej podložke je porovnať rôzne kombinácie valivého odporu pri rôznom zaťažení pneumatík s rôzny hustiacim tlakom. Je to docielené meraním ľažnej sily na zariadení ktorá sa ukladá do počítača pomocou softwaru. Následne sú využívané programy Excel a Statistica ktoré slúžia na tabuľkové a grafické vyhodnotenie údajov a sformulovanie záveru.

Kľúčové slová: valenie pneumatiky, valivý odpor, , analýza, agrolesnícke pneumatiky

INTRODUCTION

The majority of used agro-forestry machines have a wheel chassis, as these chassis mostly correspond to the soil conditions in our area. In agro-forestry machines, these tires are subject to great strain, resulting from the growing performance of agro-forestry machinery. By choosing the right tire and inflation pressure, we can reduce rolling resistance, reducing wear and tear, reducing time to work and, in particular, reducing fuel consumption. An important advantage is the reduction of soil compaction, which is a very important factor in the use of heavy energy vehicles carried and towed. (Beneš P., 2009) (Antos G., 2009)

At present, the deformation properties of the entire tire are investigated by finite element method calculations. The predictive ability of the calculation results can only be verified by a real tire test. In addition, according to the test results, the calculation can be adjusted to allow calculations to be made more precise with regard to the input of material and other inputs. That is why it is very important for the tires to be tested. The endeavor is for the tests to be as close as possible to the actual load during operation and to make the results comparable to each other. (Bauer F. et al., 2013) (Lajbl L., Antos G., 2007)

Rolling Resistance Coefficient

The rolling resistance coefficient f is affected by several factors. The most important is the road surface. Other factors affecting the rolling resistance coefficient include deformation and wheel speed of the vehicle. For a tire with a low inflation pressure, deformation occurs to a greater extent than when the tire is inflated to a higher pressure. As the tire pressure decreases, the rolling resistance increases. This is due to a higher value of deformation and damping work. The last factor is the wheel speed of the vehicle. (Dočkal V., Kovanda J. and Hrubec F., 1998) (Bálimt Tóth J., 2011) (Delanne, Y. 1994) (Huang, J. 2011))

Experimental rolling resistance measurement

Measurement of tire rolling resistance is relatively simple. For this purpose, we use a guiding frame with side guides. The measurement is based on the drawing of the pulling force required to traverse the main and auxiliary guide frame of the wheel by means of the brake reel. The main sensed physical magnitude is in this case the pulling force required to pull the wheel and guide frame. This is captured by the HBM S9M sensor. (Helexa, 2012) (Bložon, 2008) (Schwalbe, 2011)

MATERIAL AND METHODS

The basis of our test facility is to guide the subframe. Its length is 9,000 mm, which can be extended to the required value by connecting other welded steel beams. The support rails are also fastened to the concrete floor of the laboratory by means of threaded anchors. This ensures its stable position and capture, in particular, the lateral and vertical forces acting on the subframe. The auxiliary frame (or lateral guide) serves to longitudinally guide the subframe, the main purpose of which is to guide the main support frame of the test wheel (s) in the straight line. The guide frame and the main frame with the wheel are connected together by means of four square bars. The main support frame of the wheel includes a wheel drive mechanism and also carries additional weights through which the wheel's vertical load can be changed. The main frame of the wheel itself has a weight of 222 kg, with the additional weight being increased up to 734 kg. The drive of the test wheel is provided by the Siemens 1LA7 133-4AA electric motor of 7.5 kW. The Siemens 1LA7 113-4AA winding electric motor with a power of 4 kW serves for the backward movement of the entire steering and wheel drive mechanism. A picture. (Helexa, 2012) (Grappe, F.; Candau, R.; Barbier, B.; Hoffman, M.D.; Belli, A. & Rouillon, J.D. 1999)

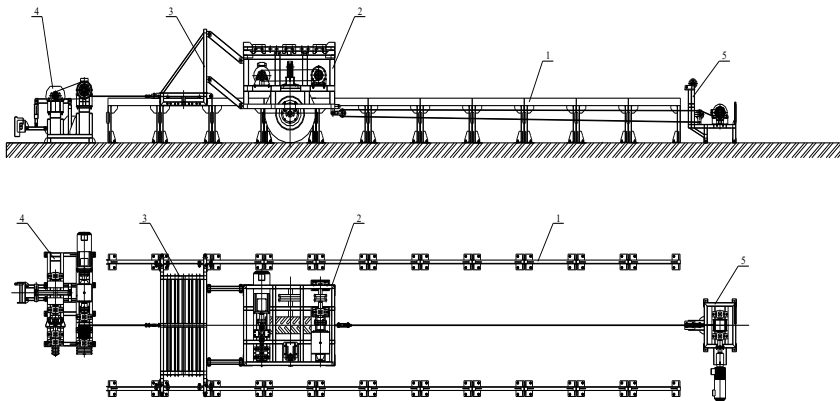


Fig. 1 Soil Testing Channel (Measurement on Concrete Floor)
 Side guides, 2. Main wheel support frame with drive, 3. Guiding frame, 4. Braking device,
 5. Reversing winch [Helexa, 2012]

Obr. 1 Kanál na testovanie pôdy (meranie na betónovej podlahe)
 1. Bočné vodiace lišty, 2. Rám nosného kolesa s pohonom, 3. Vodiaci rám, 4. Brzdové zariadenie,
 5. Reverzný naviják [Helexa, 2012]

Used tyres

Tires to carry out the measurement were selected by Mitas. Specific type of TS tread for agroforestry machines. From this series we used two models to measure. Specifically TS-04 and TS-05. We chose them mainly because of their availability and similarity because they are from the same manufacturer of the same type. Further, they have been selected for their appropriate dimensions for the device used and their parameters that are suitable for measurement.

Table 1 Technical data of Mitas TS-04 tires

Tabuľka 1 Technické údaje pneumatík Mitas TS-04

Casing size	6,00 – 16	Load Index / Speed Index	79/91 A8
PR	6 PR	Frame / Frame (allowed)	4.00Ex16/4.50Ex16
Profile Width (mm)	–	Outer diameter (mm)	735
Static radius (mm)	345	Effective circuit (mm)	2160
Weight (kg)	10	Load (kg)	–
Hose pressure (kPa)	280	Tubeless (TL) / Tubetype (TT)	TT
Inner tube / Inserts	6,00 – 16	EAN code	8590341017314

Table 2 Technical data of Mitas TS-05 tires

Tabuľka 2 Technické údaje pneumatík Mitas TS-05

Casing size	10,0/75 – 15.3	Load Index / Speed Index	111/122 A8
PR	10 PR	Frame / Frame (allowed)	9,00x15,3
Profile Width (mm)	264	Outer diameter (mm)	780
Static radius (mm)	360	Effective circuit (mm)	2295
Weight (kg)	20	Load (kg)	–
Hose pressure (kPa)	400	Tubeless (TL) / Tubetype (TT)	TL
Inner tube / Inserts	10-15 HS / 10/75-15	EAN code	8590341016874

RESULTS AND DISCUSSION

We used the Catman program from DAQ Software, which belongs to HBM, from which we also used the QuantumX MX840A signal strength and signal amplifier to guarantee compatibility and accuracy of measurement.

The accuracy of the measurement is given by the manufacturer of the silomer HBM S9N, namely 0.02%. So, in this case, we need to take into account the measurement deviation because it represents a negligible part of the result. We've set the scanning frequency from the sensor to 5Hz, so every second we get 5 values, which is enough because the main frame goes through the entire usable path of the device in about 40 seconds.

Measurement procedure

Put the selected tire on the main frame of the measuring device without using the drive and, after it has been inflated to the required pressure, weigh the main frame of the measuring device by weighing the necessary weight. We move the main and auxiliary frames using a winch to the starting position where the winch is disconnected and the rope is attached from the main winch, which is tensioned manually to reduce the vibrations of the trolley. On the computer, we run the measurement record and run the main reel until the trolley reaches the final position where the reel stops. We stop recording the measurement that we store and prepare for further measurement with other loads or other tire pressures.

Measuring parameters

Table 3 Mitas TS-04 tire input parameters

Tabul'ka 3 Vstupné parametre pneumatik Mitas TS-04

Tire inflation pressure [kPa]	Tire Load Size [kg]
100	222
150	350
200	478
250	542
300	606
	670

Table 4 Mitas TS-05 tire input parameters

Tabul'ka 4 Vstupné parametre pneumatik Mitas TS-05

Tire inflation pressure [kPa]	Tire Load Size [kg]
100	222
150	350
200	478
250	606
300	734

Calculation of measured data

For each measurement, we received approximately 200 values, and after reviewing, we found that the measured values had a scattering which is the smallest in 2 areas. This scattering can be caused by several factors. We can divide the values into 2 regions, namely A and B, and from each region we chose a 10 second section in which the values were the least scattered to maintain the highest accuracy and consistency of the measurement. As an example for the enclosed graph, we chose Range A for Area A between 16 and 26 seconds, and Area B ranges between 38 and 48 seconds.

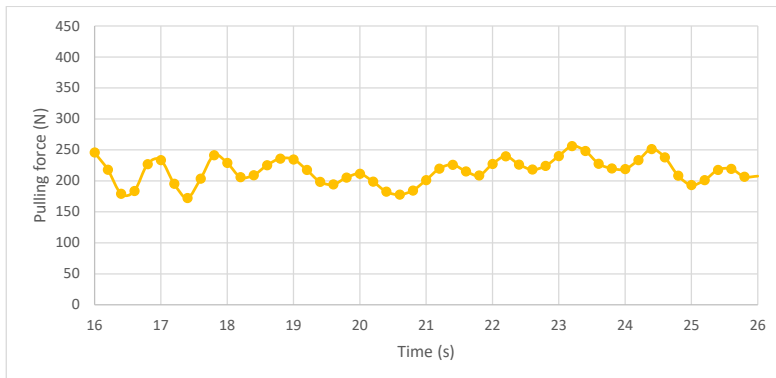


Fig. 2 Graph of values showing dependence of pulling force by time from area A

Mitas TS04 6,00 – 16 6PR p = 150 kPa, m = 478 kg

Obr. 2 Graf hodnôt zobrazujúci závislosťťahovej sily od času z oblasti A

Mitas TS04 6,00 – 16 6PR p = 150 kPa, m = 478 kg

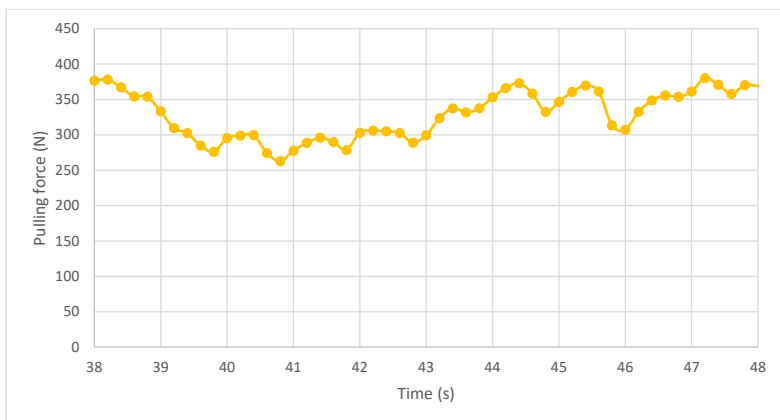


Fig. 3 Graph of values showing dependence of pulling force by time from area B

Mitas TS04 6,00 – 16 6PR p = 150 kPa, m = 478 kg

Obr. 3 Graf hodnôt zobrazujúci závislosťťahovej sily od času z oblasti B

Mitas TS04 6,00 – 16 6PR p = 150 kPa, m = 478 kg

Subsequently, we added values from each area to Statsoft's Statistica, which allowed us to calculate, for example, the mean and the standard deviation of the measured values. We used the values of the mean in the resulting graphs and we used the standard deviation values as a check. If the standard deviation value was too large, we did not match that measurement into a graphical representation. This situation can be considered a measurement error that is mainly due to the instability of the device's lateral guidance and non-repeat measurement. Finally, we used an area that had a smaller measurement error.

As a result, however, we only got the total resistance when pulling the trolley. To determine the magnitude of the rolling resistance, we still had to calculate all other resistances in the device and deduce them from the total resistance.

To calculate the resistance of the trolley, we proceeded as in the total resistance measurement. The only difference was that no tire was mounted on the main frame and was unloaded onto the guiding frame in order not to rush on the ground.

Evaluation of measurement results

We calculated the resulting calculated values visually into graphs for better interpretation. For the most appropriate evaluation of the results, we have chosen three types of dependencies that best show the dependence of the rolling resistors. To view the example, we chose the Mitas TS04.

Example 1

In the first example of the dependence of rolling resistance on wheel load at different inflation pressures, we should see a linear dependence on theoretical knowledge, where the roller resistance should also increase when increasing the load on the wheel. Along with the increasing inflation pressure, the resistance of the vane should decrease.

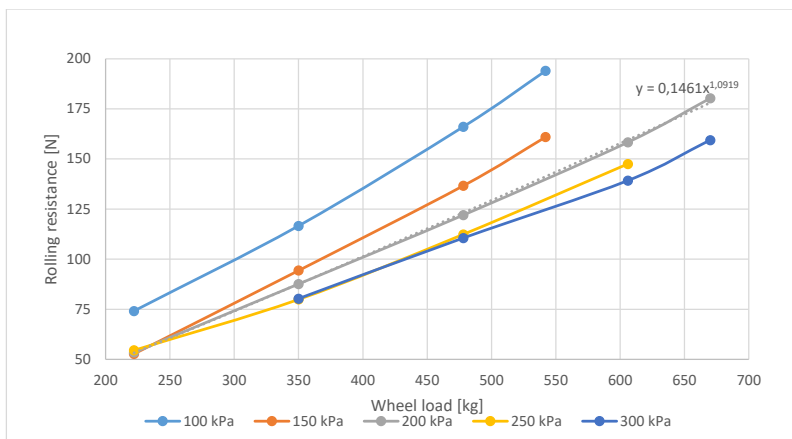


Fig. 4 Dependence of rolling resistance on wheel load

Mitas TS04 6,00–16 6PR A

Obr. 4 Závislost' valivého odporu na zaťažení kolesa

Mitas TS04 6,00–16 6PR A

As we can see in Fig. 4, the measurement has confirmed the theory and therefore, with increasing tire load, the rolling resistance is almost linear, and the rolling resistance decreases with the increasing inflation pressure. At the lowest tire pressure measured, the tire pressure is considerably higher at the lowest pressure, but at all other inflation pressures the rolling resistance does not change. This is due to the fact that, at low inflation pressures, most of the load is transmitted to the sidewall of the tire which in this case can not handle even a low load and its deformation results in an increase in rolling resistance. At higher inflation pressures, the sidewall is relieved to the extent that the increase in inflation pressure no longer reduces rolling resistance, as with higher loads. When measuring with a tire that has a stronger sidewall already this trend at a low load we can not see what we can confirm in the Fig. 4.

At the same time, the function of dependence on the pressure value of 200 kPa is still described in the graph, since it is the mean value of the pressure and should describe this dependence as accurately as possible.

$$y = 0,1461x^{1,0919} \quad (1)$$

Example 2

In the second example, the dependence of the rolling resistance on the tire inflation pressure. Here, according to theoretical knowledge, we should see the decreasing tendency of rolling resistance with increasing tire inflation pressure. At the same time with the increasing load, the rolling resistance should also increase.

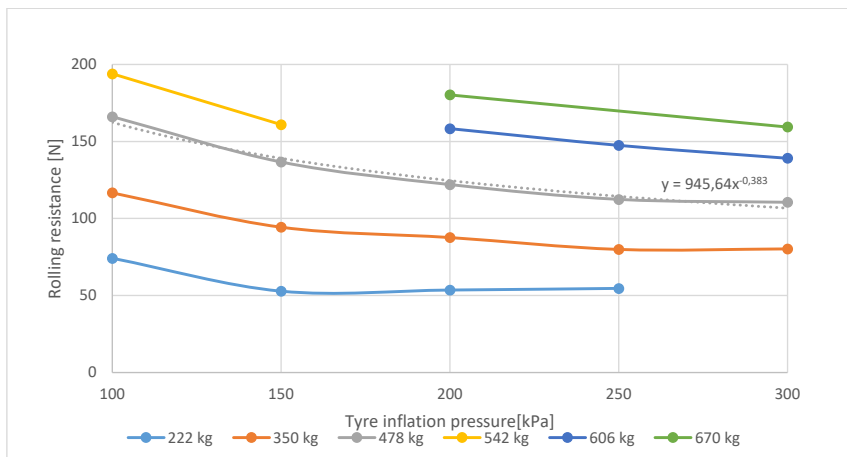


Fig. 5 Dependence of rolling resistance on tire pressure

Mitas TS04 6,00–16 6PR A

Obr. 5 Závislost' valivého odporu na tlaku v pneumatikách

Mitas TS04 6,00–16 6PR A

Figure 5 shows the confirmation of the theoretical part. Rolling resistance has a decreasing tendency with increasing tire inflation pressure. We can also see that, at lower loads, the inflation pressure value begins to stagnate from a certain inflation pressure value. This means that the tire is sufficiently infiltrated and has sufficient strength to prevent further deformation, and further pressure increases no longer affect the rolling resistance.

Also, a dependency function for a load of 478kg is described in the graph, since it is the average load value and should describe this dependence as accurately as possible.

$$y = 945,64x^{-0,383} \quad (2)$$

Example 3

In the latter example, we have the dependence of the rolling resistance coefficient on the inflation pressure of the tire, which is essentially the same as in the previous example, except that the rolling resistance is calculated on the tire load unit. According to theoretical knowledge, we should see the same dependence as in the previous example, namely the decreasing tendency of the rolling resistance coefficient with the gradually increasing tire inflation pressure. The roller resistance coefficient should remain the same with varying load.

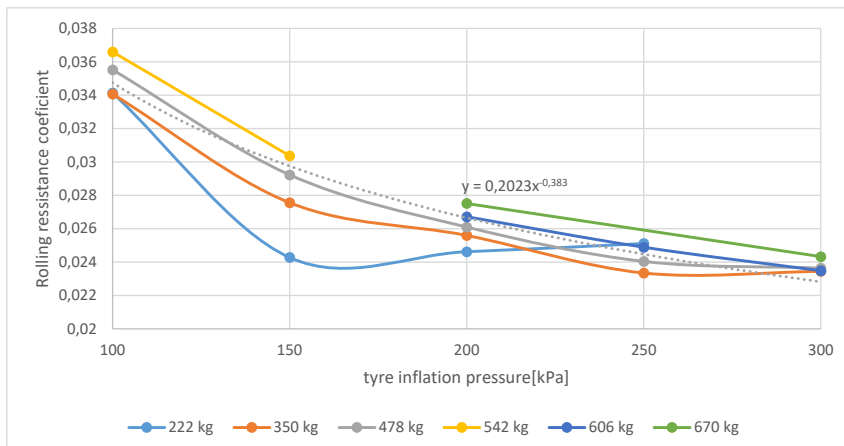


Fig. 6 Dependence Rolling resistance coefficient of tire inflation pressure

Mitas TS04 6,00–16 6PR A

Obr. 6 Závislosť Koeficient odporu valenia pneumatikového hľuku

Mitas TS04 6,00–16 6PR A

As we can see in Figure 6, the theoretical part is mostly confirmed and we see a very similar dependence as in the previous example. Values are scattered but not too large. This scattering may be due to less stability of the lateral guidance of the device when increasing the tire load. We can also see the measurement uncertainty at a load of 222kg. This inaccuracy is probably caused by the imperfectly flat surface of the laboratory on which the measurements were made, as the error occurred at a low load and in the previous example of dependence the error did not appear.

As in the previous example, the chart depicts a dependence function for a load of 478kg, since it is the average load value and should describe this dependence as accurately as possible.

$$y = 0,2023x^{-0,383} \quad (3)$$

Measurement errors

As with each measurement, this measurement also had measurement errors. Errors may have been caused mainly by the imperfections of the construction of the equipment and of the laboratory environment where the measurement was carried out. Errors have been attempted to remove the best of measurement by using the measured values averages and using the data from the two most steady areas of measurement.

CONCLUSION

Based on the theoretical knowledge gained in the first part, we were able to evaluate and compare the measured and calculated measurement data with theoretical values based on the calculations only. All the measured and calculated results were confirmed in all three cases.

In the first example, we have confirmed that the rolling resistance of the tire almost linearly increases with increasing load, but we can partially reduce it by increasing the inflation pressure in the tire. We have also found that the used Mitas TS04 tire has sufficient strength with a measured load of 222kg and a spraying pressure of 150kPa, where the rolling resistance value did not fall below a certain value even with increasing inflation pressure. It results from the fact that the tire's sidewall is strong enough and the tire has a low deformation so that it is not necessary to increase the inflation pressure above a certain value for a low load or a sufficiently rigid tire to reduce the rolling resistance.

The second example confirmed that the rolling resistance decreases with the increasing inflation pressure. However, at a certain value of the inflation pressure, rolling resistance stops falling and begins to stagnate. This value of inflation pressure is rising along with the increasing load.

In the third example, we came to the same conclusion as the second example. The only difference in these examples is the use of the rolling resistance coefficient instead of rolling resistance directly. This change should eliminate the tire load and the resulting coefficient values should be the same. We almost succeeded in measuring and computing. The resulting values of the rolling resistance coefficient are almost the same. Small differences in these values are likely to cause mistakes and measurement inaccuracies, even though we have tried to eliminate them as much as possible.

Measurement errors have occurred and are still visible for some measurements despite our efforts to eliminate them. Measuring the measurement values and collecting the seemingly best value ranges was not enough. The incompleteness of the laboratory environment, and especially the rigid substrate, contributed to inaccuracies and measurement errors. Another important factor of accuracy is the number of repeated measurements.

LITERATURE

- ANTOS G. 2009. Milyen a jó traktorgumi ? [online], Available at: <http://www.haszonagrар.hu/mezogepek/201-milyen-a-jo-traktorgumi.html>
- BAUER F. (ed.), 2013. Traktory a jejich využití. 2. vyd. Praha: Profi Press, 223 s. ISBN 978-80-86726-52-6
- BÁLIMT TÓTH J. 2011. A gumiabroncs lelke a légyomás, Agrárágazat, 2011/Prosinec, 62-66 s.
- BEKKER M.G., 1955. Theory of land locomotion [online]. Michigan: University of Michigan Press. Available at: <http://babel.hathitrust.org/cgi/pt?id=mdp.39015000986904;view=1up;seq=87>
- BENEŠ P. 2009. Přínos změny tlaku v pneumatikách [online]. [cit. 2018-04-23]. Available at: <http://zemedelec.cz/prinos-zmeny-tlaku-v-pneumatikach/>
- BLOŽON b. 2008. Testovanie kvality v gumárenskom priemysle. [online] [cit. 2017-06-02]. Available at: http://www.atpjournal.sk/rubriky/aplikacie/testovanie-kvality-v-gumarenskom-priemysle.html?page_id=7243
- DELANNE, Y. 1994. The influence of pavement unevenness and macrotexture on fuel consumption. American Society for Testing and Materials, 1225: 240-247.
- DOČKAL V., KOVANDA J. & HRUBEC F. 1998. Pneumatiky. Vydavatelství ČVUT, Praha, 71 s. ISBN 80-01-01882-2
- Firemný materiál. 2013. Mitas, Zemědělské pneumatiky, [online]. Available at: http://www.best-drive.cz/cs/download/52-mitas_agri_databook_cz_12th.pdf
- GRAPPE, F.; CANDAU, R.; BARBIER, B.; HOFFMAN, M.D.; BELL, A. & ROUILLO, J.D. 1999. Influence of tyre pressure and vertical load on coefficient of rolling resistance, 42(10): 1361–1371.
- HELEXA, M. 2012. Metodika merania valivých odporov pneumatikových kolies v pôdnom skúšobnom kanály. Zvolen: Technická univerzita vo Zvolene, 2012
- HELEXA, M. 2012. Návrh pôdneho skúšobného kanála pre skúšky pojazdových ústrojenstiev. Zvolen: Technická univerzita vo Zvolene, 2012
- HUANG, J. 2011. Tech feature: The work of wheel energy. Available at: [<http://www.cyclingnews.com/features/tech-feature-the-work-of-wheel-energy>].
- LAJB, L., ANTOS, G. 2007. A korszerű traktor gumiabroncsokról, Agrárágazat, 2007/Březen, 70–73 s.
- Rolling Resistance Tire Tester. [online] [cit. 2018-06-30].Available at: http://www.polinggroup.com/testing_end_rrt_tb.php
- SCHWALBE. 2011. Rolling resistance. Available at: [http://www.schwalbetyres.com/tech_info/rolling_resistance]. Retrieved on 19 March 2012.

This article was developed as part of the VEGA project no. 1/0642/18 „Analysis of the impact of structural parts of forestry mechanisms in the forest environment in terms of energy and ecology“.

Corresponding author:

Ján Kováč, tel. +421 45 5206 517, E-mail: jan.kovac@ituzvo.sk

DESIGN OF A DEVICE FOR VERIFICATION OF A HYDRAULIC PUMP OPERATION

KONŠTRUKCIA ZARIADENIA NA OVEROVANIE PREVÁDZKY HYDRAULICKÉHO ČERPADLA

Jozef Nosian¹, Marek Halenár¹ Peter Kuchar¹, Juraj Tulík¹,
Adam Fürstenzeller², Marian Kučera³

¹Department of Transport and Handling, Faculty of Engineering, Slovak University of Agriculture in Nitra, Tr. A. Hlinku 2, 949 76, Nitra, Slovakia, xnosian@uniag.sk,

²Department of Machine Design, Faculty of Engineering, Slovak University of Agriculture in Nitra, Tr. A. Hlinku 2, 949 76, Nitra, Slovakia, xfurstenzell@uniag.sk

³Department of Machine Design, Faculty of Engineering, Slovak University of Agriculture in Nitra, Tr. A. Hlinku 2, 949 76, Nitra, Slovakia, marian.kucera@uniag.sk

ABSTRACT: This article deals with the design of a hydraulic device that serves to verify the flow characteristics of the hydraulic pump. In this article is created design of device that is used to verify the characteristics of a hydraulic pump outside the tractor. This design to measure of the tractor hydraulic pump was used. Article aims is to verify the measurement of the proposed laboratory device. Laboratory tests and measurements were carried out in the laboratory of the Department of transport and handling, Faculty of Engineering, Slovak University of Agriculture in Nitra. By using the verification measurement, we have shown that the designed device is suitable for verifying characteristics of a hydraulic pump as well as for hydraulic pump testing. Measurement was performed at individual revolutions. Specifically at $n_1 = 500$ rpm, $n_2 = 750$ rpm, $n_3 = 1000$ rpm, $n_4 = 1250$ rpm and $n_5 = 1500$ rpm. By measuring, we found out the hydraulic pump flow at given speeds and then we calculated the pump efficiency. The highest efficiency was found at nominal revolutions ($\eta = 1500$ rpm), $\eta = 98,02\%$.

Key words: hydraulic pump, flow efficiency, flow characteristics.

ABSTRAKT: Tento článok sa zaobrá návrhom hydraulického zariadenia, ktoré slúži na overenie charakteristik prietoku hydrogenerátora. V danom článku je vytvorený návrh zariadenia, ktoré slúži pre overenie charakteristik hydrogenerátora mimo traktora. Tento návrh bol použitý na meranie hydrogenerátora použitého v traktoroch ZETOR. Cieľom je overiť meranie navrhovaného laboratórneho zariadenia. Laboratórne testy a merania boli vykonané v Laboratóriu Slovenskej poľnohospodárskej univerzity v Nitre na Technickej Fakulte. Použitím overovacieho merania sme preukázali, že navrhnuté zariadenie je vhodné na overenie charakteristik hydrogenerátora ako aj na testovanie hydrogenerátorov. Meranie sa vykonallo pri jednotlivých otáčkach. Konkrétnie pri $n_1 = 500$, $n_2 = 750$, $n_3 = 1000$, $n_4 = 1250$ a $n_5 = 1500$. Meraním sme zistili prietok hydrogenerátora pri daných otáčkach a následne sme vypočítali účinnosť čerpadla. Najvyššiu účinnosť sme zistili pri nominálnych otáčkach ($n = 1500$), $\eta = 98,02\%$.

Kľúčové slová: hydrogenerátor, prietková účinnosť, charakteristiky prietoku.

INTRODUCTION

Hydraulic systems have recently become an important means of modernizing and automating machines. He can develop enough strength to lifting, transmission and many other operations. The main goal is to transfer energy and reduce work requirements. Hydraulic devices have a broad upturn in the mechanisms of propulsion of agricultural and forestry machinery as well as in other areas. The development of hydraulic components is currently focused mainly on increasing energy transfer, reducing energy intensity, minimizing environmental pollution and increasing the technical life and reliability of the machine (Tkáč et al., 2008). Hydraulic pump operating conditions greatly affect pump efficiency, it is very important to understand how pump efficiency depends on operating conditions of the hydraulic pump (Inaguma and Yoshida, 2013, Rundo, 2017). Hydraulic mechanisms have several advantages over other mechanisms, the most important of which are high performance, good reliability and simplicity. The flow rate of the hydraulic pump is used to determine the hydraulics of the hydraulic pump. The working conditions of the hydraulic pump significantly affect pump efficiency, it is very important to understand how the pump efficiency depends on the operating conditions of the hydraulic pump (Inaguma and Yoshida, 2013, Rundo, 2017). Current trends present greater demands on hydraulic mechanisms. The aim of this article is to design a device for measuring the properties of a hydraulic pump. This device allows us to measure the flow characteristics to see if the hydraulic pump is correctly measured and mechanically or otherwise damaged.

MATERIAL AND METHODS

Hydraulic pump – is a source of pressure medium in the hydraulic circuit, which serves to drive hydro motors. The device is used to convert the mechanical energy of the rotary motion of the shaft into the kinetic and pressure energy of the fluid. We require sufficient flow and pressure from the hydraulic pump. The agricultural industry is mainly used for tractors that are used to create pressure in the tractor's hydraulic circuit. In designing a hydraulic laboratory device for testing hydrostatic pumps, it is based on the following calculations (Máchal et al., 2013, Kim and Kim, 2013, Hao et al., 2016):

- Internal diameter

$$d = \sqrt{\frac{4Q}{\pi \cdot w}}$$

Where:

$$Q - \text{flow rate } [\text{m}^3 \cdot \text{s}^{-1}], \quad (1)$$

W – energy [J],

- Wall thickness

$$S = \frac{p_{max} \cdot d}{2\sigma_{dov}} \cdot k \quad (2)$$

p_{max} – maximum pressure [Pa],

σ_{dov} – Allowing tensile stress [Pa],

k – Absolute roughness of the oven [m],

– Power of collar

$$P_v = \frac{\Delta T \cdot C_{01} \cdot \varrho_{01} \cdot V}{t_{.60}} \quad (3)$$

ΔT – temperature difference [°C],

C_{01} – capacity,

ϱ_{01} – consistency [kg·m⁻³],

V – bulk [m³],

– Tank area to remove heat produced

$$S_{CH1} = \frac{Q_\tau}{k_n \cdot \Delta t} \quad (4)$$

Q_τ – Total heat power [m³·s⁻¹],

k_n – Heat transfer coefficient [W·m⁻²·K⁻¹],

– Heat power

$$Q_{tn} = k_n \cdot S_n \cdot \Delta t \quad (5)$$

S_n – shallow waterreservoir [m²],

– Overall heat power

$$Q_\tau = P_s - Q_{tn} \quad (6)$$

P_s – power dissipation [W],

Q_{tn} – Heat delivered by the tank [°C],

STATISTICAL ANALYSIS

Standard deviation σ is defined as a positive square root of variance. Standard deviation is calculated if we have a complete set of possible states of the process (system). In probability theory and in statistics, standard deviation or mean square deviation is a measure of statistical dispersion. Simply said, it refers to how widely are the values distributed in a set (Hill and Lewicky, 2006).

$$\sigma = \sqrt{\frac{1}{n} \sum_{i=1}^n (x_i - \bar{x})^2} \quad (7)$$

where:

n – population size,

x_i – individual values of population,

\bar{x} – arithmetic average of population.

We say that a continuous random variable x has normal (Gaussian) distribution with parameters μ , σ^2 if density is:

$$f(x) = \frac{1}{\sigma\sqrt{2\pi}} \cdot e^{-\frac{(\bar{x}-\alpha)^2}{2\sigma^2}} \quad \text{for } x \in R, \alpha \in (-\infty, \infty), \sigma > 0 \quad (8)$$

where:

e – base of natural logarithm,

σ – standard deviation,

x – arithmetic average of population.

If a variable x has normal distribution with parameters \bar{x} , σ^2 , then, after transformation:

$$Z_i = \frac{x_i - \bar{x}}{\sigma} \quad (9)$$

where:

σ – standard deviation,

x_i – individual values of population,

\bar{x} – arithmetic average of population,

Z_i – variable with normal distribution,

The variable has normal distribution with mean value 0 and variation 1 (then standard deviation is also 1). This distribution is called as standardized normal distribution (Hill and Lewicky, 2006).

- When selecting a value from the range -1σ , $+1\sigma$, the probability of standard normal distribution is 68,27%;
- When selecting a value from the range -2σ , $+2\sigma$, the probability of standard normal distribution is 95,46%;
- When selecting a value from the range -3σ , $+3\sigma$, the probability of standard normal distribution is 99,73%.

We have chosen to evaluate the data of -1σ and $+1\sigma$ so that we obtain the values as close as possible to the nominal pressure of the hydraulic pump ($p = 16$ MPa). When choosing the range of -1σ and $+1\sigma$, the credibility of results is 68,27%. The flow efficiency of the hydraulic pump was calculated from this sample of values.

RESULTS AND DISCUSSION

In the present article a gear hydraulic pump was measured. The measured hydraulic pump is the UD 25 is a gearhead hydraulic pump. This hydraulic pump has a relatively wide range of geometric volumes, namely $V_g = 5 - 40 \text{ cm}^3 / \text{rpm}$. The pump achieves nominal working pressures up to 30 MPa. The measured hydraulic pump is used in the latest Zetor Forterra tractors. The device for verifying the characteristics of the hydraulic pump operation consists of two hydraulic circuits. The left hand side of the hydraulic circuit serves to drive the HP2 hydraulic pump. Three phases the HG 1 output is directly connected to the output of the HM (HP1 is a control axial piston pump). The change of flow rate on the HP1 hydraulic pump serves to adjust the velocity on the HP2 pump. In the case of high pressure, there is a risk of damage to the part of the circuit and the risk of damage to the device, which is why the pressure valves PV1 and PV2, which have a safety valve

function in this circuit, are included. The proportional pressure regulator PRV (from $p = 0$ MPa to $p = 20$ MPa) is used to adjust the pressure values. Make sure that all connections are watertight and do not run out of them, which could cause deformation of measurement and results. Check the functionality of individual sensors and sensors. Before we measure, we perform a verification test to determine the functionality of the device. Measurement took place at the Laboratory of the Slovak Agricultural University in Nitra. We measured the flow of UD 25 and its efficiency.

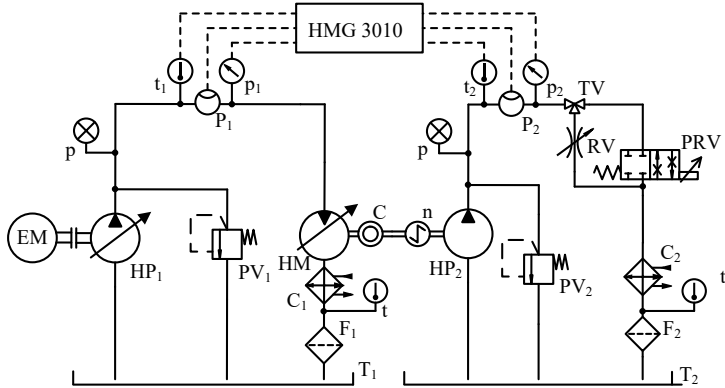


Fig. 1. Scheme of the laboratory testing device for hydraulic pump testing

Obr. 1. Schéma laboratórneho testovacieho zariadenia pre testovanie hydraulických púmp
 EM – elektromotor, HP_1 – regulárny hydraulický pumpe, PV_1 , PV_2 – tlakový ventil, HM – regulárny hydraulický motor, HP_2 – testovaná hydraulická pumpe, C_1 , C_2 – chladič, t – teplotný senzor pre nádoby, p – tlakomera, RV – smerujúci ventil, PRV – proporcionalny smerujúci ventil, C – spojka, n – otáčkový senzor, t_1 , t_2 – ETS 4148-H-006-000 teplotné senzory, P_1 , P_2 – EVS 3108-H-0300-000 prúdové senzory, p_1 , p_2 – HDA 4748-H-0400-000 tlakové senzory

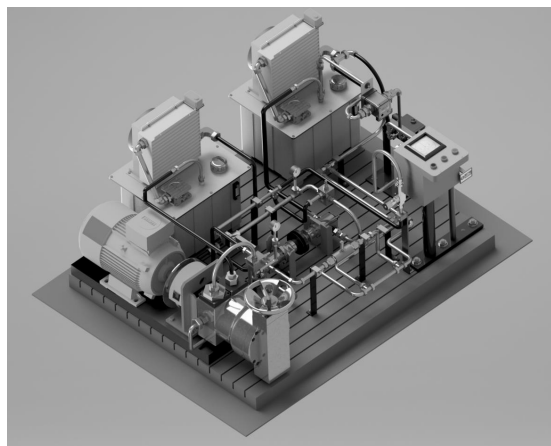


Fig. 2. Testing device for the measurement of hydraulic pump characteristics
 Obr. 2. Testovacie zariadenie na meranie charakteristiky hydraulickej pumpy

Table 1. Technical parameters of hydraulic pump UD 25
 Tabuľka 1. Technické údaje hydraulickej pumpy UD 25

Parameter	Unit	Value
Rated speed	$[min^{-1}]$	1500
Maximum speed		3000
Minimum speed		500
Maximal pressure at the inlet	$[MPa]$	0,05
Minimum inlet pressure		0,03
Nominal outlet pressure	$[MPa]$	20
Maximum outlet pressure		23
Geometric volume	$[cm^3]$	25
Maximum oil viscosity	$[mm^2 \cdot s^{-1}]$	1200
Minimum oil viscosity		10
Maximum oil temperature	$^{[^\circ C]}$	80
Minimum oil temperature		-20

Table 2. Measured values
 Tabuľka 2. Namerané hodnoty

Speed of rotation n , $[rpm]$	Number of measurements flow Q , $[dm^3 \cdot rpm]$			Average flow Q , $[dm^3 \cdot rpm]$	Efficiency η , [%]
	1	2	3		
500	11.93	11.73	11.51	11.72	93.76
750	18.47	17.72	17.55	17.91	95.52
1,000	24.02	24.16	24.09	24.09	96.36
1,250	30.74	30.52	30.35	30.53	97.69
1,500	37.02	36.6	36.67	36.76	98.02

$$\text{Average flow: } x = \frac{\sum_{i=1}^n x_i}{n} = \frac{11.93+11.73+11.51}{3} = 11.72 \text{ dm}^3 \cdot \text{rpm} \quad (10)$$

$$\text{Efficiency: } \eta = \frac{Q}{V_G \cdot n} \cdot 100 = \frac{11.72}{0.025 \cdot 500} = 93.76\% \quad (11)$$

The flow hydraulic pump efficiency was calculated from the measured flow characteristics (Tkáč et al., 2010):

$$\eta_{pr} = \frac{Q}{V_G \cdot n} \cdot 100 \quad (12)$$

where:

Q – hydraulic pump flow, $\text{dm}^3 \cdot \text{rpm}$

n – nominal speed of hydraulic pump, $1 \cdot \text{rpm}$

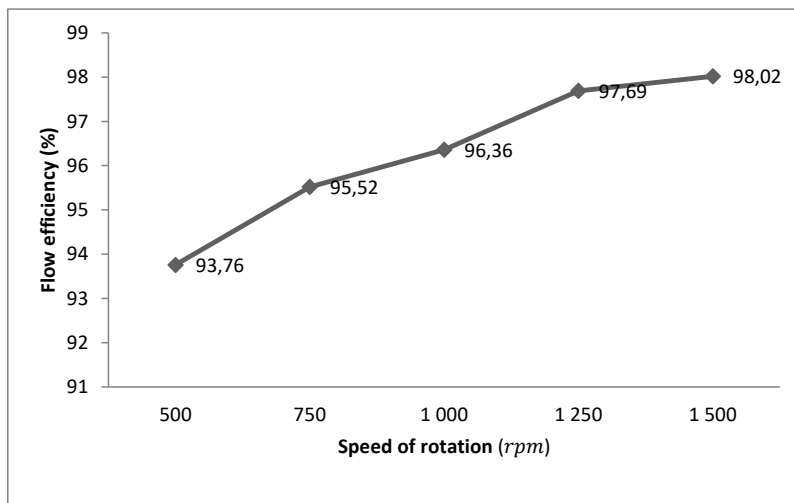


Fig. 3. Flow rate depending on individual revolutions

Obr. 3. Rýchlosť prúdenia závislá na otáčkach

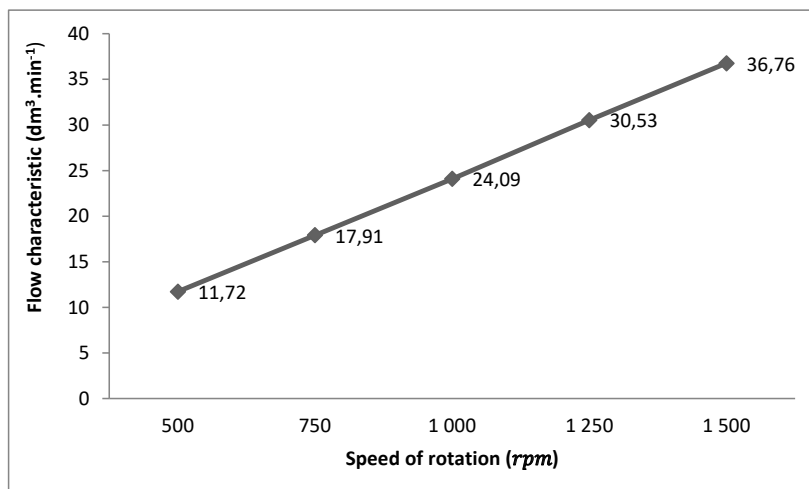


Fig.4. Flow characteristic of hydraulic pump

Obr. 4. Charakteristika prúdenia hydraulickej pumpy

Before the measurement, make sure that all connections are watertight and do not leak from them, which would distort the measurement itself and the results.

The measurements were made at five different rotation speed of the UD 25 hydraulic pump, at the rotations speed $n_1 = 500$, $n_2 = 750$, $n_3 = 1,000$, $n_4 = 1,250$, $n_5 = 1,500$.

For individual measurements for a given hydrogenerator rotations, the flow efficiency of the non-pressure system was calculated. The flow efficiency was:

$$\eta_{pr500} = 93,76 \%$$

$$\eta_{pr750} = 95,52 \%$$

$$\eta_{pr1000} = 93,36 \%$$

$$\eta_{pr1250} = 97,69 \%$$

$$\eta_{pr1500} = 98,02 \%$$

During the measurements, we found that the efficiency of the hydraulic pump increases with increasing speed. This means that the UD 25 works best at rotating speed $n = 1500$ rpm. We have found that the hydraulic pump flow increases as the speed increases. Dobrota et al. (2010) evaluated the efficiency of the hydraulic pump flow rate at rated speeds $n = 95,73\%$ depending on the pressure $p = 20$ MPa and Michael et al. (2012) evaluated flow efficiency at nominal speed $n = 95,00\%$. These values corresponded to our results.

CONCLUSION

Farm machinery manufacturers have recently tried to introduce into hydraulic systems new plant- or synthetic-based fluids and oils that are more environmentally friendly, decomposable and less damaging to water resources (Molari and Sedoni, 2008). The device for measuring the characteristics of the hydraulic pump serves to verify the flow rate as well as to measure the efficiency. These two parameters are the most important. Thanks to this device, we can also detect the damage or leakage of individual elements. The device serves to diagnose the hydraulic pump. The proposed laboratory equipment greatly facilitates the testing and assessment of the use of various energy carriers in hydraulic systems of tractors and optionally provides an opportunity to assess the effects of energy carriers on the properties of hydraulic circuit components. The laboratory equipment may also be used to compare the properties of the individual energy carriers under the same conditions.

LITERATURE

- ASAFF, Y., DE NEGRI, V.J., THEISSEN, H., MURRENHOFF, H. 2014. Analysis of the Influence of Contaminants on the Biodegradability Characteristics and Ageing of Biodegradable Hydraulic Fluids. *Strojniski Vestnik – Journal of Mechanical Engineering*, 60(6): 417-424.
- DOBROTA, D., LALIĆ, B., ORŠULIĆ, M. 2010. Experimental modelling of volumetric efficiency of high-pressure external gear pump. *Nase More*, 57(5-6): 535-240.
- HAO, X., ZHOU, X., LIU, X., SANG, X. 2016. Flow characteristics of external gear pumps considering trapped volume. *Advances in Mechanical Engineering*, 8(10): 1-10.
- HILL, P., LEWICKY, T. 2006 Statistics: Methods and applications. Statsoft Inc., Tulsa USA.
- INAGUMA, Y., YOSHIDA, N. 2013. Mathematical analysis of influence of oil temperature in hydraulic pumps for automatic transmissions. *SAE International Journal of Passenger Cars – Mechanical Systems*, 6(2): 786-798.
- KIM, J. H., KIM, S. G. 2013. The flow rate characteristics of external gear pump for EHPS. *4th International Conference on Intelligent Systems, Modelling and Simulation*: 346-349.
- KOSIBA, J., JABLONICKÝ, J., BERNÁT, R., KUCHAR, P. 2016. Effect of ecological hydraulic fluid on operation of tractor hydraulic circuit. In *Trends in agricultural engineering 2016*. 1st ed.: 317-322.

- MÁCHAL, P., TKÁČ, Z., KOSIBA, J., JABLONICKÝ, J., HUJO, L., KUČERA, M., TULÍK, J. 2013. Design of a laboratory hydraulic device for testing of hydraulic pumps. *Acta Universitatis Agriculturae et Silviculturae Mendelianae Brunensis*. 61(5): 1313-1319.
- MAJDAN, R., ABRAHÁM, R., HUJO, L., MOJŽIŠ, M., JÁNOŠKO, I., VITÁZEK, I., 2012. Technical condition of a tractor hydraulic pump during hydraulic fluid tests. In *Acta technologica agriculturae vol 15, 2012 no. 1, p.s. 12-15. ISSN 1335-2555.*
- MAJDAN, R., CVÍČELA, P., BOHÁT, M., IVANIŠOVÁ, K., 2008. The observation of hydrostatic pump deterioration during the durability test according to hydraulic fluids contamination In *X. International conference of young scientists 2008: Conference Proceedings, Czech Republic. - Prague: Czech University of Life Sciences Prague, 2008. - ISBN 978-80-213-1812-0. - S. 147-153*
- MICHAEL, P.W., KHALID, H., WANKE, T. 2012. An Investigation of external gear pump efficiency and stribbeck values. *SAE Commercial Vehicle Engineering Congres*.
- MOLARI, G., SEDONI E. 2008. Experimental evaluation of power losses in a power-shift agricultural tractor transmission. *Biosystems Engineering*, 100(2): 177-183.
- NIKOLIČ, R., SAVIN, L., FURMAN, T., TOMIĆ, M., SIMIKIĆ. 2005. : Koncepcije traktora I pogonskih mašina, Traktori I pogonskej mašine, (2005) 2, 16-24
- RUNDO, M. 2017. Theoretical flow rate in crescent pumps. *Simulation Modelling Practice and Theory*, 71(1): 1-14.
- TKÁČ, Z., DRABANT, Š., MAJDAN, R., CVÍČELA , P. 2008. Testing stands for laboratory tests of hydrostatic pump of agricultural machinery. *Research in Agricultural Engineering*, 54(1): 183–191.
- TKÁČ, Z., MAJDAN, R., DRABANT, Š., JABLONICKÝ, J., ABRAHÁM, R., CVÍČELA, P. 2010. The accelerated laboratory test of biodegradable fluid type „ertto“. *Research in agricultural engineering*. 56(1): 18-25.
- TKÁČ, Z., KOSIBA, J., HUJO, L., UHRINOVÁ, D., ŠTULAJTER, I. 2014. Hydraulic laboratory devices for testing of hydraulic pumps. *Advanced Materials Research*, 1059 (special. iss.): 111–117.

1/0155/18

Aplikovaný výskum využívania ekologických nositeľov energie v polnohospodárskej, lesníckej a dopravnej technike

Corresponding author:

Jozef Nosian, 0914 147 356, e-mail: xnosian@uniag.sk

REFERÁTY

USE OF HARVESTER HEADS IN FORESTRY

VYUŽITIE HARVESTOROVÝCH HLAVÍC V LESNÍCTVE

Veronika Ľuptáčiková, Richard Hnilica

Department of Manufacturing Technology and Quality Management, Faculty of environmental and manufacturing technology, Technical university in Zvolen, Študentská 26, 960 53 Zvolen, Slovenská republika, luptacikovav@gmail.com, hnilica@tuzvo.sk

ABSTRACT: The main reason for the development of logging and transport machines in Slovakia was their application to the processing of wood in random mining. Harvesting and processing of trees by the harvester takes place in a continuous workflow with a synchronized follow-up on the material transport tractor. The task of the Harvester Head is to span the tree, branch it, cut the tree to the specified length, and save it to the gathering. Branching is one of the most profitable operations of the mining and production process. The branches of the tree trunk serve the branch mechanism, which is the most common knife. These are basically hyperbolically shaped knives stored in the head or telescopic boom. Most harvester heads have three knives, one fixed and two movable. Between these knives they are cut off by the pulling of the branch of his branch. Therefore, the cutting blades should be able to best duplicate the shape of the strain.

Key words: branching, cutting blades, harvester head, strain

ABSTRAKT: Hlavným dôvodom rozvoja ťažbovo-dopravných strojov na Slovensku bolo ich násadenie na spracovanie dreva v náhodných ťažbách. Vyrúbanie a spracovanie stromov harvestorom prebieha v kontinuálnom pracovnom postupe so synchronizovanou nadväznosťou na traktor vykonávajúci odvoz materiálu. Úlohou harvestorovej hlavice je spliť strom, odvetvíť, narezat' strom na zadanú dĺžku a uložiť ho na zhromažďisko. Odvetvovanie je jedna z najprácejších operácií ťažbovo-výrobného procesu. Na odvetvenie kmeňa stromu slúži odvetvovací mechanizmus, ktorý býva najčastejšie nožový. Jedná sa o podstate o hyperbolicky tvarované nože, uložené v hlavici, prípadne na teleskopickom výložníku. Väčšina harvestorových hlavíc má tri nože, jeden pevný a dva pohyblivé. Medzi týmito nožmi sa pretáhovaním kmeňa jeho vetvy odrezávajú. Preto by odvetvovacie nože mali byť schopné čo najlepšie kopírovať tvar kmeňa.

Kľúčové slová: odvetvovanie, odvetvovacie nože, harvestorová hlavica, kmeň

INTRODUCTION

The main reason for the development of mining and transportation machines in the Slovak Republic was their application to the processing of wood in random mining. In

the Slovak Republic there was a change in the mining methods by eliminating the consequences of the endemic calamities in 2004. The first advantages and disadvantages of the harvester technologies were reflected here. One of the advantages was the smaller handling capacity and the labor force savings compared to manual technology by up to 70.5%, as well as the rapid and easy transfer of technological units. On the other hand, the application of harvester technology has led to an increase in production costs of up to 35.5% and the impossibility to perform a good wood preservation (Malík, V. et al., 2007).

MATERIAL AND METHODS

The harvesting and processing of trees by the harvester (Fig. 1) takes place in a continuous operation with a synchronized follow-up on the material-carrying tractor (Kalinčová, D. et al., 2016).



Fig. 1 Harvester JOHN DEERE 1470G (MERIMEX)
Obr. 1 Harvester JOHN DEERE 1470G (MERIMEX)

First, the trees are ripped off on tracks to prevent machine passages with subsequent mining interventions in the working field of the plant. Trees are harvested, harvested, cut in the length of the required assortments and deposited most often perpendicular to the export line, always on the other half of the work field than they were harvested. The angle of rotation of the pile axis to the axis of the line does not affect the efficiency of the tractor's work when exporting timber. Piles of export lines are always assembled from one assortment. Branches contain the rest of the branches on the line of export, the root system and the roots of the root line. Through the tick carpet, the machine pressure is evenly decomposed on the soil substrate and the risk of damage to the soil surface is reduced, as well as the damage of the ground-level trees (Dvořák, J. et al., 2011).

RESULTS

The task of the Harvester Head is to span the tree, branch it, cut the tree to the specified length, and save it to the gathering. There are a number of design variants of the heads. The heads are different in particular by the thickness of the treated wood, the shape and number of cutting blades, the type of feeding device, the way of measuring the lengths and thicknesses, the arrangement of the cutting part (Kováč, J. et al., 2017).

A typical harvester head (Fig. 2) consists of a chain or blade undercutting mechanism. Nowadays, however, the chain mechanism is used because it is lighter and does not pull the wood fibers on the cutting surface, does not cause cracking and pulping in the cutting area. The saw is driven hydraulically. It has a more robust chain and higher performance than any other chain that can be handled by humans (Neruda, J., 2013). There are also two or more bent cutting blades that remove the branches along the perimeter of the tree. From their curvature depends on the quality of branching as well as on the two rotating feeders working with the strain in the horizontal position. Feeders can be belt or wheel with different types of steel spikes. The side pins on the sides allow the tree to be clamped with the harvester head. The wheels rotate to force the cut tree to pass through the cutting blades (Neruda, J. et al., 2006).

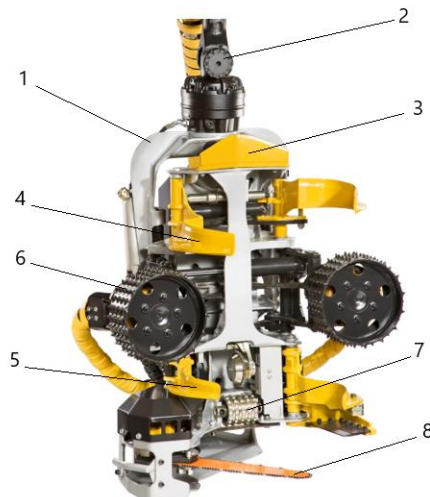


Fig. 2 Harvester head 1 – rigid head frame, 2 – rotor, 3 – fixed cutting knife, 4 – upper moving cutter blade, 5 – lower moving cutter blade, 6 – feed roller rotors, 7 – chain) (Kováč, J. et al., 2017)

Obr. 2 Harvesterová hlavica 1 – pevný rám hlavice, 2 – rotátor, 3 – pevný odvetvovací nôž, 4 – horný pohyblivý odvetvovací nôž, 5 – dolný pohyblivý odvetvovací nôž, 6 – podávacie valcové rotátory, 7 – koliesko na meranie dĺžok, 8 – rezacia jednotka (reťazová) (Kováč, J. et al., 2017)

At the end of the hydraulic crane, a rotor is installed to allow rotation at an angle of up to 280° due to the presence of a hydraulic line. Some rotators allow even continuous rotation (Neruda, J., 2013). The rotor is a suspended steel frame of a rectangular profile and there is a harvester head that ensures the operation of the mining and complex processing

of the tree. Upon arrival of the harvester near the tree, the harvester head is mounted on a tree trunk by a crane, above the rootstocks, the tree is gripped by moving cutting blades and feed rollers. Slicing knives that have an arched construction at this time fill the grab function. The cutting of the tree is followed by a saw blade, the tilting of the tree into the working position, which is enabled by a rotational bearing in the frame of the head which is still vertical (Ulrich, R., 2006). The other steps are the branch which is carried out by pulling the stem through the cutting blades at a speed of about 5 m.s⁻¹ thanks to the feeding device and the truncation of the strain to individual assortments (Malík, V. et al., 2007).

At present, there are two basic types of heads, Swedish and Finnish. The Swedish type heads are designed to work with long and straight stems, so their construction is more robust and has a longer base frame than the other type of head. It is equipped with two feed rollers (Ulrich, R., 2006). On the contrary, the Finnish-type head is characterized by a more compact structure, has a shorter base frame that is also capable of working with curved stems. The feedrate of the strain is secured by four feed rollers, which however do not have as much pulling force as in the Swedish-type head. Its lower weight facilitates manipulation with the crane (Neruda, J., 2013).

The harvester heads can also be used with wheeled or tracked chassis, where conventional accessories such as a spoon behind a drill head are shaken. However, the machine must be equipped with a system in the cab to allow the head to be controlled (Krilek, J. et al., 2013). The use of these machines is then found either on saws or forks where they are thus cut to shorter sections of the strain that are the output of the stock mining method for further processing or transport. For the needs of smaller ribs, the connection of the mining heads with the hydraulic crane fitted in the three-point hitch of the tractor is also used (Mikleš, J., 2017).

In order for the head to perform the required operations, it is equipped with the following mechanisms (Ulrich, R. et al., 2002):

- Sawing mechanism,
- Feed mechanism,
- Branching mechanism,
- Measuring, marking and other mechanisms.

Sawing mechanism

The sawing mechanism serves to trim the tree and direct the tree to the desired direction.

At present, most of the heads are equipped with a chain saw. Their precursors are hydraulic shearing knives, which are suitable for small stem diameters up to 30 cm. Some types are suitable for processing trees up to 50 cm in diameter. Today, it can be used, for example, in the processing of fast-growing woods, when one strain is multiplied by multiple strains at the same time or when preprocessed (Mikleš, M. et al., 2012). In order to make redundancy more efficient, they can be used on the hydraulic crane forklift instead of the grabber, when the spliced trees are loaded into the cargo compartment of the machine directly by the shearing head. They are also referred to as scissor heads or energy firing heads. Most of these heads are not capable of spinning. Other predecessors are the saw

blade heads. However, the saw blades were of incomparable dimensions to the diameter of the tree to be processed. The advantage of the two technologies to chain sawing is easy maintenance and simple construction (Neruda, J., 2013).

The chain saw itself consists of a 0,404 „or $\frac{3}{4}$ “ chain consisting of planing teeth, guides and connecting links. The chain is guided in the guide bar, which can reach up to 1320 mm in the most powerful machines and is usually made of alloy steel. The width of the guide groove is between 1.6 and 2 mm and there are guides and a single sprocket that is driven by a hydraulic motor, which results in the chain movement itself (Ulrich, R., 2006). The direct hydraulic motor ensures that the entire guide bar is tilted when cutting. The lubrication is carried out with oil from a separate tank and is always switched together with the chain drive motor (Kučera, M. et al., 2009). The hydrogenerator is located on a base machine from which the oil is supplied via a hose lead to a harvester head to control the drive and move the chain. The line includes two piping, pressure and return. The problem can arise at a great distance between the hydrogenerator and the harvester head (length loss of conduction), the distance of the conductor in the harvester machines can be up to 20 m (according to the size of the hydromanipulator) (Kováč, J. et al., 2017).

The chain is very prone to damage when cutting low on the ground when it may come into contact with stones or soil. Large wear also occurs in contact with sandy soil that contains fine grain sand and it gets into functional parts of the chain.

Feed mechanism

The feed mechanism provides for the longitudinal displacement of the spliced strain between the individual operating mechanisms.

In practice, we can meet the following types (Ulrich, R. et al., 2002):

- cylindrical,
- belt.
- telescopic.

The rolls are most often installed on the movable arm and the drive is secured by the rotary hydraulic motor for each cylinder separately. The cylindrical type is most commonly all metal with flat or conical spikes or ribs on the cylinder surface. The disadvantage of their use is damage to the surface of the strain in the form of imprints and scratches, therefore they are used where this damage does not matter (Malík, V. et al., 2007). On the other hand, they are characterized by a good transmission of the sliding force on the strain, which makes it impossible for the branches to be branched. They have a long service life. In cases where emphasis is placed on a good surface of the pulling assortment, rollers made of a steel rim and a rubber-coated sheath are used. This can be screwed, glued or pressurized to the hoop. For sufficient power transmission, angled anti-skid chains or a presser-tipped layer are used on the surface. However, the chains are more wear-free than the spikes and are pushed into the rubber surface, which leads to its damage (Neruda, J., 2013). For these reasons, it is necessary to perform more thorough maintenance, check the tension of the chain and, in case of wear, ensure replacement. The advantage of this is to reduce the head load in case of sudden shocks and thus to prolong their life, on the other hand the head has a higher weight. Another option is the rollers in which the surface is composed of metal bodies carried on the pins. This movable body arrangement allows

copying of the stem shape and their individual replacement in case of damage (Ulrich, R., 2006).

The belt feed device consists of one pair of belts made of steel members. The belts are located on two rollers, one of which provides tensioning and a second torque transfer from the rotary hydraulic motor. The advantage is the good quality of the timber surface and the less incline of the trunk. Both of these benefits are due to a greater contact surface. However, this results in the use of straight trees for straight trees. The disadvantage is the complexity of construction and larger dimensions (Malík, V. et al., 2007).

The last solution is the telescopic feeding device. The mining head is equipped with a telescopic arm with splitting knives. The suction procedure is as follows: „By pulling the telescopic arm is a branch of the tree. After the shoulders are pulled, the stem is firmly gripped by the front knives and the head is attached to them. With the attachment of the head, the branched strain is measured and the assortment is performed. The process is repeated until the tree is completely processed. „(Ulrich, R. et al., 2002).

Straightening mechanism

The spinning mechanism serves to branch out the tree trunk. It is usually assembled from two knife blocks having a triangular profile with a 35° cut angle. The blades are equipped with a blade on both sides, allowing the branch to be removed when the stem is moved in both directions. The mechanism of separation of branches from the strain operates on the principle of pressure. Its size depends on the thickness of the trunk and is controlled from the cabin. Knife sharpening is done manually by a file. Occasionally it is necessary to overcome the curve sections of the knife strain, which is made possible by direct hydraulic motors. If it is necessary to separate branches of larger diameters or larger densities, it is possible to use the pre-branch function. The head thus forms a predetermined lengthwise stretch without branches, in order to create a free path without obstacles for the start of the next shift (Mikleš, J., 2017).

Measuring, marking and other mechanisms

The metering mechanism serves to automatically measure the length and diameter of the tree to be processed. The measuring device performs a prognosis of the profile of a logging trunk from the stem of the logging tree at the main section and specifies it with the movement of the stem by the head. Based on the forecast, a new forecast is made.

The length of the strain is measured by the spur gear. It is rolling along a trunk with a minced head. With the rotation of the wheel, the impulses are registered, which is the specified length unit. From the number of pulses, the calculated tree length or assortment is needed to calculate the volume. Measurement is performed with an accuracy of one centimeter (Malík, V. et al., 2007).

Uncertainty of measurement can occur with tooth wear, poorly calibrated, in exceptional cases with shifted bark after the triangle in which the wheel is trapped, or in the case of the humpiness of the strain where the wheel passes through unevenness. To reduce the inaccuracy during the sinks, a wider wheel is installed or two wheels are installed on the shaft next to each other. Modifications of the measuring wheels are also possible for other specific properties of the treated woods, which may be, for example, strong storm.

The stem diameter is measured in two perpendicular directions at the ten-centimeter intervals that are averaged. Thickness sensing is performed by sensors (potentiometers) responsive to the movement of the blades or feed rolls located in the fold of the arms of the front blades or feed rollers. Signals resp. the voltage from the transmitter passes into the electronic unit and then into the operating system where it is transformed to thickness (Kováč, J. et al., 2017).

Modern harvesters are equipped with an automatic system for measuring the lengths and thicknesses of the treated strain. For the measurement of lengths, a gearwheel is mounted in the harvester head, which during the movement of the strain copies the stem surface and derives the length of the strain from the number of turns of the wheel. The thickness of the strain is derived from the size of the cutting down of the lower cutting blades that surround the stem. It is measured using a potentiometer located in the harvesting arm blades of the harvester head on the basis of the measured voltage in the potentiometer. The measurement and evaluation systems allow you to calculate the volume produced by the type of wood, thickness, length and quality. This data is captured on the harvester's computer and later can be used for further processing. Frequent problems with the wheel of the sensor of the length measuring device are often encountered during the operation of the head, as small pieces of wood accumulate in the wheel space, which impair its functionality. At present, almost all harvester manufacturers offer computer-controlled measurement and evaluation systems (Malík, V. et al., 2007).

In order to better distinguish similarly sized assortments, the mining heads may be provided with a marking device which identifies the loaded material on the front with two different colors or combinations thereof. Paint application is solved through nozzles in saw blades or cutting blades.

Further, a coniferous protection system can be utilized to dispense urea or other alternatives to the feed through the nozzle in the guide bar to prevent rot. (Neruda, J., 2013.)

DISCUSSION

The article describes the use of harvesters in forestry technology. In particular, the individual parts of the harvester head are mentioned. Specifically, they are a siphon mechanism, a feeding mechanism, a vane mechanism, and a metering and tagging mechanism. For each of them, a short section is given in the article, which mentions their basic characteristics.

CONCLUSION

At present, the technical level of the machinery used in forestry technology has seen a significant shift forward. This is achieved mainly through the introduction of automation, mechanization and information and communication technologies into forestry. The current development of technology in the world is focused on the constant improvement and application of new mechanical and electronic elements, including elements utilizing the positioning of machines. The article shows the basic use of harvesters in forestry technology. In the article, the individual parts from which the harvester heads are comprised are also brought closer together.

LITERATURE

- DVOŘÁK, J., BYSTRICKÝ, R., HOŠKOVÁ, P., HRIB, M., JARKOVSKÁ, M., KOVÁČ, J., KRILEK, J., NATOV, P., NATOVOVÁ, L. 2011. The use of harvester technology in production forests. Kostelec nad Černými lesy: Lesnická práce, 2011. 156 s. ISBN 978-80-7458-018-5.
- Company MERINEX s. r. o.: supplier of forest and mobile technology. Online: <<https://www.merimex.cz/john-deere/stroje-john-deere/harvestory/john-deere-1470g/>>.
- KALINCOVÁ, D., ŤAVODOVÁ, M., HNILICOVÁ, M., VEVERKOVÁ, D. 2016. Machinery for forest cultivation – increase of resistance to abrasive wear of the tool. In *MM science journal*. 2016. s. 1269 – 1272. ISSN 1803-1269.
- KOVÁČ, J., KRILEK, J., JOBBÁGY, J., DVOŘÁK, J. 2017. Technika a mechanizácia v lesníctve, 2017. 354 s., ISBN 978-80-228-3021-8.
- KRILEK, J., KOVÁČ, J. 2013. Energetická náročnosť sekacích strojov. Zvolen: vyd. TU Zvolen, 2013. 101 s. ISBN 978-80-228-2586-3.
- KUČERA, M., HELEXA, M. 2009. Hydrostatické mechanizmy. Zvolen: Technická univerzita vo Zvolene, 2009. 100 s. ISBN 978-80-228-2041.
- MALÍK, V., DVOŘÁK, J. 2007. Harvesterové technologie a vliv na lesní porosty: Harvester technologies and impact on forest stands. Praha: 2007. ISBN 978-80-86386-92-8.
- MIKLEŠ, M., MIKLEŠ, J. 2012. Rezné mechanizmy v lesnej ťažbe. Zvolen: Technická univerzita vo Zvolene, 2012. 83 s. ISBN 978-80-228-2428-6.
- MIKLEŠ, J. 2017. Kinematika odvetvovacej hlavice a riešenie tvaru nožov. In *Mobilné energetické prostriedky – Hydraulika – Životné prostredie – Ergonómia mobilných strojov: zborník abstraktov*. Zvolen: 2017, s. 16 – 17. ISBN 978-80-228-2995-3.
- NERUDA, J. 2013. Harvesterové technologie lesní těžby. Brno: Mendelova univerzita, 2013. ISBN 978-807375-842-4.
- NERUDA, J., SIMANOV, V. 2006. Technika a technologie v lesnictví. Brno: Mendelova zemědělská a lesnická univerzita, 2006. ISBN 80-7157-988-2.
- ULRICH, R., SCHLAGHAMERSKÝ, A., ŠTOREK, V. 2002. Použití harvesterové technologie v probírkách. Brno: Mendelova zemědělská a lesnická univerzita, 2002. ISBN 80-715-7631-X.
- ULRICH, R. 2006. Harvesterové technologie a jejich optimální užití v praxi. Brno: Mendelova zemědělská a lesnická univerzita v Brně, 2006. ISBN 80-737-5012-0.

This paper was prepared within the work on a research project APVV-16-0194 “Research on the impact of process innovation on lifespan of forestry machinery tools and components”.

Corresponding author:

Veronika Luptáčiková, luptacikovav@gmail.com

Richard Hnilica, hnilica@tuzvo.sk